

International Journal of Modern Physics A
 © World Scientific Publishing Company

Nonperturbative approach to Yang-Mills thermodynamics

Ralf Hofmann

*Institut für Theoretische Physik
 Johann Wolfgang Goethe – Universität
 Max von Laue – Str. 1
 D-60438 Frankfurt am Main
 Germany
 r.hofmann@thphys.uni-heidelberg.de*

Received 7 April 2005

Revised 26 November 2006

An analytical and nonperturbative approach to SU(2) and SU(3) Yang-Mills thermodynamics is developed and applied. Each theory comes in three phases: A deconfining, a preconfining, and a confining one. We show how macroscopic and inert scalar fields emerge in each phase and how they determine the ground-state physics and the properties of the excitations. While the excitations in the deconfining and preconfining phase are massless or massive gauge modes of spin 1 the excitations in the confining phase are massless or massive spin-1/2 fermions. The nature of the two phase transitions is investigated for each theory. We compute the temperature evolution of thermodynamical quantities in the deconfining and preconfining phase, and we estimate the density of states in the confining phase. Some implications for particle physics and cosmology are discussed.

Keywords: thermal gauge theories; holonomy; caloron; magnetic monopole; center-vortex loop; thermal ground state; thermal quasiparticles; Bose condensation; preconfinement; complete confinement; Polyakov-loop expectation; Hagedorn transition; Planck-scale axion; cosmic coincidence; CP violation; electroweak symmetry breaking; fractional Quantum Hall effect

PACS numbers: 11.15.Ex, 11.10.Wx, 11.15.Tk

1. Introduction

The beauty, richness and usefulness of nonabelian gauge theories is generally appreciated. Yet, in a perturbative approach to gauge theories like the Standard Model of particle physics (SM) and its (non)supersymmetric extensions it is hard if not impossible to convincingly address a number of recent and not so recent experimental and observational results in particle physics and cosmology: Nondetection of the Higgs particle at LEP ¹, indications for a rapid thermalization and strongly collective behavior of the plasma that emerges in the early stage of an ultra-relativistic heavy-ion collision ^{2,3} despite the fact that the ideal hydrodynamical expansion essentially obeys a free-gas equation of state, dark energy and dark matter, a strongly

2 *Ralf Hofmann*

avored epoch of cosmological inflation ^{4,7,5,6} in the very early Universe ^{8,9,10} and today's accelerated cosmological expansion, a puzzling large-angle signal in the power spectrum of the cosmic microwave background for the cross correlation of electric-field polarization and temperature fluctuations ¹², the likely existence of intergalactic magnetic fields of so far unclarified origin ^{13,14}, and the departure of $\sim 3 \times 10^{43}$ protons p. a. (and hardly any negative charges) ¹⁰³ from the sun's surface (solar wind) which clearly is contradicting the charge conservation inherent in the SM. An analytical and nonperturbative approach to strongly interacting gauge theories may further our understanding of these phenomena.

The objective of the present work is the thermodynamics of SU(2) and SU(3) Yang-Mills theories in four dimensions. It is difficult to gain insights in the dynamics of a strongly interacting four-dimensional gauge theory by analytical means if this dynamics is not severely constrained by certain global symmetries. We conjecture with Ref. ¹⁵ that a thermodynamical approach is an appropriate starting point for such an endeavor. On the one hand, this conjecture is reasonable since a strongly interacting system, being in equilibrium, communicates distortions almost instantaneously by rigid correlations, and thus a return to equilibrium takes place very rapidly. On the other hand, it turns out that the requirement of thermalization allows for an analytical and nonperturbative derivation of macroscopic ground states and the properties of their (quasiparticle) excitations in two of the three phases of each theory. A breakdown of equilibrium in a transition to the third phase is unproblematic since the dynamics then is uniquely determined by the remaining symmetry.

Let us very briefly recall some aspects of the analytical approaches to thermal SU(N) Yang-Mills theory as they are discussed in the literature. Because of asymptotic freedom ^{16,17} one would naively expect thermal perturbation theory to work well for temperatures T much larger than the Yang-Mills scale Λ since the gauge coupling constant $\bar{g}(T)$ logarithmically approaches zero for $\frac{T}{\Lambda} \rightarrow \infty$. It is known for a long time that this expectation is too optimistic since at any temperature perturbation theory is plagued by instabilities arising from the infrared sector (weakly screened, soft magnetic modes ¹⁸). As a consequence, the pressure P can be computed perturbatively only up to (and including) order \bar{g}^5 . The effects of resummations of one-loop diagrams (hard thermal loops), which rely on a scale separation furnished by the small value of the coupling constant \bar{g} , are summarized in terms of a nonlocal effective theory for soft and semi-hard modes ¹⁹. In the computation of radiative corrections, based on this effective theory, infrared effects due to soft magnetic modes still appear in an uncontrolled manner. This has led to the construction of an effective theory where soft modes are collectively described in terms of classical fields whose dynamics is influenced by integrated semi-hard and hard modes ^{20,21}. In Quantum Chromodynamics (QCD) a perturbative calculation of P was pushed up to order $\bar{g}^6 \log \bar{g}$, and an additive 'nonperturbative' term at this order was fitted to lattice results ²². Within the perturbative orders

a poor convergence of the expansion is observed for temperatures not much larger than the $\overline{\text{MS}}$ scale. While the work in ²² is a computational masterpiece it could, by definition, not shed light on the missing, nonperturbative dynamics of the infrared sector. Screened perturbation theory, which relies on a split of the tree-level Yang-Mills action by the introduction of variational parameters, is a very interesting idea. Unfortunately, this approach generates temperature dependent ultraviolet divergences in its presently used form, see ²³ for a recent review.

The purpose of the present work is to report, in a detailed way, on the development of a nonperturbative and analytical approach to the thermodynamics of SU(2) and SU(3) Yang-Mills theory (see ²⁴ for intermediate stages). The reason why we consider only these two gauge groups is that for SU(N) with $N \geq 4$ it is likely that the phase structure of the theory is not unique: In contrast to SU(2) and SU(3), which possess one confining (center), one preconfining (magnetic), and one deconfining (electric) phase, more than three phases may exist for an SU(N) Yang-Mills theory with $N \geq 4$.

Our starting point is the derivation of a macroscopic ground state in the deconfining phase. This ground state originates from instantaneous, long-range correlations mediated by field configurations of topological charge ± 1 . Technically, this situation is described by a spatially homogeneous, quantum mechanically and statistically inert scalar field ϕ , which transforms under the adjoint representation of the gauge group, and a pure-gauge configuration of trivial topology solving the Yang-Mills equations subject to a source term provided by ϕ . Both the field ϕ and the pure-gauge configuration emerge after a spatial coarse-graining over quantum fluctuations down to a resolution corresponding to the length scale $|\phi|^{-1}$. While ϕ represents the spatial average over BPS saturated, topological defects, that is, ‘large’ quantum fluctuations the pure-gauge configuration is a manifestation of averaged-over plane-wave quantum fluctuations.

Conceptually, our approach is similar to the macroscopic Landau-Ginzburg-Abrikosov theory for superconductivity in metals ^{25,26}. Recall that this theory describes the existence of a condensate of Cooper pairs in terms of a nonvanishing expectation for a complex scalar field φ (local order parameter), which is charged under the electromagnetic gauge group U(1), and in terms of a pure-gauge configuration. A nonzero value of φ is enforced by a phenomenologically introduced potential V . As a consequence, coarse-grained U(1) gauge-field modes δa_μ (photons), which are deprived of the microscopic gauge-field fluctuations contributing to the formation of Cooper pairs and their subsequent condensation, acquire a mass. Microscopically, the generation of a photon mass can be visualized as a large sequence of elastic scattering processes off the electrons residing within individual Cooper pairs in the condensate. At a given photon momentum this slows down the effective velocity of propagation in comparison to a propagation without a Cooper-pairs condensate, see Fig. 1. In the superconducting phase the U(1) gauge symmetry is spontaneously broken by the Cooper-pair condensate, and physical phenomena associated with this breakdown can be analysed in dependence of the parameters

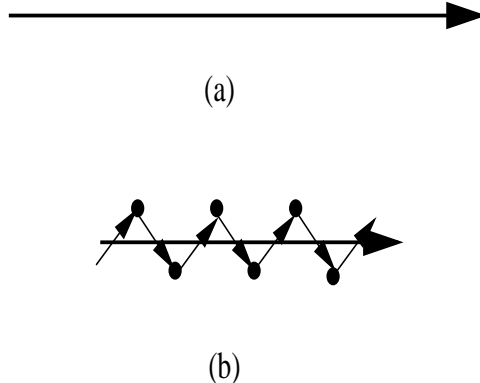
4 *Ralf Hofmann*

Fig. 1. Photon propagation without (a) and within (b) a Cooper-pair condensate.

entering an effective action and in dependence of external conditions such as a magnetic field and/or temperature.

When pursuing the idea of a dynamically generated, macroscopic ground state in each of the phases of an $SU(2)$ or $SU(3)$ Yang-Mills theory it turns out that a situation similar to superconductivity holds. Moreover, in a thermalized $SU(2)$ or $SU(3)$ Yang-Mills theory one is in the comfortable position of being able to *derive* the dynamics of macroscopic scalar fields from first principles. Thus the stabilizing potentials for each scalar field are uniquely determined (up to an undetermined mass parameter – the scale of the Yang-Mills theory). Each (gauge invariant) potential is specified by a unique microscopic definition of the scalar field’s phase (in a suitably chosen gauge) and by the assumption that a dynamically generated, constant mass scale exists. This assumption is supported by perturbation theory^{16,17} where the specification of the running of the gauge coupling requires such a boundary condition. The microscopic definition of the scalar field’s phase is an average over an (nonlocal) operator saturated by noninteracting Bogomolnyi-Prasad-Sommerfield (BPS)³⁰ saturated configurations of topological charge ± 1 . If a particular phase supports propagating gauge modes then, in a second step, interactions between the topological defects and microscopic radiative corrections are taken into account macroscopically by pure-gauge solutions to the equations of motion for gauge fields residing in the trivial-topology sector. The source term for these equations of motion is provided by the (inert) scalar fields.

More specifically, we have shown in⁴⁶ that at large temperatures upon spatial coarse-graining an adjoint scalar field ϕ emerges due to the spatial correlations mediated by trivial-holonomy calorons²⁹. (By large temperature we mean large as compared to the dynamically generated scale.) We discuss in Sec. 2.3.4 why the critical temperature T_P for the onset of ϕ ’s existence should be comparable to the cutoff-scale for a field theoretic description in four dimensions. Trivial-holonomy calorons are BPS saturated (or selfdual) solutions³⁰ to the Euclidean Yang-Mills equations at finite temperature. (The time coordinate τ is compactified on a circle, $0 \leq \tau \leq \frac{1}{T}$.) The topological charge of these configurations is integer. (Whenever we

speak of a topological soliton in this section its antisoliton is also meant.) It will turn out that only calorons with topological charge one contribute to the moduli-space average defining ϕ 's phase. The reason is that for higher-charge calorons the larger number of dimensionful moduli does not admit the definition of a dimensionless entity without the introduction of an explicit temperature dependence⁴⁶. The latter, however, ought to be absent because of a temperature independent weight on the classical level. To understand macroscopic results generated by microscopic interactions between calorons and between their constituents an investigation of the properties of quantum corrected nontrivial-holonomy calorons is necessary⁴¹.

For a given $SU(N)$ gauge-field configuration nontrivial holonomy refers to the following property: Evaluate the Polyakov-loop on this configuration at spatial infinity and observe that the result is not an element

$$\mathbb{1} \exp \left[\frac{2\pi i}{N} k \right] \quad (k = 0, \dots, N-1) \quad (1)$$

of the center Z_N of the gauge group. If this is the case then a mass scale exists in the configuration which determines the behavior $A_4(|\vec{x}| \rightarrow \infty)$. For a classical solution at finite temperature this mass scale must be temperature itself. The quantity $u \equiv T \int_0^\beta d\tau A_4(\tau, |\vec{x}| \rightarrow \infty)$ defines the holonomy of the configuration ($\beta \equiv \frac{1}{T}$). Due to a reflection symmetry $u \rightarrow -u$ one can restrict the values of u as $0 \leq u \leq 2\pi T$ for $SU(2)$.

Calorons with nontrivial holonomy are selfdual configurations that possess BPS magnetic monopole constituents^{31,32,33,34,35}: For an $SU(N)$ caloron with no net magnetic charge there are N constituent monopoles whose magnetic charges add up to zero. The masses of the monopoles are determined by the holonomy u and thus are $\propto T$. By a recent heroic calculation the one-loop quantum weight for an $SU(2)$ caloron with nontrivial holonomy was derived in⁴¹.

Since the one-loop effective action of a nontrivial-holonomy caloron scales with the spatial volume of the system one is tempted to conclude that these configurations do not contribute to the partition function of the theory in the thermodynamical limit and thus are irrelevant³⁶. This conclusion, however, is not valid since one can show that nontrivial-holonomy calorons are *unstable* under quantum corrections⁴¹. Moreover, if, on spatial average, interacting calorons are shown to be described by a quantum mechanically and statistically inert, *macroscopic* adjoint scalar field ϕ and a pure-gauge configuration a_μ^{bg} ⁴⁶ then the exponent of minus the associated effective action S_{cl} can be factored out in the partition function and thus cancels in any physical average. This situation holds even if S_{cl} scales with the spatial volume of the system and thus is infinite in the thermodynamical limit. On the microscopic level, the generation of (unstable) nontrivial holonomy is due to interactions between trivial-holonomy calorons mediated by long-wavelength fields that reside in the topologically trivial sector of the theory.

For the $SU(2)$ case it was shown in⁴¹ that the one-loop fluctuations around calorons with a small holonomy generate an *attractive* potential between the two

6 *Ralf Hofmann*

BPS monopole constituents. This implies that monopole and antimonopole annihilate shortly after they have been created. Thus the likelihood of such a process roughly is determined by the finite one-loop quantum weight of a trivial-holonomy caloron. Up to an additive correction, which depends on temperature and the caloron radius ρ and which is finite, the effective action equals the classical action $S = \frac{8\pi^2}{g^2}$. For g not too small the likelihood of generating a small holonomy is sizable. In the opposite case of a large holonomy a *repulsive* potential between the monopole constituents arises due to one-loop fluctuation⁴¹. Thus monopole and antimonopole separate back-to-back, and the caloron dissociates into a pair of an isolated monopole and an isolated antimonopole which are screened by intermediate caloron fluctuations^{53,54}. Before screening, that is, on the level of the classical solution the mass of both monopole and antimonopole is much larger than temperature³⁴. We conclude that the generation and subsequent dissociation of a large-holonomy caloron is a very rare process due to an extreme Boltzmann suppression. Thus attraction between a monopole and its antimonopole is the dominating situation in the ground-state physics of an SU(2) or SU(3) Yang-Mills theory being in the electric phase. The macroscopic manifestation of monopole-antimonopole attraction, their subsequent annihilation, and recreation is a *negative* ground-state pressure. Equating the exponent in the Boltzmann distribution of the monopole-antimonopole system before screening with the exponent in the one-loop quantum weight of the caloron allows for an estimate of the typical distance between a monopole and an antimonopole at a given temperature. We will see that, on the scale of the inverse temperature, isolated and screened monopoles are very dilute. The case of SU(2) has a straight-forward generalization to SU(3): No qualitative changes take place in the above discussion when going from SU(2) to SU(3).

From the selfduality or BPS saturation of the caloron it follows that its energy-momentum tensor vanishes identically. Since the macroscopic field ϕ originates from the spatial correlations of noninteracting trivial-holonomy calorons of topological charge one⁴⁶ ϕ 's macroscopic energy-momentum tensor vanishes in the absence of a coupling to the topologically trivial sector of the theory. This is a derived condition which needs to be imposed to fix some of the ambiguities which emerge when calculating ϕ 's phase. Namely, one insists on a BPS saturation of the τ dependence of this phase: A linear second-order equation of motion for ϕ 's phase can be derived from a microscopic definition involving a moduli-space average over a two-point correlator, and the requirement of BPS saturation determines the solution up to an irrelevant global gauge choice and an irrelevant constant phase shift⁴⁶.

Subsequently, a potential V_E for the canonically normalized field ϕ is derived by appealing to the derived information on ϕ 's phase and to the assumptions that a dynamically generated scale Λ_E exists and that the right-hand side of ϕ 's BPS equation is analytic in ϕ . (Here the subscript E refers to the electric phase.) As a consequence, ϕ 's modulus is $\propto T^{-1/2}$ and $V_E \propto T$. Thus the caloron sector contributes to thermal quantities in a power-suppressed way at large temperatures. Moreover, we will show that the ground state in the electric phase is degenerate with

respect to a global electric Z_2 (SU(2)) and a global electric Z_3 (SU(3)) symmetry. Therefore, the electric phase is *deconfining*.

In the coarse-grained theory a useful decomposition of field configurations a_μ with trivial topology (only those ones appear as explicit gauge fields) is

$$a_\mu = a_\mu^{bg} + \delta a_\mu \quad (2)$$

where a_μ^{bg} denotes a pure-gauge configuration belonging to the ground state, and δa_μ is a finite-curvature fluctuation. In unitary gauge, where $a_\mu^{bg} = 0$ and thus no coupling between δa_μ and a_μ^{bg} exists, a fluctuation δa_μ acquires a mass by the adjoint Higgs mechanism if $[\phi, \delta a_\mu] \neq 0$. Since the field ϕ dynamically breaks the gauge symmetries $SU(2) \rightarrow U(1)$ and $SU(3) \rightarrow U(1)^2$, two and six directions in the three and eight dimensional adjoint color space acquire mass, respectively.

We shall discuss why the scale Λ_E , which measures the strength of apparent gauge-symmetry breaking by calorons at a given temperature, is physically set at a temperature scale T_P where any four-dimensional gauge theory fails to describe reality. Common belief is that T_P is comparable to the Planck mass $M_P \sim 10^{19}$ GeV.

How does the existence of the temperature dependent scale $|\phi|$ influence the propagation of gauge modes in the infrared and ultraviolet? Calorons induce quasi-particle masses on tree level in the effective theory which are of the order $e|\phi|$. Here e denotes the *effective* gauge coupling. This coupling measures the interaction strength between the topologically trivial off-Cartan fluctuations (in unitary gauge) and the coarse-grained manifestation of nontrivial topology. Furthermore, it is a measure for the screening of the magnetic charge of a monopole. (As far as thermodynamical quantities are concerned, essentially all excitations are free (quasi)particles⁴⁸.) The evolution of e with temperature follows from the requirement of thermodynamical selfconsistency of this interaction. Except for a small range in temperature to the right of the electric-magnetic transition at $T_{c,E}$, where

$$e(T) \sim -\log(T - T_{c,E}), \quad (3)$$

the coupling e is constant: A manifestation of the existence of screened^a, isolated and conserved magnetic charges generated by dissociating large-holonomy calorons.

Infrared cutoffs $\sim e|\phi|$ arise from a reduction of propagation speed for off-Cartan fluctuations by their interactions with calorons, compare with the analogous situation for a superconducting material in Fig. 1. Due to the existence of these cutoffs in the loop expansions of thermodynamical quantities the problem of a magnetic instability, as encountered in perturbation theory¹⁸, is resolved^{18,48}. In the ultraviolet, $|\phi|$ acts as a compositeness constraint by setting a maximal scale for the off-shellness of quantum fluctuations. This is a consistent requirement since *all*

^aThe screening of the monopoles is due to surrounding caloron fluctuations of small holonomy and not due to Cartan *excitations* since the latter are not capable of screening static magnetic fields¹⁸.

gauge modes, on-shell or off-shell, originate from the nontrivial ground state and thus ought not be capable of destroying it. Moreover, plane-wave quantum fluctuations of an off-shellness larger than $|\phi|^2$ are contained, in a coarse-grained form, in the pure-gauge configuration a_μ^{bg} . Compositeness constraints are implemented in a physical gauge with respect to the unbroken subgroups $U(1)$ or $U(1)^2$. The usual renormalization program, needed to make sense of ultraviolet divergences in thermal perturbation theory, is abandoned in the effective theory: The ground state itself provides for a *physical* ultraviolet cutoff.

As a consequence of the simultaneous existence of both an ultraviolet and an infrared cutoff the contributions of higher loops in the expansion of thermodynamical quantities are very small. (Technically, an evaluation of two-loop corrections to the pressure is quite involved⁴⁸.) Obviously, the situation outlined so far differs substantially from the idea of a Wilsonian flow for nonabelian gauge theories in its usual implementation: One derives effective dynamics in dependence of an externally set scale^b k by integrating plane-wave modes harder than k into couplings that appear in an ansatz for an effective action. This effective action describes the dynamics of gauge modes of maximal hardness k . The dynamics of these modes is, however, not only influenced by integrated-out high-momentum fluctuations but also by (spatially) small-scale fluctuations of nontrivial topology. Recall that the later can not be expanded in terms of the former because of an essential singularity in their weight at a vanishing value of the fundamental gauge coupling. Thus we propose an approach which is the converse of the usual picture: Integrate the topological sector first and determine subsequently, that is, after spatial coarse-graining, what its average effect on the trivial-topology fluctuations is.

We have already mentioned that this approach to $SU(2)$ or $SU(3)$ Yang-Mills thermodynamics implies the existence of three rather than two phases. In the magnetic phase, where the isolated and screened magnetic monopoles of the electric phase are massless and thus condensed and where off-Cartan modes are thermodynamically decoupled, the dual gauge symmetries $U(1)_D$ or $U(1)_D^2$ are broken dynamically, and the global electric center symmetries Z_2 or Z_3 are restored in the ground state. We will show that the ground state in the magnetic phase is a Bose condensate of monopole-antimonopole systems. Each condensate is described in terms of a macroscopic and inert complex scalar field and a pure-gauge configuration.

A monopole condensate confines fundamentally charged, fermionic and static test charges. At the same time, dual and massive gauge modes *propagate* in the magnetic phase. Thus it is appropriate to refer to the magnetic phase as a pre-confining phase. The magnetic coupling g , which measures the interaction strength between dual gauge modes and condensed magnetic monopoles on the one hand

^bThis scale either is continuous, see²⁷ for a review on gauge theories, or it reflects a scale hierarchy originating from the assumed smallness of the coupling constant \bar{g} at a large temperature T , for example $k = \bar{g}T$ ¹⁹.

and the screening of center-vortex loops on the other hand, is zero at $T_{c,E}$ and rises rapidly into a logarithmic divergence of the same form as in Eq. (3) at a temperature $T_{c,M}$. For SU(2) and SU(3) we have $T_{c,M} = 0.835 \times T_{c,E}$ and $T_{c,M} = 0.877 \times T_{c,E}$, respectively. Thus the magnetic phase occupies only a small region in the phase diagram of either theory. This and the fact that the monopole condensates possess infinite correlation lengths $\sim (\text{monopole mass})^{-1}$ are the reasons why the magnetic phase has escaped its direct detection by simulations on finite-size lattices. We will show though that it is possible to observe the existence of the magnetic phase in a lattice simulations of the infrared insensitive entropy density when using the so-called differential method. The latter provides the best-controlled circumvention of the infrared problem in simulations on finite-size lattices⁷⁸.

At $T_{c,M}$, where g diverges logarithmically, another phase transition takes place. All dual gauge modes decouple and thus the monopole condensates, macroscopically described by nonfluctuating, BPS saturated complex scalar fields φ (SU(2)) and φ_1, φ_2 (SU(3)) and pure gauges, dominate the thermodynamics. As a consequence, the entropy density vanishes at $T_{c,M}$ and the equation of state is

$$\rho = -P. \quad (4)$$

Just like magnetic monopoles are isolated defects in the electric phase there are isolated and closed magnetic flux lines in the magnetic phase^c which, however, collapse as soon as they are created if the magnetic coupling g is finite: Abrikosov-Nielsen-Olesen (ANO) vortex loops⁶⁷. Only one unit of flux with respect to $U(1)_D$ (SU(2)) or either factor in $U(1)_D^2$ (SU(3)) is carried by a given vortex loop since in the electric phase only charge-one calorons dissociate into magnetic monopoles with one unit of magnetic charge^d. This allows for an interpretation of ANO vortex loops as center-vortex loops. For SU(N) the magnetic flux of the latter is determined by the differences in phase modulo N of two center elements, see Eq. (1). There is one unit of center flux for SU(2), and there are two separate units of center flux for SU(3).

^cThe fact that only closed loops occur is explained by the absence of isolated magnetic charges in a monopole condensate.

^dThe core of a vortex line, where $U(1)_D$ (SU(2)) or one factor in $U(1)_D^2$ (SU(3)) is restored, can be pictured as a directed motion of magnetic monopoles (to the right) and antimonopoles (to the left) in the rest frame of the heatbath⁶⁶, see Fig. 2. The magnetic flux, which penetrates a spatial hyperplane perpendicular to the direction of monopole or antimonopole motion, is by Stoke's theorem measured by a line integral $g \oint_{\mathcal{C}} dz_{\mu} A_{\mu}^D$ along a circular curve \mathcal{C} with infinite radius lying in this plane. Here A_{μ}^D denotes the gauge field with respect to the dual gauge group $U(1)$ (SU(2)) or either factor in $U(1)^2$ (SU(3)) generated by the moving chains of monopoles and antimonopoles. If we choose to evaluate the line integral in a covariant gauge then the contribution to $dz_{\mu} A_{\mu}^D$ of each moving monopole or antimonopole is that of a static monopole or antimonopole since the perpendicular part of the gauge field is invariant under boosts along the vortex axis. Thus the state of motion of each monopole and antimonopole is irrelevant for its effect on the total magnetic flux carried by the vortex as long as the net motion of all monopoles and antimonopoles in a given segment defines the direction of the vortex axis: The only thing that determines the magnetic flux of the vortex line is the *charge* of a monopole.

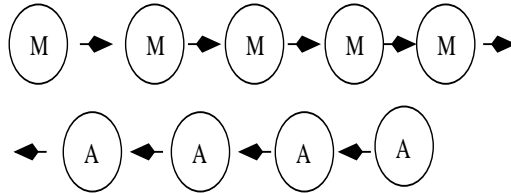


Fig. 2. Microscopics of the core of a center vortex. Monopoles (M) and antimonopoles (A) move in opposite directions.

The core-size of a center vortex is determined by the length $l_g \sim (g|\varphi|)^{-1}$ (SU(2)) or $l_{g,1} \sim (g|\varphi_1|)^{-1}, l_{g,2} \sim (g|\varphi_2|)^{-1}$ (SU(3)) of penetration of the vortex' gauge field into a direction perpendicular to the vortex. While center vortices are thick close to $T_{c,E}$ their core size vanishes at $T_{c,M}$. Since the energy of a typical center-vortex loop⁶⁷ is $\propto g^{-1}$ spin-0 systems composed of a vortex loop and its antivortex loop condense at $T_{c,M}$. We will show that there is a parameter with discrete values characterizing the possible values of a macroscopic, complex scalar field Φ which describes the vortex condensate.

The transition to the center phase is of the Hagedorn type and thus nonthermal. An order parameter for this transition is the expectation of the 't Hooft loop whose modulus measures the strength of center-vortex condensation. If the 't Hooft loop does not vanish then the *magnetic* Z_2 (SU(2)) or Z_3 (SU(3)) symmetry is dynamically broken. These center symmetries are *local* in four-dimensional space-time. Under large $U(1)_D$ (SU(2)) or large $U(1)_D^2$ (SU(3)) gauge transformations the macroscopic field Φ transforms by multiplications with center elements.

In the course of the Hagedorn transition the ground state of the magnetic phase decays through creation of single and self-intersecting center-vortex loops. In contrast to the magnetic phase, center-vortex loops are stable in the center phase, thus are particle-like, and possess a density of states which is over-exponentially rising with energy. There are precisely two polarization states for each self-intersecting or single loop (spin-1/2 fermions). After the decay of the monopole condensate is completed the new ground state is a Cooper-pair condensate of systems composed of a massless single vortex and antivortex loop. The energy-momentum tensor on this ground state *vanishes identically*. This result is protected against radiative corrections.

The center phase is truly confining: A pair of electric, static, oppositely and fundamentally charged, and fermionic test charges forms a confining electric flux tube because of the presence of condensed electric dipoles (single center-vortex loops) in the ground state, and all gauge modes are infinitely heavy. Notice that

the absence of propagating gauge modes implies that only contact interactions are possible between (thin) center fluxes and the self-intersection points of their vortex loops.

Thermal lattice simulations fail to produce physical results for infrared sensitive quantities at temperatures shortly below $T_{c,E}$: The center phase as well as the magnetic phase possess infinite correlation lengths. In the center phase this correlation length is given by the inverse (vanishing) mass of a single center-vortex loop. Thus the fermionic nature of excitations and their over-exponentially rising density of states in the center phase escapes simulations performed on finite-size lattices.

It is self-evident that what was said above has implications for particle physics and cosmology. We only would like to mention a few questions that are likely to be answered by SU(2) Yang-Mills (thermo)dynamics alone: Electroweak symmetry breaking, namely, the origin of the masses of Z_0 and W^\pm ; the mass hierarchy between the two members of a lepton family; the question of whether the neutrino is Dirac or Majorana; the smallness of the cosmological constant on particle physics scales; the nature of cosmological and clustering dark matter; cosmic coincidence; baryon and lepton asymmetries; intergalactic magnetic fields; and large-angle anomalies in some of the power spectra of fluctuations in the cosmic microwave background.

The article is organized as follows. In the first part of Sec. 2 we provide prerequisites on caloron physics. The classical solutions of trivial and nontrivial holonomy and their behavior under quantum corrections are discussed for SU(2). As an aside we estimate the separation of isolated and screened monopoles in terms of the inverse temperature in the electric phase. The second part of Sec. 2 is devoted to the derivation of the macroscopic, adjoint field ϕ in terms of a moduli-space and S_3 integral over the spatial two-point correlations in a caloron-anticaloron system. Subsequently, we discuss the full ground-state physics in the electric phase. The existence of a dynamically generated scale Λ_E needs to be assumed to determine ϕ 's modulus at a given temperature. We show that a degeneracy with respect to a global electric Z_2 (SU(2)) and Z_3 (SU(3)) symmetry occurs which proves that this phase is deconfining. The last part of Sec. 2 addresses the full thermodynamics of the electric phase, including excitations. An evolution equation for the effective gauge coupling e is derived and solved numerically. It is observed that an ultraviolet-infrared decoupling is manifest in this evolution. We present analytical results for the electric screening mass, associated with the massless mode in the SU(2) case, and for the two-loop correction to the pressure.

In Sec. 3 we investigate the magnetic phase. Prerequisites on the BPS monopole are given. Considering the average magnetic flux, generated by a screened monopole-antimonopole system in a thermal environment, through an S_2 with infinite radius, where the monopole-antimonopole system is located outside of this S_2 , a continuous parameter (proportional to the Euclidean time) is derived. This parameter governs the temporal winding of a spatially homogeneous, complex, and inert scalar field φ in the limit where monopole mass and spatial momentum of the system vanish (Bose

condensation). For SU(3) two such fields exist, each for every independent monopole species. Assuming the existence of a dynamically generated scale Λ_M , the modulus of φ is derived. We then discuss the ground-state physics in the magnetic phase. It is shown that the electric Z_2 (SU(2)) and electric Z_3 (SU(3)) degeneracy of the ground state, as observed in the electric phase, gives way to a unique ground state in the magnetic phase. Thus we derive test-charge confinement in the magnetic phase. Evolution equations for the effective magnetic coupling g are derived and solved numerically. A discussion of the full Polyakov-loop expectation (including excitations) and an analysis of the critical behavior at the electric-magnetic phase boundary are presented. We find that this transition is second order with mean-field exponents both for SU(2) and SU(3) with the difference that the peak in the specific heat is about three times smaller in the former as compared to the latter case.

In Sec. 4 we investigate the center phase. We start by providing prerequisites on the ANO vortex. In particular, we emphasize the fact that an ANO vortex generates negative pressure at finite magnetic coupling g . While a vortex-loop is a particle-like excitation at $g = \infty$ it collapses as soon as it is created for $g < \infty$. Collapsing ANO or center-vortex loops dominate the (negative) pressure inside the magnetic phase where $g < \infty$. In analogy to the monopole condensate we determine a parameter (mean center flux through an S_1 of infinite radius) which governs the expectation of a macroscopic, complex scalar field Φ describing the Bose condensate of massless vortex-antivortex-loop pairs. The values of this parameter are discrete: Two possible values for SU(2) and three possible values for SU(3). At $T_{c,M}$, where g diverges in a logarithmic way and where dual gauge modes acquire an infinite mass, the center-vortex condensate starts to form under (spin-1/2) particle creation. We construct an effective potential V_C for Φ involving a scale Λ_C . We check V_C 's uniqueness, and discuss how vortex-loop creation takes place by center jumps of Φ 's phase. An estimate for the density of fermion states, created by Φ 's relaxation to zero energy density and pressure, is provided. As a result, we analytically establish that the center-magnetic transition is of the Hagedorn type.

In Sec. 5 we discuss how the scales Λ_E and Λ_M are related by the continuity of the pressure across the electric-magnetic phase boundary. We also provide an approximate relation between Λ_M and Λ_C .

In Sec. 6 we present numerical results for the temperature dependence of thermodynamical quantities throughout the electric and the magnetic phase. The following quantities are discussed: Pressure, energy density, interaction measure, specific heat per volume, and entropy density. While the former quantities are very sensitive to the ground-state physics at low temperatures, which is determined by very large spatial correlations and thus is inaccessible to finite-size lattices, the entropy density is only sensitive to the excitations. This fact makes a comparison of our results for the entropy density with those obtained on lattices (employing the differential method) useful, all other quantities exhibit quantitative disagreements with their lattice-obtained values at low temperatures.

In Sec. 7 we discuss implications of our work for particle physics and cosmology. We start by addressing the cosmic-coincidence and the old cosmological-constant problem in view of a Planck-scale axion, originating from dynamically generated and subsequently integrated spin-1/2 fermions at the Planck scale, and in view of an SU(2) gauge theory of Yang-Mills scale close to the temperature of the cosmic microwave background (CMB) (SU(2)_{CMB}). This theory is at the electric-magnetic phase boundary, and its only massless and unscreened excitation is the photon. Throughout cosmological evolution the axion mass is provided by the axial anomaly involving nonconfining SU(N) gauge theories of Yang-Mills scales lower than the Planck scale. The presence of a Planck-scale axion may explain the particle-number asymmetries and CP violation in the weak interactions. Some of the phenomenology of the electroweak sector of the SM is addressed in view of leptons being stable solitons in the center phase of various SU(2) Yang-Mills theories. These solitons are embedded into instable higher-charge excitations with an over-exponentially rising density of states which protect their apparent structurelessness seen in scattering experiments (the photon couples to the lepton because of mixing) up to center-of-mass energies comparable to the mass of the Z boson (with exceptions at momenta comparable to the lepton masses). We postdict the mass ratio $\frac{m_{\nu_e}}{m_e}$ in terms of the mass ratio $\frac{m_e}{m_Z}$. Finally, we present some ideas on how fractionally charged light quarks and their confinement may arise in Quantum Chromodynamics (QCD) in terms of electric-magnetically dual SU(3) gauge dynamics and the fractional Quantum Hall effect.

The last section of the present work briefly summarizes our results.

2. The electric phase

2.1. Prerequisites

2.1.1. The Harrington-Shepard solution (trivial holonomy)

Calorons of trivial holonomy are the field configurations which enter the definition of the phase of the macroscopic adjoint scalar field ϕ . We only need to consider the SU(2) case since the SU(3) ground-state thermodynamics can be derived from a 'democratic' embedding of SU(2) calorons. We use the nonperturbative definition of the gauge field where the coupling constant is absorbed into the field.

(Anti)Calorons are (anti)selfdual, that is, their field strength is up to a sign equal to their dual field strength

$$F_{\mu\nu}[A^{(C,A)}] = \pm \tilde{F}_{\mu\nu}[A^{(C,A)}] \quad (5)$$

where the superscript $C(A)$ refers to caloron (anticaloron). Only calorons of topological charge one (minus one) enter the definition of ϕ 's phase and thus we will focus on this case only.

14 *Ralf Hofmann*

The Harrington-Shepard solutions²⁹ are given as

$$\begin{aligned} A_\mu^C(\tau, \vec{x}) &= \bar{\eta}_{a\mu\nu} \frac{\lambda^a}{2} \partial_\nu \ln \Pi(\tau, \vec{x}) \quad \text{or} \\ A_\mu^A(\tau, \vec{x}) &= \eta_{a\mu\nu} \frac{\lambda^a}{2} \partial_\nu \ln \Pi(\tau, \vec{x}) \end{aligned} \quad (6)$$

where the 't Hooft symbols $\eta_{a\mu\nu}$ and $\bar{\eta}_{a\mu\nu}$ are defined by

$$\begin{aligned} \eta_{a\mu\nu} &= \epsilon_{a\mu\nu} + \delta_{a\mu}\delta_{\nu 4} - \delta_{a\nu}\delta_{\mu 4} \\ \bar{\eta}_{a\mu\nu} &= \epsilon_{a\mu\nu} - \delta_{a\mu}\delta_{\nu 4} + \delta_{a\nu}\delta_{\mu 4}. \end{aligned} \quad (7)$$

In Eq. (6) λ^a , ($a = 1, 2, 3$), denote the Pauli matrices. The periodic solutions in Eq. (6), $A_\mu^{C,A}(0, \vec{x}) = A_\mu^{C,A}(1/T, \vec{x})$, are generated by a temporal mirror sum of the 'pre'potential

$$\Pi_0 = 1 + \frac{\rho^2}{x^2} \quad (8)$$

of a single BPST (anti)instanton of scale ρ ²⁸ in singular gauge⁴⁵. Here $x^2 \equiv \tau^2 + \vec{x}^2$. The scalar function $\Pi(\tau, \vec{x})$ in Eq. (6) is given as

$$\begin{aligned} \Pi(\tau, \vec{x}) &= \sum_{n=-\infty}^{\infty} \frac{\rho^2}{(\tau - n\beta, \vec{x})^2} \\ &= \bar{\Pi}(\tau, r) \equiv 1 + \frac{\pi\rho^2}{\beta r} \frac{\sinh\left(\frac{2\pi r}{\beta}\right)}{\cosh\left(\frac{2\pi r}{\beta}\right) - \cos\left(\frac{2\pi\tau}{\beta}\right)} \end{aligned} \quad (9)$$

where $r \equiv |\vec{x}|$ and $\beta \equiv 1/T$. Evaluating the integral of the Chern-Simons current over a small three-sphere S_3 , centered at the singular point ($\tau = 0, \vec{x} = 0$), one obtains plus (or minus) one unit of topological charge. For a given value of ρ the solutions in Eq. (6) can be generalized by shifting the center from $z = 0$ to $z = (\tau_z, \vec{z})$ by the (quasi) translational invariance of the classical action. (The temporal shift τ_z is restricted to $0 \leq \tau_z \leq \beta$ because of periodicity.) In addition, the color orientation of each solution can be rotated by global gauge transformations.

Computing the Polyakov loop at spatial infinity on either of the configurations $A_\mu^C(\tau, \vec{x})$ and $A_\mu^A(\tau, \vec{x})$ yields the following result

$$\mathbf{P}(|\vec{x}| \rightarrow \infty) = \mathcal{P} \exp \left[i \int_0^\beta d\tau A_4^{C,A}(\tau, |\vec{x}| \rightarrow \infty) \right] = \mathbb{1}. \quad (10)$$

Thus the Harrington-Shepard solutions possess trivial holonomy.

2.1.2. The Lee-Lu-Kraan-van Baal solution (nontrivial holonomy)

For a discussion of (anti)selfdual SU(2) configurations with nontrivial holonomy and topological charge one (minus one) we use the conventions and closely follow the presentation of³⁴ which to our taste makes the magnetic monopole content

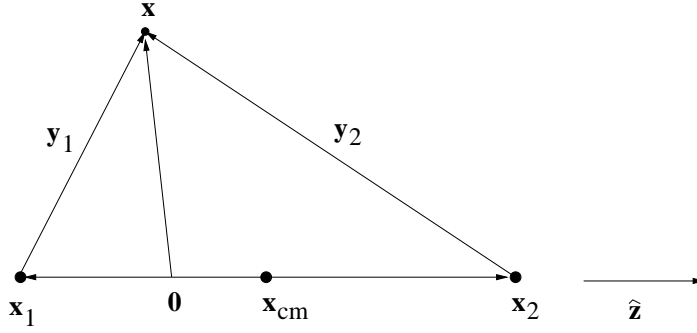


Fig. 3. Meaning of the spatial arguments \vec{y}_1, \vec{y}_2 entering the solution in Eq. (12). The points \vec{x}_1, \vec{x}_2 are the core positions of the monopole and the antimonopole. At the point $\tau = 0, \vec{x}_{\text{cm}}$ the solution is singular.

most explicit. (In ⁴¹ the constituents of nontrivial-holonomy calorons are referred to as dyons because the nonabelian magnetic and electric field of each constituent is equal and Coulomb-like for large distances away from a given monopole core. This property, however, follows from the selfduality of the caloron configuration. With respect to the unbroken U(1) the charge of a constituent monopole is purely magnetic (and not dyonic as in ⁵⁸) since the A_4 field serves as a Higgs field and not as the gauge potential for the electric field.) The existence of these solutions was shown by Nahm ³¹. Explicit analytical constructions were independently performed by Lee and Lu ³⁴ and Kraan and van Baal ^{32,33}.

Lee and Lu use antihermitian generators and parametrize the holonomy u as

$$A_4^C(\tau, |\vec{x}| \rightarrow \infty) = -i\frac{u}{2}\lambda_3 \quad (11)$$

where $0 \leq u \leq \frac{2\pi}{\beta}$. Using the Nahm data for a monopole coexisting with an antimonopole as an input to the Atiyah-Drinfeld-Hitchin-Manin-Nahm (ADHMN) equations (subject to a normalization condition), a selfdual field configuration with monopole-antimonopole constituents was constructed in ³⁴. It reads

$$\begin{aligned} A_\mu(\vec{x}, \tau) = & C_1^\dagger V_\mu(\vec{y}_1; u) C_1 + C_2^\dagger V_\mu(\vec{y}_2; \frac{2\pi}{\beta} - u) C_2 + \\ & C_1^\dagger \partial_\mu C_1 + C_1^\dagger \partial_\mu C_1 + C_2^\dagger \partial_\mu C_2 + S^\dagger \partial_\mu S \end{aligned} \quad (12)$$

where

$$\begin{aligned} V_4(\vec{x}; u) = & \frac{\lambda_a}{2i} \hat{x}_a \left(\frac{1}{|\vec{x}|} - \frac{u}{\coth(u|\vec{x}|)} \right), \\ V_i(\vec{x}; u) = & \frac{\lambda_a}{2i} \epsilon_{aij} \hat{x}_j \left(\frac{1}{|\vec{x}|} - \frac{u}{\sinh(u|\vec{x}|)} \right). \end{aligned} \quad (13)$$

16 *Ralf Hofmann*

Interpreting $V_4(\vec{x}; u)$ as an adjoint Higgs field, Eqs. (13) represent the BPS magnetic monopole⁵⁷. The matrices C_1, C_2 in Eq. (12) are given as

$$\begin{aligned} C_1 &= \sqrt{\frac{2DN_1}{\mathcal{N}}} \frac{B_1^\dagger}{\mathcal{M}} \left[\exp\left(-\frac{\vec{\lambda}}{2} \cdot \vec{s}_2\right) Q_+ + \exp\left(\frac{\vec{\lambda}}{2} \cdot \vec{s}_2\right) Q_- \right] \exp\left(-i\frac{\pi}{\beta}\tau\lambda_3\right), \\ C_2 &= \sqrt{\frac{2DN_2}{\mathcal{N}}} \frac{B_2^\dagger}{\mathcal{M}} \left[\exp\left(\frac{\vec{\lambda}}{2} \cdot \vec{s}_1\right) Q_+ + \exp\left(-\frac{\vec{\lambda}}{2} \cdot \vec{s}_2\right) Q_- \right] \end{aligned} \quad (14)$$

where $Q_\pm = \frac{1}{2}(1 \pm \lambda_3)$ are projection operators. The matrices B_1, B_2 are

$$\begin{aligned} B_1 &= \exp\left[i\frac{\pi}{\beta}\tau\right] \exp\left[-\frac{\vec{\lambda}}{2} \cdot \vec{s}_1\right] \exp\left[-\frac{\vec{\lambda}}{2} \cdot \vec{s}_2\right] - \\ &\quad \exp\left[-i\frac{\pi}{\beta}\tau\right] \exp\left[\frac{\vec{\lambda}}{2} \cdot \vec{s}_1\right] \exp\left[\frac{\vec{\lambda}}{2} \cdot \vec{s}_2\right], \\ B_2 &= \exp\left[i\frac{\pi}{\beta}\tau\right] \exp\left[-\frac{\vec{\lambda}}{2} \cdot \vec{s}_2\right] \exp\left[-\frac{\vec{\lambda}}{2} \cdot \vec{s}_1\right] - \\ &\quad \exp\left[-i\frac{\pi}{\beta}\tau\right] \exp\left[\frac{\vec{\lambda}}{2} \cdot \vec{s}_2\right] \exp\left[\frac{\vec{\lambda}}{2} \cdot \vec{s}_1\right] \end{aligned} \quad (15)$$

and the scalar \mathcal{M} is defined as

$$\mathcal{M} = 2 \left(\cosh s_1 \cosh s_2 + \hat{y}_1 \cdot \hat{y}_2 \sinh s_1 \sinh s_2 - \cos\left[\frac{2\pi}{\beta}\tau\right] \right). \quad (16)$$

In addition, one defines

$$N_i = \frac{1}{y_i} \sinh s_i, \quad (i = 1, 2), \quad (17)$$

and

$$\mathcal{N} = 1 + \frac{2D}{\mathcal{M}} (N_1(\cosh s_2 - (\hat{y}_2)_3 \sinh s_2) + N_2(\cosh s_1 + (\hat{y}_1)_3 \sinh s_1)), \quad (18)$$

and

$$S = \frac{1}{\sqrt{\mathcal{N}}} \exp\left[-i\frac{u}{2}\tau\lambda_3\right]. \quad (19)$$

The spatial arguments of the configuration in Eq. (12), compare with Fig. 3, are defined as

$$\begin{aligned} \vec{y}_i &= \vec{x} - \vec{x}_i, & y_i &= |\vec{y}_i|, & s_i &= |\vec{s}_i| & (i = 1, 2), \\ \vec{s}_1 &= u\vec{y}_1, & \vec{s}_2 &= \left(\frac{2\pi}{\beta} - u\right)\vec{y}_2, & D &= |\vec{x}_2 - \vec{x}_1|. \end{aligned} \quad (20)$$

(A $\hat{\cdot}$ -sign indicates a unit vector.) Kraan and van Baal show that the distance D between the two BPS monopoles can be expressed by the scale ρ of a trivial-holonomy caloron which is deformed to nontrivial holonomy³³. One has

$$D = \frac{\pi}{\beta} \rho^2. \quad (21)$$

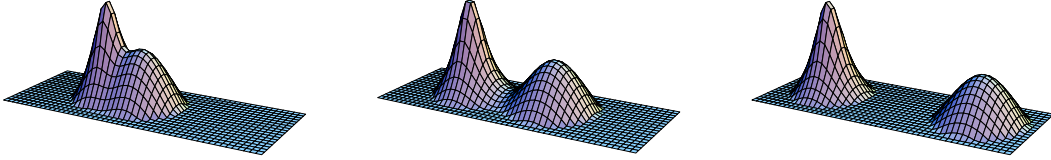


Fig. 4. Action density of an $SU(2)$ caloron with nontrivial holonomy plotted on a two-dimensional spatial slice. The caloron radius ρ and therefore the separation D (Eq. (21)) increases from left to right while temperature and holonomy are fixed. Figures are taken from a paper by Kraan and van Baal. The peaks of the action density coincide with the core positions of the constituent BPS monopoles.

It was shown in ³⁴ that for $y_1 \ll D$

$$C_2, S \sim \frac{1}{\sqrt{D}} \quad (22)$$

and

$$C_1 = \frac{\lambda_3 \cosh \frac{s_1}{2} - \vec{\lambda} \cdot \hat{y}_1 \sinh \frac{s_1}{2}}{\sqrt{\cosh s_1 - (\hat{y}_1)_3 \sinh s_1}} + \mathcal{O}(1/D). \quad (23)$$

Thus C_1 is a single-valued unitary matrix, and for $y_1 \ll D$ the configuration in Eq. (12) is an approximate gauge transform of a BPS monopole. Similarly, for $y_2 \ll D$ C_2 is a unitary matrix. The difference as compared with C_1 for $y_1 \ll D$ is that for $y_2 \ll D$ the matrix C_2 induces a large gauge rotation due to an extra factor $\exp\left[-i\frac{\pi}{\beta}\tau\lambda_3\right]$. This gauge transformation inverts the charge of the BPS monopole at \vec{x}_2 as compared to the charge of the BPS monopole at \vec{x}_1 . There is a singularity of the solution at the point $(\tau = 0, \vec{x}_{\text{cm}})$ where

$$\vec{x}_{\text{cm}} = \frac{\beta u}{2\pi} \vec{x}_1 + \left(1 - \frac{\beta u}{2\pi}\right) \vec{x}_2. \quad (24)$$

This point carries one unit of topological charge. One can show this by expanding the solution about $(\tau = 0, \vec{x}_{\text{cm}})$ and by performing the integral of the Chern-Simons current over a small S_3 centered at this point. A plot of the action density of a nontrivial-holonomy caloron with varying radius ρ at a fixed temperature and a fixed holonomy is presented in Fig. 4.

On the classical level the masses of the monopoles at \vec{x}_1 and \vec{x}_2 are given as

$$m_1 = 4\pi u \quad m_2 = 4\pi \left(\frac{2\pi}{\beta} - u\right), \quad (25)$$

respectively. For a large holonomy, that is $u \sim \frac{\pi}{\beta}$, we have $m_1 \sim m_2 \sim 4\pi^2 T \sim 40 T$. Thus large holonomy is extremely Boltzmann suppressed.

18 *Ralf Hofmann*

2.1.3. One-loop quantum weights

In this section we first present the results for the one-loop effective action of a trivial-holonomy caloron, which was obtained by Gross, Pisarski, and Yaffe³⁶ by appealing to the results obtained in^{37,38,39} and the pioneering work of 't Hooft⁴⁰. Subsequently, we sketch the results obtained recently by Diakonov, Gromov, Petrov, and Slizovskiy⁴¹ for the one-loop quantum weight of a caloron with non-trivial holonomy. Both results are important for a grasp of the microphysics of the ground-state physics in the electric phase.

Harrington-Shepard solution:

The functional determinant around a Harrington-Shepard caloron was calculated in³⁶. The result for the quantum weight $\exp[-S_{\text{eff}}]$ of this configuration is given in terms of the effective action as

$$S_{\text{eff}} = \frac{8\pi^2}{\bar{g}^2} + \frac{4}{3}\sigma^2 + 16A(\sigma) \quad (26)$$

where the dimensionless quantity σ is defined as $\sigma \equiv \pi \frac{\rho}{\beta}$ and

$$A(\sigma) \equiv \frac{1}{12} \left[\int_0^\beta d\tau \frac{d^3x}{16\pi^2} \left(\frac{(\partial_\mu \Pi)^2}{\Pi^2} \right)^2 - \int \frac{d^4x}{16\pi^2} \left(\frac{(\partial_\mu \Pi_0)^2}{\Pi_0^2} \right)^2 \right]. \quad (27)$$

The weight $\exp[-S_{\text{eff}}]$ is relevant for the integration over the classical moduli space in the presence of one-loop quantum fluctuations. (The nonflat metric is the same as in the zero-temperature situation.)

In Eq. (27) the scalar quantities Π and Π_0 are defined in Eqs. (9) and (8), respectively. The first integral in Eq. (27) is over $S_1 \times \mathbb{R}^3$ while the second integral is over \mathbb{R}^4 . It is worth mentioning how $A(\sigma)$ behaves in the high- and low-temperature limits $\sigma \rightarrow \infty$ and $\sigma \rightarrow 0$:

$$A(\sigma) \rightarrow -\frac{1}{6} \log \sigma, \quad (\sigma \rightarrow \infty), \quad A(\sigma) \rightarrow -\frac{\sigma^2}{36}, \quad (\sigma \rightarrow 0). \quad (28)$$

At a given caloron radius ρ the correction to the classical action $\frac{8\pi^2}{\bar{g}^2}$ thus is large in the high-temperature regime, indicating that the contribution of trivial-holonomy calorons to the partition function is suppressed, while it is small at low temperatures, implying the increasing importance of calorons as the temperature of the system drops. The distinction between high and low temperatures is made by a dynamically generated scale Λ_E which also determines the ρ dependence of the coupling constant \bar{g} in Eq. (26). The latter, by zero-temperature one-loop renormalization-group running^{16,17}, estimatedly becomes larger than unity for $\rho^{-1} \sim \Lambda_E$ and is logarithmically small for $\rho^{-1} \gg \Lambda_E$.

Lee-Lu-Kraan-van Baal solution

The calculation of the one-loop quantum weight for a caloron of nontrivial holonomy is much harder than for the trivial case. This explains why this result only appeared in the literature⁴¹ more than six years after the analytical form of the nontrivial-holonomy solution was published in^{34,33}. The expressions are so involved that the contribution $\mathcal{Z}_{\text{n.h.}}$ of an isolated, quantum-blurred caloron to the total partition function \mathcal{Z} of the theory has so far only been stated in closed analytical form in the limit

$$\frac{D}{\beta} = \pi \left(\frac{\rho}{\beta} \right)^2 \gg 1. \quad (29)$$

This, however, is the relevant physical situation, see Sec. 2.1.5 where it is shown that (trivial-holonomy) calorons with $\rho \gg \beta$ dominate the phase of the macroscopic adjoint scalar field ϕ . As we shall see, the ground-state physics in the electric phase is dominated by small-holonomy deformations of the trivial case.

Apart from the restriction in Eq. (29) the result obtained in⁴¹ for $\mathcal{Z}_{\text{n.h.}}$ is valid for any value of the holonomy, $0 \leq u \leq \frac{2\pi}{\beta}$. After the (trivial) integrations of the overall color orientation and time translations are performed one obtains⁴¹

$$\begin{aligned} \mathcal{Z}_{\text{n.h.}} = & C\beta^{-6} \int d^3x_1 \int d^3x_2 \left(\frac{8\pi^2}{\bar{g}^2} \right)^4 \left(\frac{\Lambda e^{\gamma_E \beta}}{4\pi} \right)^{22/3} \left(\frac{\beta}{D} \right)^{5/3} \times \\ & (2\pi + \beta u \bar{u} D)(uD + 1)^{\frac{4}{3\pi}u\beta-1} (\bar{u}D + 1)^{\frac{4}{3\pi}\bar{u}\beta-1} \times \\ & \exp[-V P(u) - 2\pi D P''(u)], \quad (D \gg \beta). \end{aligned} \quad (30)$$

(The number of independent integration variables in Eq. (30) is four because $\int d^3x_1 \int d^3x_2 = 4\pi \int d^3x \int dDD^2$ where $\vec{x} = \frac{1}{2}(\vec{x}_1 + \vec{x}_2)$). In Eq. (30) $C \sim 1.0314$, \vec{x}_1 and \vec{x}_2 are the core positions of the monopoles in the classical solution (compare with Fig. 3), $\bar{u} \equiv \frac{2\pi}{\beta} - u$, γ_E is the Euler constant, V denotes the typical spatial volume belonging to the one-caloron system, and Λ is a scale which is a one-loop renormalization group invariant (dimensional transmutation). The functions $P(u)$ and $P''(u)$ are given as

$$\begin{aligned} P(u) &= \frac{\beta}{12\pi^2} u^2 \bar{u}^2, \\ P''(u) &= \frac{\beta}{\pi^2} \left[\frac{\pi}{\beta} \left(1 - \frac{1}{\sqrt{3}} \right) - u \right] \left[\bar{u} - \frac{\pi}{\beta} \left(1 - \frac{1}{\sqrt{3}} \right) \right]. \end{aligned} \quad (31)$$

The function $P(u)$ is always positive for $u \neq 0, \frac{2\pi}{\beta}$. The occurrence of the spatial volume V in the exponent in Eq. (30) would mean total suppression of nontrivial holonomy in the naive thermodynamical limit $V \rightarrow \infty$. This, however, is not a valid conclusion since nontrivial-holonomy calorons are unstable: They either dissociate into a pair of BPS monopoles (large holonomy) or they collapse back onto trivial holonomy by an annihilation of their BPS monopole constituents. This can be checked by investigating the second contribution to the exponent in Eq. (30).

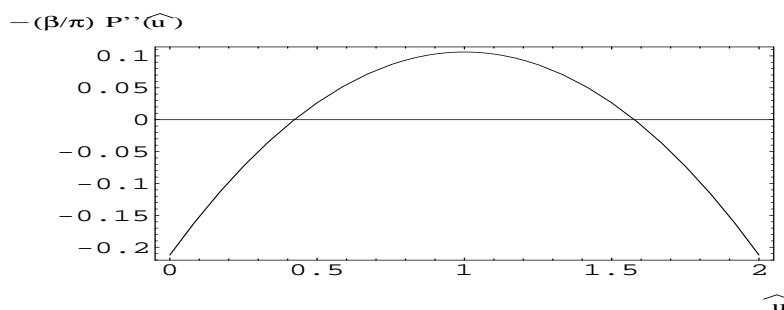
20 *Ralf Hofmann*

Fig. 5. The quantity $-\frac{\beta}{\pi}P''(\hat{u})$, compare with Eq. (30), as a function of the dimensionless holonomy $\hat{u} \equiv \frac{u}{\pi T}$.

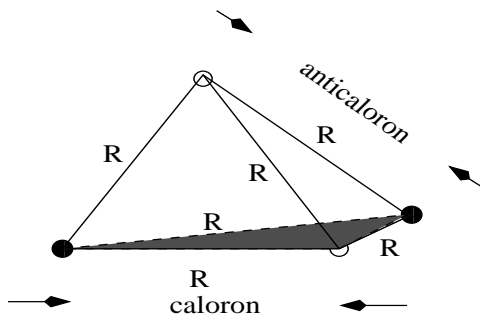


Fig. 6. The typical volume spanned by two pairs of BPS monopoles created by the dissociation of two calorons whose large holonomy was generated by the interaction of trivial-holonomy calorons.

In Fig. 5 a plot of $-\frac{\beta}{\pi}P''(\hat{u})$ is shown. For $0 \leq u \leq \frac{\pi}{\beta}(1 - \frac{1}{\sqrt{3}})$ and for $\frac{\pi}{\beta}(1 + \frac{1}{\sqrt{3}}) \leq u \leq 2\frac{\pi}{\beta}$ the quantity $P''(u)$ is positive (small holonomy) while it is negative in the complementary range (large holonomy). According to Eq. (30) this means that in the former (latter) case the BPS monopoles experience a linear attractive (repulsive) potential. Let us now make an estimate of the typical size of an equilateral tetrahedron whose corners are the positions of (screened) magnetic monopoles, see Fig. 6, which are generated by the dissociation of a caloron and an anticaloron whose large holonomy was created by their interaction. The edge length R of the tetrahedron is the typical maximal distance between two BPS monopoles generated by a caloron with a holonomy close to maximally nontrivial, $u_{\max} = \frac{\pi}{\beta}$. Once a large holonomy has been created the dissociation of the caloron generates the stabilized distance R with probability one. (Once a monopole is at rest with respect to the heat bath there is no screening of its magnetic charge by Cartan fluctuations¹⁸ but only by small-holonomy calorons in its surroundings. Thus the screening of magnetic charge is not described by Eq. (30).) Thus it is appropriate to

equate the probability for reaching the distance R , where monopoles are sufficiently screened to be at rest, governed by Eq. (30), with the thermal probability for exciting the monopoles in a caloron of large holonomy to start with. Since monopoles also are at rest shortly after being created the latter probability is roughly given as

$$\exp[-\beta(m_1 + m_2)], \quad m_1 \sim m_2 \sim \frac{4\pi^2}{\beta}, \quad (32)$$

see Eq. (25). Taking only the exponentially sensitive part of the caloron weight into account and substituting for V the volume of the tetrahedron, $V = \frac{1}{6\sqrt{2}}R^3$, this translates into the following condition:

$$-\frac{\pi^2}{72\sqrt{2}}\left(\frac{R}{\beta}\right)^3 + \frac{2}{3}\pi\frac{R}{\beta} + 8\pi^2 = 0. \quad (33)$$

There exists only a single real and positive solution to this equation. Numerically, we obtain $R \sim 10.1\beta$. So on the scale of the inverse temperature the gas of screened magnetic monopoles is dilute. This fits nicely with the lattice results obtained in 53,54.

While the (extremely small) likelihood for the generation of large-holonomy calorons depends on the value of the holonomy only (and not on the distance D) this is not true for a caloron with holonomy close to trivial. Since the latter configuration always collapses back onto trivial holonomy the likelihood for its generation is determined by the caloron weight $\exp[-S_{\text{eff}}]$ with S_{eff} given in Eq. (26). A strong dependence of S_{eff} on D (or ρ) at a given temperature exists. In contrast to $\exp[-\beta(m_1 + m_2)] \sim \exp[-8\pi^2]$ the weight $\exp[-S_{\text{eff}}]$ is sizable at S_{eff} 's minimum σ_{min} .

We conclude that *attraction* between a BPS monopole and its antimonopole (small holonomy), which are in equilibrium with respect of their creation and annihilation, by far dominates the ground-state physics as compared to the case where monopole and antimonopole *repulse* one another (large holonomy). Macroscopically, this situation expresses itself by a *negative* pressure of the ground state. We shall compute the temperature dependence of this pressure in Sec. 2.1.6.

2.1.4. Microscopic definition for the phase of an adjoint and macroscopic scalar field ϕ

The results that were discussed in the last two subsections are important for an understanding of the infrared physics in the electric phase. The detailed microscopic dynamics is very complicated and, as it seems, it is impossible to derive macroscopic quantities such as the pressure or the energy density or the mass of thermal quasi-particles by performing literal ensemble averages on the microscopic level. What turns out to be feasible and thermodynamically exhaustive is to compute the spatial average (spatial coarse-graining) over the physics generated by the topologically nontrivial sector. This procedure introduces the concept of a macroscopic, thermal

ground state. As far as thermodynamics is concerned one still obtains exact results this way. The advantage of such an approach is that the complications of a microscopic calculation are avoided. Once the ground-state physics is understood and quantitatively described its effect on the propagation of trivial-topology modes can be investigated.

If the ground state is to be characterized by a macroscopic field other than a pure-gauge configuration then, by spatial isotropy, this macroscopic field must be a Lorentz scalar ϕ . Moreover, in a pure Yang-Mills theory, where all local fields transform under the adjoint representation of the gauge group, the composite field ϕ needs to transform in an adjoint way under the remnants of a microscopic, spacetime dependent gauge transformations. Since space dependent gauge transformations are constant on the macroscopic level (due to the spatial average) no space dependence of ϕ occurs in any chosen gauge. Apart from its modulus, which is governed by a dynamically emerging scale Λ_E and temperature, the only nontrivial information on ϕ is the τ dependence of its color orientation in a given gauge. In the following we will refer to ϕ 's color orientation as ϕ 's phase.

Let us imagine a (hypothetical) Yang-Mills world where the only field configurations allowed to contribute to the partition function are classical and noninteracting caloron configurations of trivial holonomy. We will show in Sec 2.1.5 that it is consistent to adopt this point of view in the derivation of the *macroscopic* ground-state physics. Since the Yang-Mills scale Λ_E can not be computed we focus on the computation of ϕ 's phase first. Because ϕ 's phase is a ratio of the field and its modulus and hence dimensionless the associated measure for the ρ -average is flat.

We closely follow the presentation in ⁴⁶ for the remainder of this section and for Sec. 2.1.5. Due to the selfduality of calorons any local definition of ϕ 's phase yields

the trivial result zero. Thus we start by defining:

$$\begin{aligned}
\frac{\phi^a}{|\phi|}(\tau) \sim \text{tr} \left[\right. \\
& \beta^0 1! \int d^3 x \int d\rho \\
& \quad \frac{\lambda^a}{2} F_{\mu\nu}[A_\alpha(\rho, \beta)]((\tau, 0)) \{(\tau, 0), (\tau, \vec{x})\} [A_\alpha(\rho, \beta)] \times \\
& \quad F_{\mu\nu}[A_\alpha(\rho, \beta)]((\tau, \vec{x})) \{(\tau, \vec{x}), (\tau, 0)\} [A_\alpha(\rho, \beta)] + \\
& \beta^{-1} 2! \int d^3 x \int d^3 y \int d\rho \\
& \quad \frac{\lambda^a}{2} F_{\mu\lambda}[A_\alpha(\rho, \beta)]((\tau, 0)) \{(\tau, 0), (\tau, \vec{x})\} [A_\alpha(\rho, \beta)] \times \\
& \quad F_{\lambda\nu}[A_\alpha(\rho, \beta)]((\tau, \vec{x})) \{(\tau, \vec{x}), (\tau, \vec{y})\} [A_\alpha(\rho, \beta)] \times \\
& \quad F_{\nu\mu}[A_\alpha(\rho, \beta)]((\tau, \vec{y})) \{(\tau, \vec{y}), (\tau, 0)\} [A_\alpha(\rho, \beta)] + \\
& \beta^{-2} 3! \int d^3 x \int d^3 y \int d^3 u \int d\rho \\
& \quad \frac{\lambda^a}{2} F_{\mu\lambda}[A_\alpha(\rho, \beta)]((\tau, 0)) \{(\tau, 0), (\tau, \vec{x})\} [A_\alpha(\rho, \beta)] \times \\
& \quad F_{\lambda\nu}[A_\alpha(\rho, \beta)]((\tau, \vec{x})) \{(\tau, \vec{x}), (\tau, \vec{y})\} [A_\alpha(\rho, \beta)] \times \\
& \quad F_{\nu\kappa}[A_\alpha(\rho, \beta)]((\tau, \vec{y})) \{(\tau, \vec{y}), (\tau, \vec{u})\} [A_\alpha(\rho, \beta)] F_{\kappa\mu}[A_\alpha(\rho, \beta)]((\tau, \vec{u})) \times \\
& \quad \{(\tau, \vec{u}), (\tau, 0)\} [A_\alpha(\rho, \beta)] + \dots \left. \right]. \tag{34}
\end{aligned}$$

A number of comments are in order: The dots in (34) stand for the contributions of higher n -point functions and for reducible, that is, factorizable contributions with respect to the spatial integrations. The factors $(n-1)!$ in front of the n -point contribution measures the multiplicity of the corresponding integral. Factors β^{n-2} are needed to make the contribution dimensionless. The argument $A_\alpha(\rho, \beta)$ (spacetime dependence suppressed) refers to either a caloron or an anticaloron configuration, the Harrington-Shepard solutions of Sec. 2.1.1. Moreover, the following definitions apply:

$$\begin{aligned}
|\phi| &\equiv \frac{1}{2} \text{tr} \phi^2, \\
\{(\tau, 0), (\tau, \vec{x})\} [A_\alpha] &\equiv \mathcal{P} \exp \left[i \int_{(\tau, 0)}^{(\tau, \vec{x})} dy_\beta A_\beta(y, \rho) \right], \\
\{(\tau, \vec{x}), (\tau, 0)\} [A_\alpha] &\equiv \mathcal{P} \exp \left[-i \int_{(\tau, 0)}^{(\tau, \vec{x})} dy_\beta A_\beta(y, \rho) \right] \tag{35}
\end{aligned}$$

where \mathcal{P} is the path-ordering symbol. Under a microscopic gauge transformation

24 *Ralf Hofmann*

$\Omega(y)$ we have:

$$\begin{aligned}
& \{(\tau, 0), (\tau, \vec{x})\} [A_\alpha] \rightarrow \Omega^\dagger((\tau, 0)) \{(\tau, 0), (\tau, \vec{x})\} [A_\alpha] \Omega((\tau, \vec{x})), \\
& \{(\tau, \vec{x}), (\tau, 0)\} [A_\alpha] \rightarrow \Omega^\dagger((\tau, \vec{x})) \{(\tau, \vec{x}), (\tau, 0)\} [A_\alpha] \Omega((\tau, 0)), \\
& F_{\mu\nu}[A_\alpha]((\tau, \vec{x})) \rightarrow \Omega^\dagger((\tau, \vec{x})) F_{\mu\nu}[A_\alpha]((\tau, \vec{x})) \Omega((\tau, \vec{x})), \\
& F_{\mu\nu}[A_\alpha]((\tau, 0)) \rightarrow \Omega^\dagger((\tau, 0)) F_{\mu\nu}[A_\alpha]((\tau, 0)) \Omega((\tau, 0)).
\end{aligned} \tag{36}$$

As a consequence of Eq. (36) the right-hand side of (34) transforms as

$$\frac{\phi^a}{|\phi|}(\tau) \rightarrow R_{ab}(\tau) \frac{\phi^b}{|\phi|}(\tau) \tag{37}$$

where the $SO(3)$ matrix $R_{ab}(\tau)$ is defined as

$$R^{ab}(\tau)\lambda^b = \Omega((\tau, 0)) \lambda^a \Omega^\dagger((\tau, 0)). \tag{38}$$

Thus we have defined an adjointly transforming scalar in (34). In addition, we have just shown that only the time-dependent part of a microscopic gauge transformation survives on the macroscopic level. (Shifting the spatial part of the argument $(\tau, 0) \rightarrow (\tau, \vec{z})$ in (34) introduces a finite *parameter* \vec{z} to the gauge rotation R^{ab} : $R^{ab}(\tau) \rightarrow R^{ab}(\tau, \vec{z})$. Such a shift, however, introduces an arbitrary but finite mass scale $|\vec{z}|^{-1}$ into the definition of ϕ 's phase which, on the classical level, is absent. Also, a finite value of $|\vec{z}|$ would introduce an explicit breaking or rotational symmetry into the definition (34). Thus we have $\vec{z} = 0$. Moreover, the integration path connecting the points $(\tau, 0)$ with (τ, \vec{x}) in Eq. (35) ought to be a straight line since a spatial curvature would imply the existence of a mass scale other than temperature on the classical level.) Integrations over shifts $\tau \rightarrow \tau + \tau_s$ ($0 \leq \tau_s \leq \beta$) project a nontrivial (periodic) τ dependence of ϕ 's phase onto zero and thus are forbidden. Integrations over global gauge rotations are forbidden for the same reason. Spatial shifts $\vec{x} \rightarrow \vec{x} + \vec{x}_s, \vec{y} \rightarrow \vec{y} + \vec{x}_s, \dots$ leave the integrals in (34) invariant. These averages are already performed. Thus the only admissible integration over moduli-space parameters is over ρ with a flat measure.

In (34) the \sim sign indicates that both left- and right-hand sides satisfy the same homogeneous evolution equation in τ

$$\mathcal{D} \left[\frac{\phi}{|\phi|} \right] = 0. \tag{39}$$

Here \mathcal{D} is a differential operator such that Eq. (39) represents a homogeneous differential equation. As it will turn out, Eq. (39) is a *linear* second-order equation which, up to global gauge rotations and a choice of winding sense, determines the first-order or BPS equation whose solution ϕ 's phase is. (The ambiguities in the evaluation of the right-hand side span the solution space of Eq. (39), and thus \mathcal{D} is uniquely determined by (34).)

We now discuss why n -point functions with $n > 2$ do not contribute to the right-hand side of (34). Since the classical (anti)caloron action $S = \frac{8\pi^2}{g^2}$ and the classical moduli-space metric are independent of temperature we conclude that no *explicit*

dependence on β may occur in the definition of ϕ 's phase. For $n > 2$, however, explicit β dependences do occur, see (34). We conclude that these contributions to ϕ 's phase do not exist.

What about calorons of higher topological charge? Some of these solutions have been constructed, see for example ^{43,44}. The essential difference to the charge-one case is that more dimensionful moduli occur than just the parameter ρ . For example, for charge-two configurations there is a spatial core separation between the two seed instantons and an additional instanton radius ρ' . The reader may now convince himself that along the lines of (34) a nonlocal definition of ϕ 's *dimensionless* phase, which would also have to include integrations over the additional moduli of dimension length, is impossible for higher-charge calorons. (This is certainly true for the integral over two-point functions. For every increment in n there is an increase in power of length scale by one unit arising from an additional $d^3x \times F_{\mu\nu}$. This makes the situation even worse in comparison to the two-point case.)

2.1.5. Essentials of the calculation

Before we dive into the essential parts of the calculation, which will lead to the unique determination of the operator \mathcal{D} in Eq.(39), we would like to discuss a condition which severely constrains the possible solutions to this equation.

By (anti)selfduality the energy-momentum tensor vanishes identically on a caloron or an anticaloron,

$$\theta_{\mu\nu}[A_\alpha^{(C,A)}] \equiv 0. \quad (40)$$

Since ϕ 's phase is obtained by an average over (the admissible part of) the moduli space of a caloron-anticaloron system (no interactions) the macroscopic energy-momentum tensor $\bar{\theta}_{\mu\nu}[\phi]$ should vanish identically as well,

$$\bar{\theta}_{\mu\nu}[\phi] \equiv 0. \quad (41)$$

In a thermal equilibrium situation, described by Euclidean dynamics, this is true if and only if the τ dependence of ϕ (or ϕ 's phase) is BPS saturated. Thus ϕ solves the first-order equation

$$\partial_\tau \phi = V_E^{(1/2)} \quad (42)$$

where $V_E^{(1/2)}$ denotes the 'square-root' of a suitable potential. (The fact that an ordinary and not a covariant derivative appears in Eq.(42) is, of course, tied to our specific gauge choice. If we were to leave the (singular) gauge for the seed (anti)instanton, in which the solutions of Eq.(6) are constructed, by a time-dependent gauge rotation $\bar{\Omega}(\tau)$ then a pure-gauge configuration $A_\mu^{p.g.}(\tau) = i\delta_{\mu 4}\bar{\Omega}^\dagger \partial_\tau \bar{\Omega}$ would appear in a *covariant* derivative on the left-hand side of Eq.(42). Also recall the fact that the heat bath breaks boost invariance. This is encoded in the noninvariance of Eq.(42) under O(4) rotations.) $V_E \equiv \text{tr} \left(V_E^{(1/2)} \right)^\dagger V_E^{(1/2)}$. As

26 *Ralf Hofmann*

we will see below, the right-hand side of Eq. (42) is determined only up to a global gauge rotation and a choice of winding sense.

Let us now discuss essential details of the calculation of the right-hand side of (34) which, after what was said in Sec. 2.1.4, reduces to

$$\frac{\phi^a}{|\phi|}(\tau) \sim \text{tr} \int d^3x \int d\rho \frac{\lambda^a}{2} F_{\mu\nu}[A_\alpha(\rho, \beta)] ((\tau, 0)) \{(\tau, 0), (\tau, \vec{x})\} [A_\alpha(\rho, \beta)] \times \\ F_{\mu\nu}[A_\alpha(\rho, \beta)] ((\tau, \vec{x})) \{(\tau, \vec{x}), (\tau, 0)\} [A_\alpha(\rho, \beta)] \quad (43)$$

where a sum over the contributions of a trivial-holonomy caloron and an anticalorons is to be performed.

Since the integrand in the exponent of the Wilson line $\{(\tau, 0), (\tau, \vec{x})\} [A_\alpha^{C,A}]$ is a hedgehog the path-ordering prescription can be omitted. For the caloron contribution one obtains

$$\left. \frac{\phi^a}{|\phi|} \right|_C \sim i \int d\rho \int d^3x \frac{x^a}{r} \times \\ \left[\frac{(\partial_4 \Pi(\tau + \tau_C, 0))^2}{\Pi^2(\tau + \tau_C, 0)} - \frac{2}{3} \frac{\partial_4^2 \Pi(\tau + \tau_C, 0)}{\Pi(\tau + \tau_C, 0)} \right] \left\{ 4 \cos(2g(\tau + \tau_C, r)) \times \right. \\ \left[\frac{\partial_r \partial_4 \Pi(\tau + \tau_C, r)}{\Pi(\tau + \tau_C, r)} - 2 \frac{(\partial_r \Pi(\tau + \tau_C, r)) (\partial_4 \Pi(\tau + \tau_C, r))}{\Pi^2(\tau + \tau_C, r)} \right] + \\ \sin(2g(\tau + \tau_C, r)) \left[4 \frac{(\partial_4 \Pi(\tau + \tau_C, r))^2 - (\partial_r \Pi(\tau + \tau_C, r))^2}{\Pi^2(\tau + \tau_C, r)} + \right. \\ \left. \left. 2 \frac{\partial_r^2 \Pi(\tau + \tau_C, r) - \partial_4^2 \Pi(\tau + \tau_C, r)}{\Pi(\tau + \tau_C, r)} \right] \right\} \quad (44)$$

where

$$g(\tau + \tau_C, r) \equiv \int_0^1 ds \frac{r}{2} \partial_4 \ln \Pi(\tau + \tau_C, sr), \quad (45)$$

the function $\Pi(\tau, r)$ is defined in Eq. (9), and τ_C refers to a constant but arbitrary temporal shift of the caloron center ($0 \leq \tau_C \leq \beta$). It is worth mentioning that the integrand in Eq. (45) is proportional to $\delta(s)$ for $r \gg \beta$. The dependences on ρ and β are suppressed in the integrands of (44) and Eq. (45).

As compared to the contribution of the caloron there are ambiguities in the contribution of the anticaloron: First, the τ dependence of the contribution of the anticaloron may be shifted by τ_A ($0 \leq \tau_A \leq \beta$). Second, the color orientation of caloron and anticaloron contributions may be different. Third, the normalization of the two contributions may be different. To see that this is true, we need to investigate the convergence properties of the radial integration in (44). It is easily checked that all terms give rise to a converging r integration except for the following one:

$$2 \frac{x^a}{r} \sin(2g(\tau + \tau_C, r)) \frac{\partial_r^2 \Pi(\tau + \tau_C, r)}{\Pi(\tau + \tau_C, r)}. \quad (46)$$

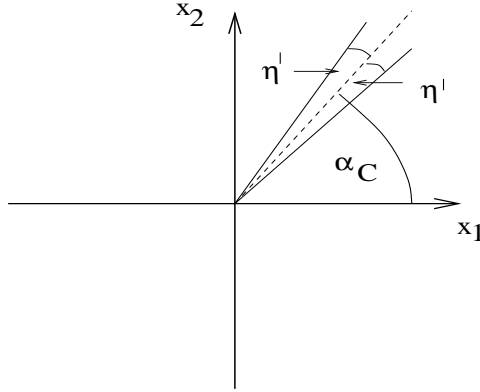


Fig. 7. The axis for the regularized azimuthal integration.

Namely, for $r > R \gg \beta$ (46) goes over in

$$4 \frac{x^a \pi \rho^2 \sin(2g(\tau + \tau_C, r))}{r \beta r^3}. \quad (47)$$

Thus the r -integral of the term in (46) is logarithmically divergent in the infrared: (The integral converges for $r \rightarrow 0$.)

$$4 \frac{\pi \rho^2}{\beta} \int_R^\infty \frac{dr x^a}{r} \sin(2g(\tau + \tau_C, r)). \quad (48)$$

Recall, that $g(\tau + \tau_C, r)$ behaves like a constant in r for $r > R$. The angular integration, on the other hand, would yield zero if the radial integration was regular. Thus a logarithmic divergence can be cancelled by the angular integral to yield some finite and real answer. To investigate this in more detail, both angular and radial integration need to be regularized.

One introduces a regularization, conveniently we have chosen dimensional regularization in ⁴⁶ with a dimensionless regularization parameter $\eta_C > 0$, for the r -integral in Eq. (48) while the angular integration can be regularized by introducing defect (or surplus) angles $2\eta'_C$ in the θ integration (azimuthal angle in the $x_1 x_2$ plane). Any other plane for the azimuthal angular integration could have been chosen. Moreover, the value of α_C is determined by a (physically irrelevant) initial condition, as we will show below, see Fig. 7. Together, the choice of the regularization plane and of the angle α_C amount to a global choice of gauge: an apparent breaking of rotational symmetry by the angular regularization is nothing but a gauge choice.) Without restriction of generality (global gauge choice) we may also for the contribution of the anticaloron use an axis for the angular regularization

28 *Ralf Hofmann*

which lies in the x_1x_2 plane, but with a different angle α_A . Then we have

$$\begin{aligned} \frac{\phi^a}{|\phi|} &= \frac{\phi^a}{|\phi|}\Big|_C + \frac{\phi^a}{|\phi|}\Big|_A \\ &= \pm \Xi_C (\delta_{a1} \cos \alpha_C + \delta_{a2} \sin \alpha_C) \mathcal{A} \left(\frac{2\pi(\tau + \tau_C)}{\beta} \right) \\ &\quad \pm \Xi_A (\delta_{a1} \cos \alpha_A + \delta_{a2} \sin \alpha_A) \mathcal{A} \left(\frac{2\pi(\tau + \tau_A)}{\beta} \right) \\ &\neq 0, \end{aligned} \tag{49}$$

where Ξ_C , Ξ_A , τ_C , τ_A , α_C , and α_A are undetermined. (Ξ_C , Ξ_A are the ratios of $\eta_{C,A}$ and $\eta'_{C,A}$, respectively.) The function $\mathcal{A} \left(\frac{2\pi(\tau)}{\beta} \right)$ is defined as

$$\begin{aligned} \mathcal{A} \left(\frac{2\pi\tau}{\beta} \right) &\equiv \frac{32}{3} \frac{\pi^7}{\beta^3} \int d\rho \left[\lim_{r \rightarrow \infty} \sin(2g(\tau, r)) \right] \times \\ &\quad \rho^4 \frac{\pi^2 \rho^2 + \beta^2 \left(2 + \cos \left(\frac{2\pi\tau}{\beta} \right) \right)}{\left[2\pi^2 \rho^2 + \beta^2 \left(1 - \cos \left(\frac{2\pi\tau}{\beta} \right) \right) \right]^2}. \end{aligned} \tag{50}$$

Eq. (49) and Eq. (50) provide the basis for fixing the operator \mathcal{D} in Eq. (39). To evaluate the function $\mathcal{A} \left(\frac{2\pi\tau}{\beta} \right)$ in Eq. (50) numerically, we introduce the same cutoff for the ρ integration in the caloron and anticaloron case as follows:

$$\int d\rho \rightarrow \int_0^{\zeta\beta} d\rho, \quad (\zeta > 0). \tag{51}$$

This introduces an additional dependence of \mathcal{A} on ζ . In Fig. 8 the τ dependence of \mathcal{A} for various values of ζ is depicted. Therefore we have

$$\begin{aligned} \frac{\phi^a}{|\phi|} &\sim 272 \zeta^3 \left(\Xi_C (\delta_{a1} \cos \alpha_C + \delta_{a2} \sin \alpha_C) \sin \left(\frac{2\pi}{\beta} (\tau + \tau_C) \right) \right. \\ &\quad \left. + \Xi_A (\delta_{a1} \cos \alpha_A + \delta_{a2} \sin \alpha_A) \sin \left(\frac{2\pi}{\beta} (\tau + \tau_A) \right) \right) \\ &\equiv \hat{\phi}^a. \end{aligned} \tag{52}$$

Just like the numbers Ξ_C and Ξ_A are undetermined on the classical level due to the invariance of the classical action under spatial scale transformations so is the number ζ . It is clear, however, from Eq. (52) that the integral in \mathcal{A} is strongly dominated by ρ -values close to the upper integration limit. Let us now discuss the physical content of (52). For fixed values of the parameters $\zeta^3 \Xi_C$, $\zeta^3 \Xi_A$, $\frac{\tau_C}{\beta}$ and $\frac{\tau_A}{\beta}$ the right-hand side of Eq. (52) resembles an elliptic polarization in the x_1x_2 plane of adjoint color space. For a given polarization plane the two independent numbers (normalization and phase-shift) for each of the two oscillations parametrize the solution space of the second-order linear differential equation

$$\mathcal{D}\hat{\phi} = 0. \tag{53}$$

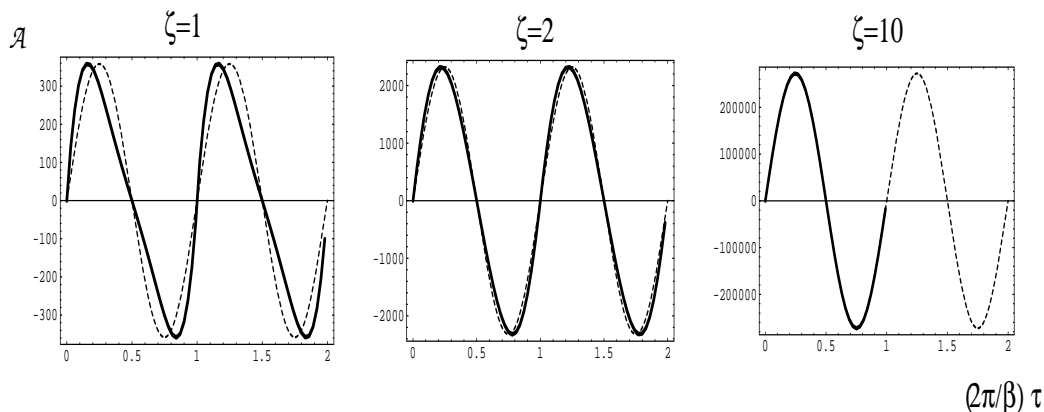


Fig. 8. \mathcal{A} as a function of $\frac{2\pi}{\beta}\tau$ for $\zeta = 1, 2, 10$. For each case the dashed line is a plot of $\max \mathcal{A} \times \sin\left(\frac{2\pi}{\beta}\tau\right)$. We have fitted the asymptotic dependence on ζ of the amplitude of \mathcal{A} as $\mathcal{A}\left(\frac{2\pi}{\beta}\tau = \frac{\pi}{2}, \zeta\right) = 272\zeta^3$, ($\zeta > 10$). The fit is stable under variations of the fitting interval. For the case $\zeta = 10$ the difference between the two curves can not be resolved anymore.

From (52) we observe that the operator \mathcal{D} is

$$\mathcal{D} = \partial_\tau^2 + \left(\frac{2\pi}{\beta}\right)^2. \quad (54)$$

The ambiguities in Eq. (52) parameterize the solution space of Eq. (53) for a given polarization plane which depends on a global choice of gauge. Thus the differential operator \mathcal{D} is *uniquely* determined by Eq. (52). What is needed to assure the validity of Eq. (41) is a BPS saturation of the solution to the linear Eq. (53) since the modulus of ϕ may not depend on τ in thermal equilibrium.

Thus we need to find first-order equations whose solutions are traceless, hermitian and solve the second-order equation (53). The relevant two first-order equations are

$$\partial_\tau \hat{\phi} = \pm \frac{2\pi i}{\beta} \lambda_3 \hat{\phi}. \quad (55)$$

Obviously, the right-hand sides of Eqs. (55) are subject to a global gauge ambiguity (associated with the choice of polarization plane in which the regularization of the azimuthal angular integration is carried out) and a choice of sign: Any normalized generator other than $\pm\lambda_3$ could have appeared. Moreover, a solution to either of the two equations (55) also solves Eq. (53) for a given polarization plane,

$$\partial_\tau^2 \hat{\phi} = \pm \frac{2\pi i}{\beta} \lambda_3 \partial_\tau \hat{\phi} = \frac{2\pi i}{\beta} \lambda_3 \frac{2\pi i}{\beta} \lambda_3 \hat{\phi} = - \left(\frac{2\pi}{\beta}\right)^2 \hat{\phi}. \quad (56)$$

Solutions to Eqs. (55) are given as

$$\hat{\phi} = C \lambda_1 \exp\left(\mp \frac{2\pi i}{\beta} \lambda_3 (\tau - \tau_0)\right) \quad (57)$$

30 *Ralf Hofmann*

where C and τ_0 denote real integration constants which both are undetermined. We set $\tau_0 = 0$ in what follows. The solutions in Eq. (57) represent a circular polarization in the $x_1 x_2$ plane of adjoint color space and thus indicate that the field ϕ winds along an S_1 on the group manifold S_3 of $SU(2)$. Both winding senses appear but can not be distinguished physically: A change in winding sense does not affect the potential nor does it affect the admissibility of the transformation to unitary gauge, see Sec. 2.2.2.

2.1.6. ϕ 's modulus and potential

SU(2) case:

The information in Eq. (57) on ϕ 's phase can be used to infer its modulus once the existence of an externally given mass scale Λ_E is assumed. (The scale Λ_E determines the typical distance between caloron centers at a given temperature.) As long as no interactions between trivial-holonomy calorons are allowed for this is consistent since the BPS saturation of ϕ forbids the occurrence of (gravitationally) measurable effects: The macroscopic energy-momentum tensor $\bar{\theta}_{\mu\nu}$ vanishes identically, and thus assuming the existence of the scale Λ_E does not yet influence the ground-state physics. We have

$$\phi = |\phi|(\beta, \Lambda_E) \hat{\phi} \left(\frac{\tau}{\beta} \right). \quad (58)$$

In order to reproduce the phase in Eq. (57) a *linear* dependence on ϕ must appear on the right-hand side of the BPS equation (42). Moreover, this right-hand side ought not depend on β explicitly and must be analytic in ϕ . The former requirement derives from the fact that ϕ and its potential V are obtained by functionally integrating over the (admissible part of the) moduli space of a caloron-anticaloron system with no interactions. The associated part of the partition function does not exhibit an explicit β dependence since the action and thus the weight are β independent on the moduli space. Thus a β dependence of V or $V^{(1/2)}$ can only be generated via the periodicity of ϕ itself. The latter requirement derives from the demand that the thermodynamics at temperature $T + \delta T$ to any given accuracy must be smoothly derivable from the thermodynamics at temperature T for δT sufficiently small provided no phase transition occurs at T . This is done by expanding the right-hand side of the BPS equation (finite radius of convergence) which, in turn, is the starting point for a perturbative treatment with expansion parameter $\frac{\delta T}{T}$.

Linearity, analyticity, and no explicit dependence of β only allow the BPS equation for ϕ to be one the two following possibilities:

$$\partial_\tau \phi = \pm i \Lambda_E \lambda_3 \phi \quad (59)$$

or

$$\partial_\tau \phi = \pm i \Lambda_E^3 \lambda_3 \phi^{-1} \quad (60)$$

where $\phi^{-1} \equiv \frac{\phi}{|\phi|^2}$. Recall that

$$\phi^{-1} = \phi_0^{-1} \sum_{n=0}^{\infty} (-1)^n \phi_0^{-n} (\phi - \phi_0)^n \quad (61)$$

has a finite radius of convergence. According to Eqs. (58) and (57) we may write

$$\phi = |\phi|(\beta, \Lambda_E) \times \lambda_1 \exp\left(\mp \frac{2\pi i}{\beta} \lambda_3 \tau\right). \quad (62)$$

Substituting Eq. (62) into Eq. (59) yields

$$\Lambda_E = \frac{2\pi}{\beta} \quad (63)$$

which is unacceptable since Λ_E is a constant scale. For the other possibility Eq. (60), we obtain

$$|\phi|(\beta, \Lambda_E) = \sqrt{\frac{\beta \Lambda_E^3}{2\pi}} = \sqrt{\frac{\Lambda_E^3}{2\pi T}} \quad (64)$$

when substituting Eq. (62) into Eq. (60). This is acceptable and indicates that at $T \gg \Lambda_E$ ϕ 's modulus is small. The right-hand side of Eq. (60) defines the 'square-root' $V^{(1/2)}$ of a potential $V(|\phi|) \equiv \text{tr} (V^{(1/2)})^\dagger V^{(1/2)} = \Lambda_E^6 \text{tr} \phi^{-2}$. The equation of motion (60) can be derived from the following action:

$$S_\phi = \text{tr} \int_0^\beta d\tau \int d^3x (\partial_\tau \phi \partial_\tau \phi + \Lambda_E^6 \phi^{-2}). \quad (65)$$

Notice that due to BPS saturation it is not possible to add a constant to the potential in Eq. (65) without changing the ground-state physics. (In fact, adding a constant, the modified BPS equation would not admit periodic solutions anymore.) The scale $|\phi|$ must be interpreted as the maximal resolution that remains after the spatial coarse-graining over calorons and anticalorons is performed. As we shall show later, a critical temperature $2\pi T_{c,E} = 13.867 \Lambda_E$ exists. Thus, expressing the critical cutoff $|\phi|^{-1} = \sqrt{\frac{2\pi}{\Lambda_E^3 \beta_{c,E}}}$ in units of $\beta_{c,E}$, yields 8.22; for $T > T_{c,E}$ this number grows as $(T/T_{c,E})^{3/2}$. But cutting off the ρ - and r -integration at $> 8.22 \beta$ perfectly represents the infinite-volume limit in Eq. (50)!

The ratios of the mass-squared of ϕ -field fluctuations, $\partial_{|\phi|}^2 V(|\phi|)$, and the compositeness scale $|\phi|$ squared or T^2 are given as

$$\frac{\partial_{|\phi|}^2 V_E}{|\phi|^2} = 12 \lambda_E^3, \quad \frac{\partial_{|\phi|}^2 V_E}{T^2} = 48 \pi^2, \quad (66)$$

where $\lambda_E \equiv \frac{2\pi T}{\Lambda_E}$. We will show in Sec. 2.3.4 that $\lambda_E \geq 13.867$ in the electric phase. Thus both ratios in Eq. (66) are much larger than unity: The field ϕ is quantum mechanically and statistically inert. It represents a *background* for the dynamics of the topologically trivial sector after spatial coarse-graining. As a consequence, our assumption that only noninteracting calorons of trivial holonomy contribute to the

32 *Ralf Hofmann*

average in Eq. (43) is consistent.

SU(3) case:

For SU(3) we write three sets of SU(2) generators as

$$\lambda_1 = \begin{pmatrix} 0 & 1 & 0 \\ 1 & 0 & 0 \\ 0 & 0 & 0 \end{pmatrix}, \quad \lambda_2 = \begin{pmatrix} 0 & -i & 0 \\ i & 0 & 0 \\ 0 & 0 & 0 \end{pmatrix}, \quad \lambda_3 = \begin{pmatrix} 1 & 0 & 0 \\ 0 & -1 & 0 \\ 0 & 0 & 0 \end{pmatrix}, \quad (67)$$

and

$$\bar{\lambda}_1 = \begin{pmatrix} 0 & 0 & 1 \\ 0 & 0 & 0 \\ 1 & 0 & 0 \end{pmatrix}, \quad \bar{\lambda}_2 = \begin{pmatrix} 0 & 0 & -i \\ 0 & 0 & 0 \\ i & 0 & 0 \end{pmatrix}, \quad \bar{\lambda}_3 = \begin{pmatrix} 1 & 0 & 0 \\ 0 & 0 & 0 \\ 0 & 0 & -1 \end{pmatrix}, \quad (68)$$

and

$$\tilde{\lambda}_1 = \begin{pmatrix} 0 & 0 & 0 \\ 0 & 0 & 1 \\ 0 & 1 & 0 \end{pmatrix}, \quad \tilde{\lambda}_2 = \begin{pmatrix} 0 & 0 & 0 \\ 0 & 0 & -i \\ 0 & i & 0 \end{pmatrix}, \quad \tilde{\lambda}_3 = \begin{pmatrix} 0 & 0 & 0 \\ 0 & 1 & 0 \\ 0 & 0 & -1 \end{pmatrix}. \quad (69)$$

One generator is dependent. This just reflects the fact that the group manifold of SU(3) locally is not $S_3 \times S_3 \times S_3$ but $S_3 \times S_5$ ^{59,60}. A set of independent generators is obtained by replacing the two matrices $\bar{\lambda}_3$ and $\tilde{\lambda}_3$ by the single matrix

$$\lambda_8 = \frac{1}{\sqrt{3}} (\bar{\lambda}_3 + \tilde{\lambda}_3) = \frac{1}{\sqrt{3}} \begin{pmatrix} 1 & 0 & 0 \\ 0 & 1 & 0 \\ 0 & 0 & -2 \end{pmatrix} \quad (70)$$

and by keeping the other matrices. The result is the familiar set of Gell-Mann matrices generating the group SU(3).

For the case of SU(3) the field ϕ may wind in each of the above SU(2) algebras. Except for the points $\tau = 0, \frac{\beta}{3}, \frac{2\beta}{3}$, where it jumps into a new algebra, a solution to the BPS equation

$$\partial_\tau \phi = \pm i \Lambda_E^3 \begin{cases} \lambda_3 \frac{\phi}{|\phi|^2}, & (0 \leq \tau < \frac{\beta}{3}) \\ \bar{\lambda}_3 \frac{\phi}{|\phi|^2}, & (\frac{\beta}{3} \leq \tau < \frac{2\beta}{3}) \\ \tilde{\lambda}_3 \frac{\phi}{|\phi|^2}, & (\frac{2\beta}{3} \leq \tau < \beta) \end{cases} \quad (71)$$

is given as

$$\phi(\tau) = \sqrt{\frac{\Lambda_E^3}{2\pi T}} \begin{cases} \lambda_1 \exp\left(\mp \frac{2\pi i}{\beta} \lambda_3 \tau\right), & (0 \leq \tau < \frac{\beta}{3}) \\ \bar{\lambda}_1 \exp\left(\mp \frac{2\pi i}{\beta} \bar{\lambda}_3 \left(\tau - \frac{\beta}{3}\right)\right), & (\frac{\beta}{3} \leq \tau < \frac{2\beta}{3}) \\ \tilde{\lambda}_1 \exp\left(\mp \frac{2\pi i}{\beta} \tilde{\lambda}_3 \left(\tau - \frac{2\beta}{3}\right)\right), & (\frac{2\beta}{3} \leq \tau < \beta). \end{cases} \quad (72)$$

Notice that the potential $V_E = 2 \frac{\Lambda_E^6}{|\phi|^2}$ is the same on the configuration $\phi(\tau)$ in Eq. (72) as for the SU(2) case and that by the same calculation one shows its quantum mechanical and statistical inertness.

2.2. A macroscopic ground state

The action Eq. (65) governs the dynamics of ϕ . We have not yet included caloron interactions, mediated by the topologically trivial sector, which change the holonomy of calorons and induce interactions between their (BPS monopole) constituents. This is the objective of the present section.

2.2.1. Pure-gauge configuration

The action Eq. (65) can be extended to include topologically trivial configurations a_μ . This is accomplished by a minimal coupling $\partial_\tau\phi \rightarrow \partial_\mu\phi + ie[\phi, a_\mu] \equiv D_\mu\phi$ and by adding a kinetic term for these configurations. Here e denotes the *effective* gauge coupling. The total Yang-Mills action S , governing the electric phase, can thus be rewritten as

$$S = \text{tr} \int_0^\beta d\tau \int d^3x \left(\frac{1}{2} G_{\mu\nu} G_{\mu\nu} + D_\mu\phi D_\mu\phi + \Lambda_E^6 \phi^{-2} \right), \quad (73)$$

where $G_{\mu\nu} = G_{\mu\nu}^a \frac{\lambda^a}{2}$ and $G_{\mu\nu}^a = \partial_\mu a_\nu^a - \partial_\nu a_\mu^a + e f^{abc} a_\mu^b a_\nu^c$. The classical equation of motion for a_μ , derived from the action (73), reads

$$D_\mu G_{\mu\nu} = ie[\phi, D_\nu\phi] \quad (74)$$

There is a pure-gauge solution a_μ^{bg} to Eq. (74) with $D_\nu\phi = 0$. Thus the total action density of the ground state (ϕ, a_μ^{bg}) is the potential $V_E = 4\pi \Lambda_E^3 T$, corresponding to an energy-momentum tensor $\theta_{\mu\nu} = V_E \delta_{\mu\nu}$ or $P^{gs} = -\rho^{gs} = -4\pi \Lambda_E^3 T$ (P^{gs}, ρ^{gs} the ground-state pressure and energy density, respectively): The so-far hidden scale Λ_E becomes (gravitationally) measurable by coarse-grained interactions between calorons.

SU(2) case:

In the background

$$\phi(\tau) = \sqrt{\frac{\Lambda_E^3}{2\pi T}} \lambda_1 \exp\left(\mp \frac{2\pi i}{\beta} \lambda_3 \tau\right) \quad (75)$$

we have

$$a_\mu^{bg} = \pm \delta_{\mu 4} \frac{\pi}{e\beta} \lambda_3. \quad (76)$$

SU(3) case:

In the background ϕ of Eq. (72) the pure-gauge solution to Eq. (74) with $D_\nu\phi = 0$ reads

$$a_\mu^{bg} = \pm \delta_{\mu 4} \frac{\pi}{e\beta} \begin{cases} \lambda_3, & (0 \leq \tau < \frac{\beta}{3}) \\ \bar{\lambda}_3, & (\frac{\beta}{3} \leq \tau < \frac{2\beta}{3}) \\ \tilde{\lambda}_3, & (\frac{2\beta}{3} \leq \tau < \beta). \end{cases} \quad (77)$$

34 *Ralf Hofmann*

2.2.2. Polyakov loop and rotation to unitary gauge

Here we would like to investigate whether the ground state, described by (ϕ, a_μ^{bg}) , is degenerate with respect to the global electric Z_2 (SU(2)) or Z_3 (SU(3)) symmetry under which the Polyakov loop \mathbf{P} transforms as $\mathbf{P} \rightarrow Z\mathbf{P}$ where $Z \in Z_2$ (SU(2)) or $Z \in Z_3$ (SU(3)). We will refer to the gauge, where ϕ 's phase is τ dependent as in Eq. (62) or in Eq. (72), as winding gauge. (Microscopically, this is the singular gauge for an instanton in which the Harrington-Shepard solution is constructed.)

SU(2) case:

Evaluating the Polyakov loop on the configuration a_μ^{bg} of Eq. (76), we have

$$\mathbf{P}[a_\mu^{bg}] = \exp[\pm i\pi\lambda_3] = -\mathbb{1}_2. \quad (78)$$

We are searching a gauge transformation $\tilde{\Omega} \in \text{SU}(2)$ to the unitary gauge $\phi = |\phi|\lambda_3$ and $a_\mu^{bg} = 0$. A periodic but not differentiable gauge transformation $\tilde{\Omega}$ doing this can be obtained from a nonperiodic but smooth gauge transformation Ω by multiplication with a local center transformation Z and by multiplication with a global gauge transformation Ω_{gl} :

$$\tilde{\Omega} = \Omega(\tau)Z(\tau)\Omega_{gl}, \quad (79)$$

where $\Omega(\tau) \equiv \exp[\mp i\pi\frac{\tau}{\beta}\lambda_3]$, $Z(\tau) = \left(2\Theta(\tau - \frac{\beta}{2}) - 1\right)\mathbb{1}_2$, and $\Omega_{gl} = \exp[-i\frac{\pi}{4}\lambda_2]$. Θ denotes the Heavyside step function:

$$\Theta(x) = \begin{cases} 0, & (x < 0), \\ \frac{1}{2}, & (x = 0), \\ 1, & (x > 0). \end{cases} \quad (80)$$

Applying $\tilde{\Omega}$ to $a_\mu = a_\mu^{bg} + \delta a_\mu$, where δa_μ is a *periodic* fluctuation in winding gauge, we have

$$\begin{aligned} a_\mu &\rightarrow \tilde{\Omega}^\dagger(a_\mu^{bg} + \delta a_\mu)\tilde{\Omega} + \frac{i}{e}\partial_\mu\tilde{\Omega}^\dagger\tilde{\Omega} \\ &= \Omega_{gl}^\dagger\left(\Omega^\dagger(a_\mu^{bg} + \delta a_\mu)\Omega + \frac{i}{e}\left((\partial_\mu\Omega^\dagger)\Omega + (\partial_\mu Z)Z\right)\right)\Omega_{gl} \\ &= \Omega_{gl}^\dagger\left(\Omega^\dagger\delta a_\mu\Omega + \frac{2i}{e}\delta\left(\tau - \frac{\beta}{2}\right)Z\right)\Omega_{gl} \\ &= (\Omega\Omega_{gl})^\dagger\delta a_\mu\Omega\Omega_{gl}. \end{aligned} \quad (81)$$

Since $\Omega\Omega_{gl}(0) = -\Omega\Omega_{gl}(\beta)$ we conclude that if the fluctuation δa_μ is periodic in winding gauge then it is also periodic in unitary gauge. It thus is irrelevant whether we integrate out the fluctuations δa_μ in winding or unitary gauge in a loop expansion of thermodynamical quantities: Hosotani's mechanism⁴⁷ does not take place. What changes though under the gauge transformation $\tilde{\Omega}$ is the Polyakov loop evaluated on the background configuration a_μ^{bg} :

$$\mathbf{P}[a_\mu^{bg}] = -\mathbb{1}_2 \rightarrow \mathbf{P}[a_\mu^{bg} = 0] = \mathbb{1}_2. \quad (82)$$

We conclude that the theory has two equivalent ground states and that the global electric Z_2 symmetry is dynamically broken. Thus we have shown that the electric phase is *deconfining*.

SU(3) case:

Let us now compute the Polyakov loop on the configuration a_μ^{bg} of Eq. (77). We have

$$\begin{aligned} \mathbf{P}[a_\mu^{bg}] &= \exp\left[\pm i\frac{\pi}{3}\tilde{\lambda}_3\right] \exp\left[\pm i\frac{\pi}{3}\bar{\lambda}_3\right] \exp\left[\pm i\frac{\pi}{3}\lambda_3\right] \\ &= \exp\left[i\frac{\pi}{3}(\pm\tilde{\lambda}_3 \pm \bar{\lambda}_3 \pm \lambda_3)\right]. \end{aligned} \quad (83)$$

The + or – sign can be chosen independently for each SU(2) algebra. The following combinations are possible:

$$\begin{aligned} \pm\left(+\tilde{\lambda}_3 + \bar{\lambda}_3 + \lambda_3\right) &= \pm 2\bar{\lambda}_3, \\ \pm\left(-\tilde{\lambda}_3 - \bar{\lambda}_3 + \lambda_3\right) &= \pm 2\tilde{\lambda}_3, \\ \pm\left(-\tilde{\lambda}_3 + \bar{\lambda}_3 + \lambda_3\right) &= \pm 2\lambda_3, \\ \pm\left(+\tilde{\lambda}_3 - \bar{\lambda}_3 + \lambda_3\right) &= 0. \end{aligned} \quad (84)$$

The corresponding values of the Polyakov loop are

$$\begin{aligned} \mathbf{P}_1^\pm &= \begin{pmatrix} \exp[\pm\frac{2\pi i}{3}] & 0 & 0 \\ 0 & 1 & 0 \\ 0 & 0 & \exp[\mp\frac{2\pi i}{3}] \end{pmatrix}, & \mathbf{P}_2^\pm &= \begin{pmatrix} 1 & 0 & 0 \\ 0 & \exp[\pm\frac{2\pi i}{3}] & 0 \\ 0 & 0 & \exp[\mp\frac{2\pi i}{3}] \end{pmatrix}, \\ \mathbf{P}_3^\pm &= \begin{pmatrix} \exp[\pm\frac{2\pi i}{3}] & 0 & 0 \\ 0 & \exp[\mp\frac{2\pi i}{3}] & 0 \\ 0 & 0 & 1 \end{pmatrix}, & \mathbf{P}_4 &= \mathbb{1}_3. \end{aligned} \quad (85)$$

\mathbf{P}_4 is a trivial representation of the center group. The set $\mathbf{P}_1^\pm, \mathbf{P}_2^\pm, \mathbf{P}_3^\pm$ closes under multiplication with the center elements $\mathbf{P} = \exp[\pm\frac{2\pi i}{3}]\mathbb{1}_3, \mathbb{1}_3$. It is a six dimensional, reducible representation of the center group. The two three dimensional irreducible representations, which collapse on one another, are spanned by

$$\frac{1}{3}\mathbb{1}_3(\mathbf{P}_1^\pm + \mathbf{P}_2^\mp + \mathbf{P}_3^\pm), \quad \frac{1}{3}\exp[\mp\frac{2\pi i}{3}]\mathbb{1}_3(\mathbf{P}_1^\pm + \mathbf{P}_2^\mp + \mathbf{P}_3^\pm). \quad (86)$$

We conclude that the ground state has a Z_3 degeneracy: The electric Z_3 symmetry is dynamically broken and thus we have discussed a *deconfining* phase.

What about a gauge rotation to unitary gauge $a_\mu^{bg} = 0$ and $\phi = |\phi|\lambda_3$ or $\phi = |\phi|\bar{\lambda}_3$ or $\phi = |\phi|\tilde{\lambda}_3$? Such a gauge transformation $\tilde{\Omega}$ is given as

$$\tilde{\Omega} = \begin{cases} \exp[\mp i\frac{\pi}{\beta}\tau\lambda_3] \exp[-i\frac{\pi}{4}\lambda_2], & (0 \leq \tau < \frac{\beta}{3}) \\ \exp[\mp i\pi\frac{\pi}{\beta}(\tau - \frac{\beta}{3})\bar{\lambda}_3] \exp[-i\frac{\pi}{4}\bar{\lambda}_2], & (\frac{\beta}{3} \leq \tau < \frac{2\beta}{3}) \\ \exp[\mp i\frac{\pi}{\beta}(\tau - \frac{2\beta}{3})\tilde{\lambda}_3] \exp[-i\frac{\pi}{4}\tilde{\lambda}_2], & (\frac{2\beta}{3} \leq \tau < \beta). \end{cases} \quad (87)$$

36 *Ralf Hofmann*

By construction $\tilde{\Omega}$ is periodic, at $\tau = \beta$ it jumps back to its value at $\tau = 0$, and thus a fluctuation δa_μ , which is periodic in winding gauge, is also periodic in unitary gauge.

A comment concerning $SU(N)$ theories with $N \geq 4$ is in order. We only discuss the case when N is even. Since at any τ the maximal number of *independent* $SU(2)$ subgroups contributing with calorons of topological charge one to the macroscopic field ϕ is $N/2$ the dynamical gauge-symmetry breaking is not as maximal as it is for $SU(2)$ and $SU(3)$. For example, $SU(4)$ breaks only down to $SU(2)^2 \times U(1)$. The question is whether there is a single critical temperature $T_{c,E}$ where the unbroken nonabelian subgroups get broken to $U(1)$ factors by the condensation of color magnetic monopoles into macroscopic adjoint Higgs fields and pure gauges, and where the abelian magnetic monopoles with respect to the remaining $U(1)$ factors condense as soon as they are created, or whether this is a stepwise process. The lattice seems to favor the former situation⁸³ which, however, does not appear natural to the author.

2.3. Excitations

Now that the derivation of a macroscopic ground state for the electric phase is completed we are in a position to discuss the properties of its on-shell excitations and the role of residual quantum fluctuations. The temperature dependent mass is a measure for the strength of coupling between gauge modes and the nontrivial ground state. The evolution of this coupling with temperature is a manifestation of the thermodynamical selfconsistency of the separation into topological configurations and gauge modes with trivial topology. As we shall see, this evolution represents a decoupling between high and low temperature physics and, for temperatures sufficiently above the critical temperature $T_{c,E}$, indicates the conservation of magnetic charge associated with the isolated and screened BPS monopoles that are liberated by the dissociation of calorons with a large holonomy.

2.3.1. Mass spectrum of thermal quasiparticles

We first discuss some general aspects of the mass spectrum and then specialize to the cases $SU(2)$ and $SU(3)$. We refer to gauge modes which acquire a quasiparticle mass on tree level by the adjoint Higgs mechanism as tree-level heavy (TLH) and to those which remain massless as tree-level massless (TLM).

In unitary gauge the mass spectrum calculates as

$$m_a^2 = -2e^2 \text{tr} [\phi, t^a][\phi, t^a], \quad (88)$$

where t^a are the group generators normalized as $\text{tr} t^a t^b = \frac{1}{2} \delta^{ab}$. For $SU(N)$ off-diagonal generators can be chosen as

$$\begin{aligned} t_{rs}^{IJ} &= 1/2 (\delta_r^I \delta_s^J + \delta_s^I \delta_r^J), & \mathbf{t}_{rs}^{IJ} &= -i/2 (\delta_r^I \delta_s^J - \delta_s^I \delta_r^J), \\ (I &= 1, \dots, N; J > I; r, s = 1, \dots, N). \end{aligned} \quad (89)$$

This yields

$$m_{IJ}^2 = \mathbf{m}_{IJ}^2 = e^2(\phi_I - \phi_J)^2 \quad (90)$$

where ϕ_I, ϕ_J denote the diagonal elements of ϕ in unitary gauge.

SU(2) case:

In this case ϕ breaks the gauge symmetry dynamically down to U(1). Thus we have one TLM mode and two TLH modes whose degenerate masses are, according to Eqs. (75) and (90), given as

$$m_{12}^2 = \mathbf{m}_{12}^2 = 4e^2|\phi|^2 = 4e^2\frac{\Lambda_E^3}{2\pi T}. \quad (91)$$

SU(3) case:

Here ϕ is diagonal in either one of the three SU(2) subgroups, and the gauge symmetry is dynamically broken to U(1)². We have

$$\begin{aligned} m_{12}^2 &= \mathbf{m}_{12}^2 = 4e^2\frac{\Lambda_E^3}{2\pi T}, \\ m_{13}^2 &= \mathbf{m}_{13}^2 = m_{23}^2 = \mathbf{m}_{23}^2 = e^2\frac{\Lambda_E^3}{2\pi T}, \quad \text{or} \\ m_{13}^2 &= \mathbf{m}_{13}^2 = 4e^2\frac{\Lambda_E^3}{2\pi T}, \\ m_{12}^2 &= \mathbf{m}_{12}^2 = m_{23}^2 = \mathbf{m}_{23}^2 = e^2\frac{\Lambda_E^3}{2\pi T}, \quad \text{or} \\ m_{23}^2 &= \mathbf{m}_{23}^2 = 4e^2\frac{\Lambda_E^3}{2\pi T}, \\ m_{12}^2 &= \mathbf{m}_{12}^2 = m_{13}^2 = \mathbf{m}_{13}^2 = e^2\frac{\Lambda_E^3}{2\pi T}. \end{aligned} \quad (92)$$

For T sufficiently far above $T_{c,E}$ we will see in Sec. 2.3.4 that e is practically independent of T . As a consequence, the TLH masses die off according to the power law in Eqs. (91) and (92). Moreover, the energy density and the pressure of the ground state are only linear in T , $P^{gs} = -\rho^{gs} = -4\pi\Lambda_E^3 T$. We will show in Sec. 2.4 that the one-loop result for thermodynamical quantities is reliable on the 0.1% level throughout the electric phase. Thus the Stefan-Boltzmann limit $P = \frac{\pi^2}{15}T^4$ and $\rho = \frac{\pi^2}{5}T^4$ (SU(2)) or $P = \frac{8\pi^2}{45}T^4$ and $\rho = \frac{8\pi^2}{15}T^4$ (SU(3)) is reached very quickly apart from a factor arising from the extra polarizations of TLH modes. This result is in agreement with early lattice simulations using the differential method.

2.3.2. Thermodynamical selfconsistency

In this section we provide a conceptual basis for the notion of thermodynamical selfconsistency.

As a result of the existence of a nontrivial macroscopic ground state, which is built of interacting calorons of topological charge-one, the ground-state physics and the properties of the excitations are temperature dependent. We have discussed in

Sec. 2.2 how the temperature dependence of the ground-state pressure and its energy density arises due to caloron interactions. These interactions are encoded in a pure-gauge configuration on the macroscopic level. For topologically trivial fluctuations δa_μ the two following properties are induced by the ground-state physics. First, in unitary gauge off-Cartan fluctuations are massive in a temperature dependent way, compare with Eqs. (91) and (92). Notice that the quasiparticle masses are related to the ground-state pressure by their respective dependences on temperature if the temperature dependence of the effective gauge coupling e is known. Second, there are constraints for the maximal off-shellness of the fluctuations δa_μ arising from the compositeness of the ground-state field ϕ . Namely, a fluctuation δa_μ , which was generated in a thermal equilibrium situation by the ground state, is not capable of destroying this ground state: In a physical gauge vacuum fluctuations or scattering processes with momenta or momentum transfers larger than the (temperature dependent) scale $|\phi|$ are forbidden.

Thermodynamical quantities such as the pressure, the energy density, or the entropy density are interrelated by Legendre transformations. These transformations can be derived from the partition function of the fundamental theory where the temperature dependence only occurs in an explicit way through the Boltzmann weight. A reformulation of the theory into a spatially coarse-grained Lagrangian, where certain parameters are temperature dependent (implicit temperature dependences) by virtue of a separation into a ground state and (very weakly interacting) excitations, see Eq. (73), must not alter the Legendre transformations between thermodynamical quantities. For this to be true in the effective theory one needs to impose that in each transformation law the total derivatives with respect to temperature involves the explicit temperature dependences only. That is, derivatives with respect to implicit temperature dependences ought to cancel in a given Legendre transformation.

A particular and essential Legendre transformation maps the total pressure onto the total energy density as

$$\rho = T \frac{dP}{dT} - P. \quad (93)$$

If the effective theory has temperature dependent quasiparticle fluctuations of mass $m_a = c_a m$, where c_a are dimensionless constants, and a ground-state pressure P^{gs} , which can be regarded a function of m , then the condition of thermodynamical selfconsistency is expressed as ⁵¹

$$\partial_m P = 0. \quad (94)$$

Eq. (94) assures that in Eq. (93) only derivatives with respect to the explicit temperature dependence of P contribute since $\frac{dP}{dT} = \partial_T P + \partial_m P \frac{dm}{dT}$. In $\partial_m P = 0$ the derivative of the pressure contribution arising from fluctuations cancels against that arising from the ground state. Eq. (94) governs the temperature evolution of the effective coupling e at any loop order that P is expanded in.

The higher the loop order the more complicated the implementation of Eq. (94). In Sec. 2.3.4 we perform an analysis on the one-loop level (noninteracting quasipar-

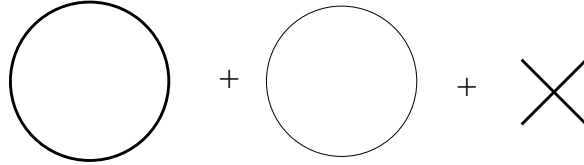


Fig. 9. Diagrams contributing to the pressure when radiative corrections are ignored. A thick line corresponds to TLH modes and a thin one to TLM modes. The cross depicts the ground-state contribution that arises from interacting calorons.

ticles) which is more than sufficient for many practical purposes. A discussion of Eq. (94) on the two-loop level is given in Sec. 2.4.2.

2.3.3. Compositeness constraint and pressure at one loop

We work in a physical gauge where TLM modes are transverse (two polarizations, Coulomb gauge with respect to the unbroken gauge group), and where TLH modes have three polarizations and do not interact with the pure-gauge configuration of the ground state (unitary gauge), for details see Sec. 2.4. This is a physical gauge fixing which needs no introduction of additional fields since the Coulomb ghosts decouple from the dynamics.

On the one-loop level, see Fig. 9, there are no interactions between the fluctuations δa_μ . The only relevant compositeness constraint, related to the maximal off-shellness of a quantum fluctuation created by the ground state, thus is

$$\begin{aligned} |p^2 - m_a^2| &\leq |\phi|^2 && \text{(Minkowskian signature)} \\ p^2 + m_a^2 &\leq |\phi|^2 && \text{(Euclidean signature)}. \end{aligned} \quad (95)$$

SU(2) case:

Before we discuss the thermal contribution to the one-loop pressure let us investigate what the constraints (95) imply for the one-loop quantum correction $-\Delta V_E$. Setting $m_a \equiv 0$ in (95) and considering two polarizations for TLM and three polarizations for TLH modes, an upper bound on $|\Delta V_E|$ can be obtained as

$$|\Delta V_E| < \frac{1}{\pi^2} \int_0^{|\phi|} dp p^3 \log \left(\frac{p}{|\phi|} \right) = \frac{|\phi|^4}{16\pi^2}. \quad (96)$$

Thus we have

$$\left| \frac{\Delta V_E}{V_E} \right| < \frac{1}{32\pi^2} \left(\frac{|\phi|}{\Lambda_E} \right)^6 = \frac{\lambda_E^{-3}}{32\pi^2}. \quad (97)$$

Since $\lambda_E > 13.867$ when omitting ΔV_E in the one-loop evolution of e , see Sec. 2.3.4, this omission is justified: One-loop quantum corrections to the pressure are suppressed as compared to the tree-level result by a factor less than 2×10^{-6} .

40 *Ralf Hofmann*

Omitting the tiny quantum part, the one-loop expression for the pressure, including the ground-state contribution, reads:

$$P(\lambda_E) = -\Lambda_E^4 \left\{ \frac{2\lambda_E^4}{(2\pi)^6} [2\bar{P}(0) + 6\bar{P}(2a)] + 2\lambda_E \right\} \quad (98)$$

where $\lambda_E \equiv \frac{2\pi T}{\Lambda_E}$ and

$$a \equiv \frac{m}{2T} = e \frac{|\phi|}{T} = e \sqrt{\frac{\Lambda_E^3}{2\pi T^3}} = 2\pi e \lambda_E^{-3/2}. \quad (99)$$

The (negative) function $\bar{P}(a)$ is defined as

$$\bar{P}(a) \equiv \int_0^\infty dx x^2 \log[1 - \exp(-\sqrt{x^2 + a^2})]. \quad (100)$$

SU(3) case:

Here a similar estimate for the quantum contribution to the one-loop pressure holds as in Eq. (96), and thus, again, we only have to consider the thermal part. It reads

$$P(\lambda_E) = -\Lambda_E^4 \left\{ \frac{2\lambda_E^4}{(2\pi)^6} [4\bar{P}(0) + 3(4\bar{P}(a) + 2\bar{P}(2a))] + 2\lambda_E \right\} \quad (101)$$

with the same definitions as in the SU(2) case.

2.3.4. One-loop evolution of effective gauge coupling

Let us now implement the condition (94). We have

$$\partial_m P = 0 \quad \Leftrightarrow \quad \partial_{(aT)} P = 0. \quad (102)$$

SU(2) case:

Substituting Eq. (98) into Eq. (102) yields the following evolution equation

$$\partial_a \lambda_E = -\frac{24 \lambda_E^4 a}{(2\pi)^6} \frac{D(2a)}{1 + \frac{24 \lambda_E^3 a^2}{(2\pi)^6} D(2a)}, \quad (103)$$

where the function $D(a)$, see Fig. 10, is defined as

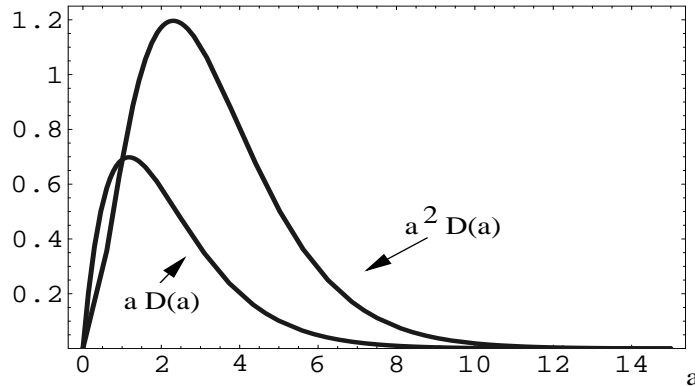
$$D(a) \equiv \int_0^\infty dx \frac{x^2}{\sqrt{x^2 + a^2}} \frac{1}{\exp(\sqrt{x^2 + a^2}) - 1}. \quad (104)$$

SU(3) case:

The evolution equation is obtained by substituting Eq. (101) into Eq. (102):

$$\partial_a \lambda_E = -\frac{12 \lambda_E^4 a}{(2\pi)^6} \frac{D(a) + 2 D(2a)}{1 + \frac{12 \lambda_E^3 a^2}{(2\pi)^6} (D(a) + 2 D(2a))}. \quad (105)$$

Each of the Eqs. (103) and (105) has two fixed points, one at $a = 0$ and one at $a = \infty$, see Fig. 10. The points $\lambda_{P,E} \equiv \lambda_E(a \rightarrow 0)$ and $\lambda_{c,E} \equiv \lambda_E(a = \infty)$ are associated with the highest and the lowest temperatures, respectively, which are attainable in the electric phase.

Fig. 10. The functions $a D(a)$ and $a^2 D(a)$.

Above $\lambda_{P,E}$ the ground state would be trivial (topological fluctuations are absent) and thus no tree-level quasiparticle mass were generated by a caloron induced Higgs mechanism. This re-introduces the problem of the diverging loop expansion as it is encountered in thermal perturbation theory¹⁸ and thus makes the thermalized Yang-Mills theory inconsistent as an interacting field theory. We conclude that $\lambda_{P,E}$ marks the point in temperature where the field theoretic implementation of the gauge principle breaks down. For a physics model, whose gauge group is a product of SU(2) and/or SU(3) groups, we expect that $\lambda_{P,E} \sim \frac{2\pi M_P}{\Lambda_E}$ where $M_P = 1.22 \times 10^{19}$ GeV is the Planck mass.

As we shall see below, the point $\lambda_{c,E}$, where each tree-level quasiparticle mass diverges, marks a transition to a (pre-confining) phase with condensed magnetic monopoles, dynamically broken dual gauge symmetries $U(1)_D$ (SU(2)) and $U(1)_D^2$ (SU(3)), and isolated but instable center-vortex loops: The magnetic phase.

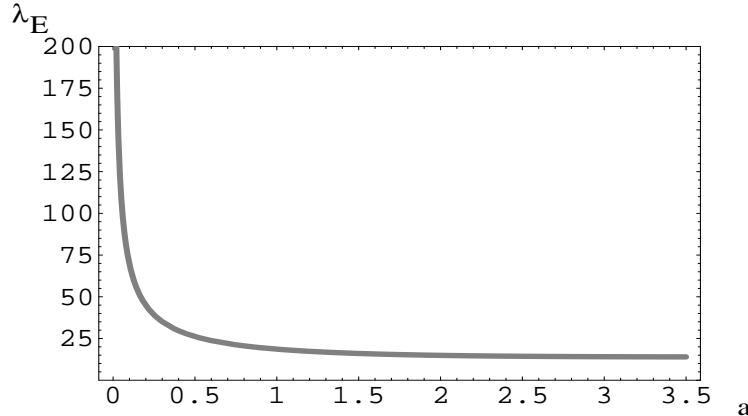
Notice that the right-hand sides of Eqs. (103) and (105) are negative definite. As a consequence, the solutions $\lambda_E(a)$ to Eqs. (103) and (105) can be inverted, and, according to Eq. (99), one obtains the evolution of the effective gauge coupling e with temperature as

$$e(\lambda_E) = \frac{1}{2\pi} a(\lambda_E) \lambda_E^{3/2}. \quad (106)$$

Inspecting the right-hand of Eqs. (103) and (105) in the vicinity of the point $\lambda_{c,E}$, it follows with Eq. (106) that e diverges logarithmically at $\lambda_{c,E}$:

$$e(\lambda_E) \sim -\log(\lambda_E - \lambda_{c,E}). \quad (107)$$

In Fig. 11 a solution to Eq. (103) subject to the initial condition $\lambda_{P,E} \equiv \lambda_E(a=0) = 10^7$ is shown. We have noticed numerically that the low-temperature behavior of $\lambda_E(a)$ is practically independent of the value $\lambda_{P,E}$ as long as $\lambda_{P,E}$ is sufficiently large. Let us show this analytically. For a sufficiently smaller than unity we may expand the right-hand side of Eq. (103) only taking the linear term in a into account.

42 *Ralf Hofmann*Fig. 11. The solution $\lambda_E(a)$ to Eq. (103) subject to the initial condition $\lambda_{P,E} = 10^7$.

In this regime, the inverse of the solution $\lambda_E(a)$ is of the following form

$$a \propto \lambda_E^{-3/2} \sqrt{1 - \left(\frac{\lambda_E}{\lambda_{E,P}}\right)^3}. \quad (108)$$

If λ_E is sufficiently smaller than $\lambda_{P,E}$ then this can be approximated as

$$a \propto \lambda_E^{-3/2}. \quad (109)$$

Thus the dependence in Eq. (109) is an *attractor* of the downward-in-temperature evolution as long as a remains sufficiently small: If we are only interested in the behavior of the theory not too far above $\lambda_{c,E}$ then it is *irrelevant* what the value of $\lambda_{P,E}$ is as long as it is sizably larger than $\lambda_{c,E}$. This result is reminiscent of the ultraviolet-infrared perturbative decoupling property of the renormalizable, underlying theory. Notice that the dependence of a on λ_E in Eq. (109) is canceled by the explicit dependence of e on λ_E in Eq. (106). Thus a plateau value $e(\lambda_E) = \text{const}$ is reached rapidly.

In Fig. 12 the temperature dependence of e for SU(2) and SU(3), subject to the initial condition $\lambda_{P,E} = 10^7$, is shown for $\lambda_E \leq 500$. Before we interpret our results a remark on the interpretation of the effective gauge coupling constant e is in order. Since e determines the strength of the interaction between topologically trivial gauge field fluctuations δa_μ and the *macroscopic* manifestation ϕ of interacting calorons in the ground state e is *not* equal to the perturbatively generated gauge coupling constant \bar{g} of the fundamental Yang-Mills theory. From Fig. 12 we see that the effective gauge coupling e evolves to values larger than unity. Naively, one would conclude that the theory is strongly coupled and that the one-loop evolution of e contradicts itself. This, however, is an incorrect conclusion. Because of compositeness constraints and the infrared regularization provided by TLH masses higher loop orders turn out to be very small as compared to the one-loop result for the pressure, see Sec. 2.4.2.

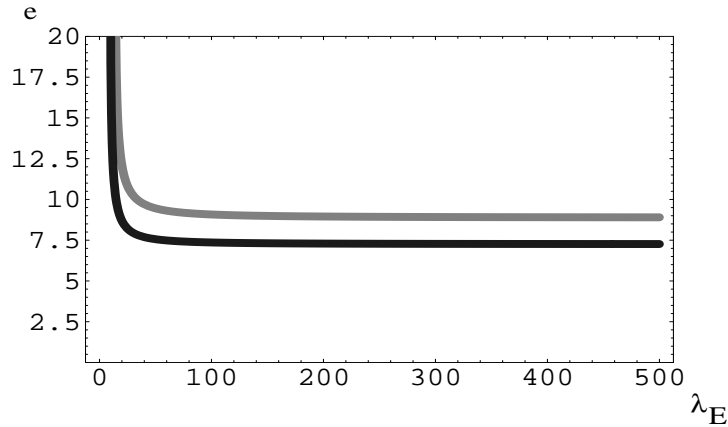


Fig. 12. The temperature evolution of the gauge coupling e in the electric phase for SU(2) (grey line) and SU(3) (black line). The gauge coupling diverges logarithmically, $e \propto -\log(\lambda_E - \lambda_{c,E})$, at $\lambda_{c,E} = 13.867$ (SU(2)) and $\lambda_{c,E} = 9.475$ (SU(3)). The respective plateau values are $e = 8.89$ and $e = 7.26$.

We interpret the fact that the gauge coupling constant e is constant for λ_E sizably larger than $\lambda_{c,E}$ as another indication for the existence of spatially isolated and conserved magnetic charges in the system. These charges are screened by calorons with a small holonomy, and thus e measures the *effective* magnetic charge of a BPS monopole which is given as $g = \frac{4\pi}{e}$. The plateau values for e are $e \sim 8.89$ (SU(2)) and $e \sim 7.26$ (SU(3)). At $\lambda_{c,E} = 13.867$ (SU(2)) or $\lambda_{c,E} = 9.475$ (SU(3)) both the core size $\sim \frac{\beta}{e}$ of a screened BPS monopole and its mass $\sim \frac{4\pi}{e} u_{\max} = \frac{4\pi^2}{e\beta}$ *vanish*, see Sec. 3.1.1. (Notice that monopoles are very massive at high temperatures.) Thus monopoles are not well separated anymore at $\lambda_{c,E}$ because it is extremely easy to move them. Local magnetic charge conservation is violated since in a typical volume β^3 the number of monopoles no longer is conserved. The increasing mobility of monopoles and the increasing violation of local charge conservation can be seen in the evolution of e for $\lambda_E \searrow \lambda_{c,E}$ where an increase of e as compared to the plateau value is observed, see Fig. 12 and Eq. (107).

For $\lambda_E \searrow \lambda_{c,E}$ TLH modes decouple (their masses diverge) and thus the (small) interaction between TLM modes dies off. This is the macroscopic manifestation of the fact that the magnetic charge of (dynamical and screened) BPS monopoles vanishes at $\lambda_{c,E}$ making them unavailable as ‘scattering centers’ for TLM modes. This is, indeed, seen as a result of a two-loop calculation of the SU(2) pressure in the electric phase^{48,49}, see Sec. 2.4.2.

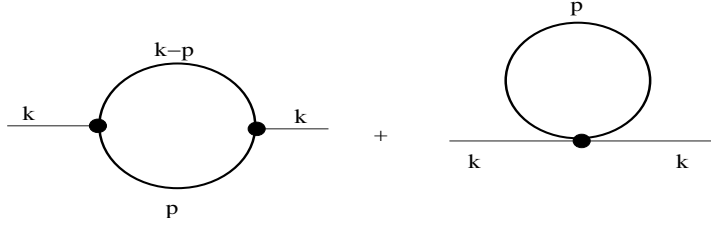


Fig. 13. Diagrams for the TLM polarization tensor at one loop. Thick and thin lines denote TLH and TLM propagation, respectively.

2.4. Radiative corrections for $SU(2)$

2.4.1. Electric screening mass for TLM modes

In this section we investigate for $SU(2)$ the one-loop contribution to the electric screening mass for the TLM mode.

In unitary gauge the analytically continued propagator of a free TLH mode $D_{\mu\nu,ab}^{\text{TLH},IJ,0}(k, T)$ is that of a massive vector boson⁶²

$$D_{\mu\nu,ab}^{\text{TLH},IJ,0}(k, T) = -\delta_{ab} \left(g_{\mu\nu} - \frac{k_\mu k_\nu}{4(e|\phi|)^2} \right) \times \left[\frac{i}{k^2 - 4(e|\phi|)^2} + 2\pi\delta(k^2 - 4(e|\phi|)^2)n_B(|k_0|/T) \right], \quad (110)$$

where $n_B(x) = \frac{1}{e^x - 1}$ is the Bose distribution and $k_0 = \pm\sqrt{\vec{k}^2 + 4(e|\phi|)^2}$. The electric (or Debye) screening mass m_D is related¹⁸ to the 00-component of the polarization tensor $\Pi_{\mu\nu}(k)$ in the limit $k_0 = 0, \vec{k} \rightarrow 0$. $\Pi_{\mu\nu}(k)$ is calculated according to the diagrams in Fig. 13. The vertices for the interactions of TLH and TLM modes are the usual ones. In addition to the compositeness constraint (95) we have constraints associated with the maximally allowed momentum transfer in a four vertex. Let the three independent momenta be p_1, p_2 , and p_3 . Then we have⁵⁰:

$$\begin{aligned} |p_1 + p_2|^2 &\leq |\phi|^2, & (s \text{ channel}) & & |(p_3 - p_1)^2| &\leq |\phi|^2, & (t \text{ channel}) \\ |p_2 - p_3|^2 &\leq |\phi|^2, & (u \text{ channel}). & & & & \end{aligned} \quad (111)$$

One can easily see that these constraints together with the constraint (95) do not allow for any (neither from quantum nor from thermal propagation of the intermediate states) contribution of the local (or tadpole) diagrams in Fig. 13 in the limit $k_0 = 0, \vec{k} \rightarrow 0$ and for $e_{\text{plateau}} = 8.89$ ($SU(2)$). A calculation of the nonlocal diagram reveals that only thermal intermediate states contribute in the limit $k_0 = 0$ and for $e = 13.867$. Notice that in perturbation theory the nonlocal diagram does not

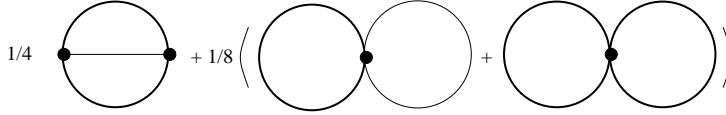


Fig. 14. Nonvanishing two-loop diagrams contributing to the pressure. Thick lines denote propagators of TLH modes, thin lines those of TLM modes.

contribute to $\Pi_{00}(k_0 = 0, \vec{k})$. The result for $\Pi_{00}(k_0 = 0, \vec{k})$ reads^e

$$\begin{aligned} \Pi_{00}(k_0 = 0, \vec{k}) = & \frac{ie^2}{2\pi} \left\{ \frac{1}{2} \left(\frac{12}{|\vec{k}|} + 4 \frac{|\vec{k}|}{4(e|\phi|^2)} + \frac{|\vec{k}|^3}{(4(e|\phi|^2)^2)} \right) \times \right. \\ & \int_{\frac{|\vec{k}|}{2}}^{\infty} d|\vec{p}| |\vec{p}| \sqrt{|\vec{p}|^2 + 4(e|\phi|^2)^2} \left[n_B \left(\frac{\sqrt{|\vec{p}|^2 + 4(e|\phi|^2)^2}}{T} \right) \right]^2 - \\ & \left. \left(4|\vec{k}| + \frac{|\vec{k}|^3}{4(e|\phi|^2)^2} \right) \int_{\frac{|\vec{k}|}{2}}^{\infty} d|\vec{p}| \frac{|\vec{p}|}{\sqrt{|\vec{p}|^2 + 4(e|\phi|^2)^2}} \left[n_B \left(\frac{\sqrt{|\vec{p}|^2 + 4(e|\phi|^2)^2}}{T} \right) \right]^2 \right\}. \end{aligned} \quad (112)$$

Thus $\Pi_{00}(k_0 = 0, \vec{k})$ is purely *imaginary* and *diverges* for $|\vec{k}| \rightarrow 0$: The electric screening mass m_D , which is the positive square root of $\Pi_{00}(k_0 = 0, \vec{k} \rightarrow 0)$, has an infinite and positive real part at *finite* coupling e : Static electric fields of long wavelength are completely screened by calorons. For $e \rightarrow \infty$ the Boltzmann factors in the integrals in Eq. (112) make $\Pi_{00}(k_0 = 0, \vec{k})$ vanish at any momentum \vec{k} .

2.4.2. Two-loop result for the $SU(2)$ pressure

The nonvanishing two-loop diagrams contributing to the $SU(2)$ pressure in the electric phase⁶² are shown in Fig. 14. Because of the strong screening of near-to-static electric modes, compare with Sec. 2.4.1, the TLM propagator in Coulomb gauge can safely be approximated as

$$D_{\mu\nu,ab}^{\text{TLM},0}(k, T) = -\delta_{ab} \left\{ P_{\mu\nu}^T \left(\frac{i}{k^2} + 2\pi\delta(k^2)n_B(|k_0|/T) \right) - i \frac{u_\mu u_\nu}{k^2} \right\} \quad (113)$$

^eThe author would like to thank Ulrich Herbst for performing this calculation.

46 *Ralf Hofmann*

where

$$\begin{aligned} P_{00}^T &= P_{0i}^T = P_{i0}^T = 0, \\ P_{ij}^T &= \delta_{ij} - \frac{k_i k_j}{k^2}, \end{aligned} \quad (114)$$

$k_0 = \pm|\vec{k}|$, and $u_\mu = \delta_{0\mu}$.

The result of a calculation of the diagrams in Fig. 14 was published in 48. We do only outline this (lengthy) calculation here.

The following nomenclature is useful. Each diagram can be split into contributions arising from the vacuum (v), the Coulomb (c) ($\propto u_\mu u_\nu$ in Eq. (113)), and the thermal (t) parts of the involved propagators. Moreover, if a TLH propagator contributes to a given diagram then this situation is abbreviated by H , in the other case by M . With e being larger than the one-loop plateau value $e_{\text{plateau}} = 8.89$ the compositeness constraint in Eq. (95) allows for the five following two-loop radiative corrections to the pressure only:

$$\frac{1}{8}\Delta P_{tt}^{HH}, \quad \frac{1}{8}\Delta P_{tt}^{HM}, \quad \frac{1}{8}\Delta P_{tv}^{HM}, \quad \frac{1}{8}\Delta P_{tc}^{HM}, \quad \frac{1}{4}(\Delta P_{ttv}^{HHM} + \Delta P_{ttc}^{HHM}). \quad (115)$$

The ratio of the two-loop corrections and the one-loop result (excluding the ground-state contribution) is plotted in Fig. 15. For $\frac{1}{8P_{1-loop}}\Delta P_{tv}^{HM}$ the plot represents only an upper bound for the modulus of the correction, all other plots are exact results. The dominating correction $\frac{1}{4P_{1-loop}}\Delta P_{ttv}^{HHM}$ arises from the nonlocal diagram in Fig. 14. It is negative. The dip is microscopically explained by the increasing effect of TLM modes scattering off of decreasingly massive magnetic monopoles close to the phase transition at $\lambda_{c,E} = 13.867$. The effect of this scattering is suppressed for $\lambda_E \gg \lambda_{c,E}$ since then the monopoles are dilute and massive scattering centers. (Recall that their mass is $\propto \frac{T}{e}$ after screening.) Notice, that the presence of massive but dilute scattering centers causes the contribution $\frac{1}{8P_{1-loop}}\Delta P_{tt}^{HM}$ to remain finite but small for asymptotically high temperatures.

A comment concerning thermodynamical selfconsistency on the two-loop level is in order. Recall that on the one-loop level we have obtained an evolution equation from the requirement of thermal selfconsistency $\partial_m P = 0$. This gave a functional relation between temperature and mass which could be inverted for all temperatures in the electric phase. After the relation Eq. (106) between coupling constant e and mass a was exploited we obtained a functional dependence of the effective gauge coupling constant e on temperature. Equivalently, we could have demanded $\partial_e P = 0$ since e is the only variable parameter (apart from the scale Λ_E) of the effective theory in the electric phase. This would *directly* have generated an evolution equation for temperature as a function of e . Because each diagram comes with a prefactor e^2 and due to the compositeness constraints radiative corrections ΔP to the pressure have a separate dependence on a and e ,

$$\Delta P = T^4 \Delta \tilde{P}(e, a, \lambda_E), \quad (116)$$

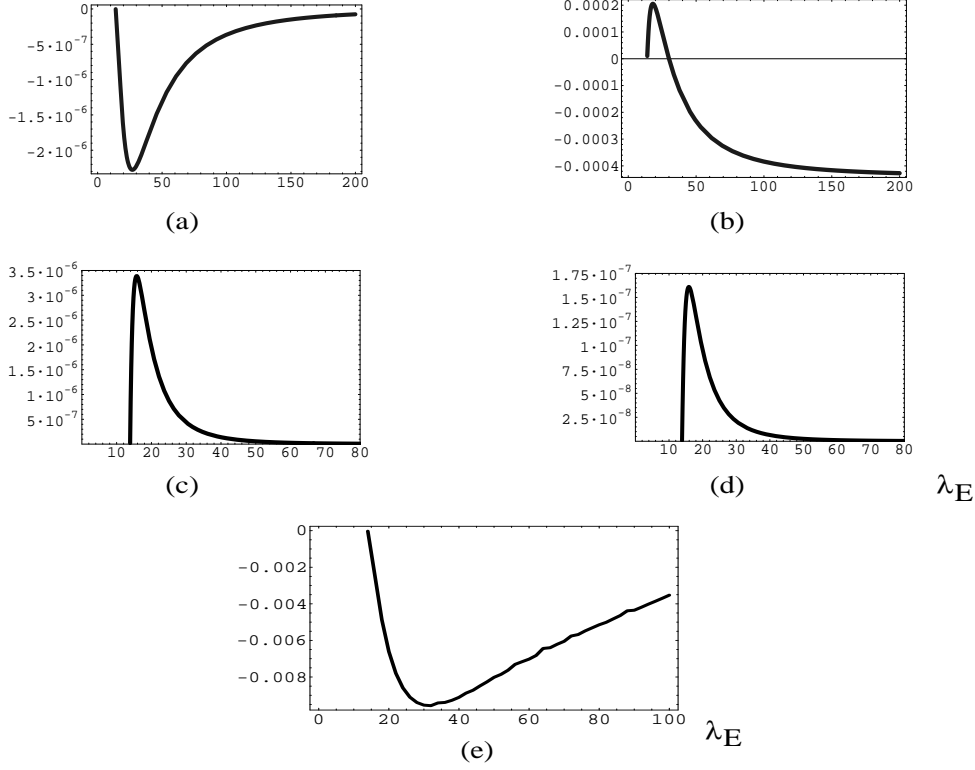


Fig. 15. Ratios (a) $\frac{1}{8P_{1-loop}}\Delta P_{tt}^{HH}$, (b) $\frac{1}{8P_{1-loop}}\Delta P_{tt}^{HM}$, (c) $\frac{1}{8P_{1-loop}}\Delta P_{tv}^{HM}$, (d) $\frac{1}{8P_{1-loop}}\Delta P_{tc}^{HM}$, and (e) $\frac{1}{4P_{1-loop}}(\Delta P_{ttv}^{HHM} + \Delta P_{ttc}^{HHM})$ as functions of temperature.

where $\Delta\tilde{P}$ is a dimensionless function of its dimensionless arguments. To implement thermodynamical self-consistency by demanding $\partial_m P = 0$ one has to express the explicitly appearing e in Eq. (116) in terms of a by means of Eq. (106) and distinguish temperature dependences arising from a simple rescaling and those arising from the T dependent ground-state physics. For SU(2) we have

$$\frac{m^2}{|\phi|^2} \equiv e^2(a, \lambda_E) = T^2 \times \frac{a^2}{|\phi|^2} = \frac{\lambda_E^2}{4\pi^2} \times a^2 \lambda_E. \quad (117)$$

The first factor on the right-hand sides of Eq. (117) arises from rescaling, so only the second factor needs to be differentiated:

$$\partial_a e^2(a, \lambda_E) = \frac{\lambda_E^2}{4\pi^2} \times (2a\lambda_E + a^2\partial_a\lambda_E). \quad (118)$$

After solving $\partial_m P = 0$ for the term $\partial_a\lambda_E$ we obtain a modified right-hand side of the evolution equation Eq. (103). The two-loop evolution of e is work in progress⁵². The investigation of the screening masses and of the two-loop pressure for SU(3) is left for future work. The latter will be of a similar magnitude as in the SU(2) case.

3. The magnetic phase

The electric phase is terminated at the temperature $T_{c,E}$ by the condensation of massless magnetic monopoles. These condensates can be described macroscopically by quantum mechanically and statistically inert complex scalar fields and pure gauges. The latter describe the interactions between monopoles which induce a negative pressure by the generation of isolated but collapsing magnetic flux loops (center-vortex loops). At $T_{c,E}$ one can not distinguish between the unbroken $U(1)$ and the dual gauge group $U(1)_D$ ($SU(2)$) or the unbroken $U(1)^2$ and the dual gauge group $U(1)_D^2$ ($SU(3)$): An exact electric-magnetic duality occurs. For $SU(2)$ the point $T_{c,E}$ is stabilized by a dip of the energy density. For $SU(3)$ a similar stabilization takes place but with a much larger slope of the energy density: The phase transition appears to be weakly first order. It turns out that the electric Z_2 ($SU(2)$) or Z_3 ($SU(3)$) degeneracy of the ground state as it was observed in the electric phase is lifted: A unique ground state characterizes the magnetic phase. On the other hand, the expectation of the Polyakov loop, though strongly suppressed as compared to that in the electric phase, does not vanish entirely in the magnetic phase. This is a manifestation of the fact that the ground state in the magnetic phase does allow for the propagation of massive dual gauge modes despite the confinement of fundamental, fermionic, and heavy test charges by the monopole condensates. In that sense, the magnetic phase is only preconfining.

The critical behavior in the vicinity of $T_{c,E}$ is investigated and compared with results that seem to be related to the Yang-Mills theory by universality arguments.

The monopole condensates are characterized by infinite correlation lengths. In a thermodynamical simulation on a finite-size lattice performed in the magnetic phase not much can be learned about thermodynamical quantities such as the pressure or the energy density which are sensitive to the infrared behavior of the theory.

3.1. Prerequisites

3.1.1. The BPS monopole

Here we provide some facts about the 't Hooft-Polyakov monopole^{55,56} in the BPS limit³⁰ since we will need them in Sec. 3.1.2. We consider an $SU(2)$ gauge model with the Lagrangian of Eq. (73) with the modification that the potential is absent. The BPS monopole is a static, particle-like solution to the equations of motion of this model saturating the BPS bound on the mass M . When centered at $\vec{x} = 0$ it is given as

$$\phi^a = \hat{x}_a |\phi| F(\rho), \quad a_4^a = 0, \quad a_i^a = \frac{\epsilon_{aij}}{er} \hat{x}_j G(\rho), \quad (119)$$

where $r \equiv |\vec{x}|$, $\hat{x}_i \equiv \frac{x_i}{r}$, $|\phi| \equiv \sqrt{\phi^a \phi^a}$ ($r \rightarrow \infty$), and $\rho = e|\phi|r$. The antimonopole solution is obtained by letting $\hat{x} \rightarrow -\hat{x}$ in Eq. (119). The functions F and G can be determined analytically. They are given as³⁰

$$F(\rho) = \coth \rho - \frac{1}{\rho}, \quad G(\rho) = 1 - \frac{\rho}{\sinh \rho}. \quad (120)$$

The mass M of a BPS monopole or antimonopole calculates as

$$M = \frac{4\pi}{e} |\phi|. \quad (121)$$

(Notice that in Eq. (121) $|\phi|$ is replaced by $u \sim u_{\max} = \frac{\pi}{\beta}$ for a screened BPS monopole generated by the dissociation of a large-holonomy caloron, compare with Eq. (13).) The magnetic charge g is obtained by integrating the 't Hooft tensor

$$\mathcal{F}_{\mu\nu} = \partial_\mu(\hat{\phi}^a a_\nu^a) - \partial_\nu(\hat{\phi}^a a_\mu^a) - \frac{1}{e} \epsilon^{abc} \hat{\phi}^a \partial_\mu \hat{\phi}^b \partial_\nu \hat{\phi}^c, \quad (\hat{\phi}^a = \frac{\phi^a}{\sqrt{\phi^b \phi^b}}), \quad (122)$$

over a two-sphere S_2 with infinite radius which is centered at $\vec{x} = 0$. It is given as

$$g = \int_{S_2, R=\infty} d\Sigma_{\mu\nu} \mathcal{F}_{\mu\nu} = \pm \frac{4\pi}{e}. \quad (123)$$

In Eq. (123) $d\Sigma_{\mu\nu}$ denotes the differential surface element.

In unitary gauge, where the color orientation of ϕ^a is 'combed' into a fixed direction in adjoint color space, the magnetic field $B_i = \mp \frac{\hat{x}_i}{er^2}$ associated with Eq. (122) is accompanied by a Dirac string along this direction in position space: If the monopole lies inside an S_2 then the magnetic flux through this S_2 of the Dirac string precisely cancels that of the hedge-hog magnetic field. If a monopole or antimonopole lies outside of an S_2 with infinite radius an finite distance b away from its surface and the monopole's or the antimonopole's Dirac string does not pierce the surface then the magnetic flux F through the surface, see Fig. 16, calculates as

$$\begin{aligned} F &= \int_{\text{plane}} d\Sigma_{\mu\nu} \mathcal{F}_{\mu\nu} \\ &= \pm \frac{1}{e} \int_0^{2\pi} d\beta \int_{-\infty}^{\infty} dx |x| \cos \alpha(x, b) \frac{1}{x^2 + b^2} \\ &= \pm \frac{4\pi}{e} b \int_0^{\infty} dx \frac{|x|}{(x^2 + b^2)^{3/2}} \\ &= \pm \frac{4\pi}{e}. \end{aligned} \quad (124)$$

We conclude that static monopoles or antimonopoles lying inside an S_2 of *infinite* radius do not contribute to the flux through S_2 while they may contribute to the flux when situated outside of this S_2 .

3.1.2. Derivation of the phases of macroscopic complex scalar fields

There is one species of magnetic monopoles in the SU(2) case while there are two independent species of magnetic monopoles for SU(3).

SU(2) case:

In unitary gauge we consider an isolated system of a monopole and an antimonopole, which both are at rest and do not interact, outside of an S_2 with *infinite* radius. We characterize their Dirac strings by unit vectors \hat{x}_m and \hat{x}_a which point away

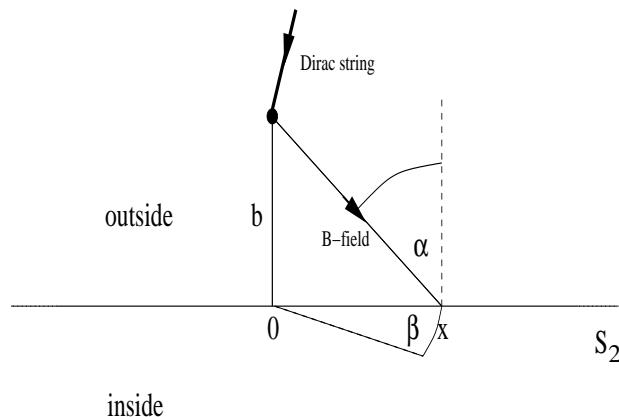


Fig. 16. A BPS monopole in unitary gauge outside of an S_2 with infinite radius. The Dirac string does not pierce the surface of the S_2 .

from the core of the monopole and the antimonopole, respectively. Let \mathbb{P} be the plane perpendicular to S_2 such that the intersection line $L = \mathbb{P} \cap S_2$ coincides with the intersection line of S_2 with the plane spanned by \hat{x}_m and \hat{x}_a . (The case where \hat{x}_m and \hat{x}_a lie in S_2 is inessential for what follows.) Whether or not this system contributes to the magnetic flux through S_2 depends on the angle $\delta = \angle(\hat{x}_m, \hat{x}_a)$ and on the angle γ which the projection of \hat{x}_m onto \mathbb{P} forms with L .

A magnetic flux through S_2 is generated if and only if either \hat{x}_m or \hat{x}_a alone pierces S_2 . For a given angle δ the angle γ is uniformly distributed. In the absence of a heat bath the probability of measuring a flux $\frac{4\pi}{e}$ or a flux $-\frac{4\pi}{e}$ through S_2 thus is given as $\frac{\delta}{2\pi}$. We conclude that for a given angle δ the average plus or minus flux through S_2 reads

$$\bar{F}_{\pm} = \pm \frac{\delta}{2\pi} \frac{4\pi}{e} = \pm \frac{2\delta}{e}, \quad (0 \leq \delta \leq \pi). \quad (125)$$

Notice that δ and $2\pi - \delta$ generate the same average flux \bar{F}_{\pm} , thus the restriction $0 \leq \delta \leq \pi$ in Eq. (125).

So far we have discussed the flux through S_2 which is generated by an isolated monopole-antimonopole system with no interactions. To derive the phase of the macroscopic complex field φ describing the Bose condensate of such systems we couple the system to the heat bath, project onto zero-momentum states (condensate) of the monopole-antimonopole system such that each constituent does not carry momentum and perform the massless limit $e \rightarrow \infty$ which takes place for $T \leq T_{c,E}$, compare with Eq. (107). (The rare case of a zero-momentum state with opposite and finite momenta of the constituents generates a closed and instable magnetic flux line, see Fig. 1. This situation takes place if a large number of large-holonomy calorons dissociate into monopole-antimonopole pairs almost simultaneously inside a small spatial volume. On the macroscopic level, the thermal average over these flux loops, which collapse as soon as they are created, will later be described by a pure gauge configuration.)

The monopole and antimonopole are generated by the dissociation of a large-holonomy caloron. According to Eq. (25) the sum of monopole and antimonopole mass, M_{m+a} , is, after screening, given as

$$M_{m+a} = \frac{8\pi^2}{e\beta}. \quad (126)$$

The thermally averaged flux of the zero-momentum system at finite coupling e is obtained as

$$\begin{aligned} \bar{F}_{\pm, \text{th}}(\delta) &= 4\pi \int d^3p \delta^{(3)}(\vec{p}) n_B(\beta|E(\vec{p})|) \bar{F}_{\pm} \\ &= \pm \frac{8\pi\delta}{e} \int d^3p \frac{\delta^{(3)}(\vec{p})}{\exp\left[\beta\sqrt{M_{m+a}^2 + \vec{p}^2}\right] - 1}. \end{aligned} \quad (127)$$

After setting $\vec{p} = 0$ in $\left(\exp\left[\beta\sqrt{M_{m+a}^2 + \vec{p}^2}\right] - 1\right)$ and by appealing to Eq. (126), the expansion of this term reads

$$\lim_{\vec{p} \rightarrow 0} \left(\exp\left[\beta\sqrt{M_{m+a}^2 + \vec{p}^2}\right] - 1\right) = \frac{8\pi^2}{e} \left(1 + \frac{1}{2} \frac{8\pi^2}{e} + \frac{1}{6} \left(\frac{8\pi^2}{e}\right)^2 + \dots\right). \quad (128)$$

Appealing to Eq. (128), the limit $e \rightarrow \infty$ can now safely be performed in Eq. (127). We have

$$\lim_{e \rightarrow \infty} \bar{F}_{\pm, \text{th}}(\delta) = \pm \frac{\delta}{\pi}, \quad (0 \leq \delta \leq \pi). \quad (129)$$

The right-hand side of Eq. (129) defines the argument of the complex and periodic function f with

$$f\left(\frac{\delta}{\pi}\right) \equiv C \frac{\varphi}{|\varphi|} \left(\frac{\delta}{\pi}\right) \quad (130)$$

where C is an undetermined (complex) constant. (Recall, that δ is an angle). Since f 's argument was obtained by a projection onto zero spatial momentum the only admissible nontrivial periodic dependence is that on the Euclidean time τ . Without restriction of generality we can thus set $\frac{\delta}{\pi} = \frac{\tau}{\beta}$. Since f is periodic, $f(\tau = 0) = f(\tau = \beta)$, it can be expanded into a Fourier series:

$$f\left(\frac{\tau}{\beta}\right) = \sum_{n=-\infty}^{n=\infty} f_n \exp\left[2\pi i n \frac{\tau}{\beta}\right] \quad (131)$$

where f_n are (complex) constants. According to Eq. (130) $f\bar{f} = |C|^2$ is constant in τ . Thus the only possibility in Eq. (131) is $f_n = C \delta_{mn}$ or $f_n = \bar{C} \delta_{(-m)n}$ for a fixed value of m . Moreover, only $m = 1$ is allowed since the physical situation generating the continuous parameter δ does not repeat itself for $0 \leq \delta \leq \frac{\pi}{m}$, $\frac{\pi}{m} \leq \delta \leq \frac{2\pi}{m}, \dots$ if $m > 1$ because no higher-charge monopoles exist. (Recall that only calorons with a large-holonomy and topological charge unity are allowed to contribute to the

52 *Ralf Hofmann*

thermodynamics in the electric phase.) We conclude that the equation of motion satisfied by f is:

$$\partial_\tau^2 f\left(\frac{\tau}{\beta}\right) + \left(\frac{2\pi}{\beta}\right)^2 f\left(\frac{\tau}{\beta}\right) = 0. \quad (132)$$

3.1.3. Derivation of the modulus of macroscopic complex scalar fields

What about φ 's modulus? The reasoning is completely analogous to that for the derivation of ϕ 's modulus. First, since φ is composed of massless, noninteracting monopoles being at rest its τ dependence ought to be BPS saturated. Second, for φ to have the phase $\exp[\pm 2\pi i \frac{\tau}{\beta}]$ the right-hand side of its BPS equation ought to be *linear* in φ . Third, for the existence of smooth deformations $\beta \rightarrow \beta + \delta\beta$, subject to a perturbative expansion in $\frac{\delta\beta}{\beta}$ away from a phase boundary, the right-hand side of the BPS equation must be analytic. Fourth, we assume that a scale Λ_M is given externally. Fifth, no explicit dependence on β may appear on the right-hand side of the BPS equation since at zero momentum the temperature dependence of the mass of a monopole cancels against the factor β in the Boltzmann weight. The only possibility for the BPS equation satisfying these conditions is

$$\partial_\tau \varphi = \pm i \frac{\Lambda_M^3 \varphi}{|\varphi|^2} = \pm i \frac{\Lambda_M^3}{\bar{\varphi}}. \quad (133)$$

From Eq. (133) it follows that φ 's modulus is given as

$$|\varphi| = \sqrt{\frac{\Lambda_M^3 \beta}{2\pi}}. \quad (134)$$

The right-hand side of Eq. (133) defines the square root of the potential V_M . In the absence of interactions between (screened) monopoles the effective theory for φ thus reads

$$S_\varphi = \int_0^\beta d\tau \int d^3x \left(\frac{1}{2} \overline{\partial_\tau \varphi} \partial_\tau \varphi + \frac{1}{2} \frac{\Lambda_M^6}{\bar{\varphi} \varphi} \right). \quad (135)$$

SU(3) case:

Here we have two independent monopole species which do not interact. The situation for each species is completely analogous to the SU(2) case. The two macroscopic fields φ_1 and φ_2 both satisfy the BPS equation (133) and are given as

$$\varphi_1(\tau) = \varphi_2(\tau) = \sqrt{\frac{\Lambda_M^3 \beta}{2\pi}} \exp\left[\pm 2\pi i \frac{\tau}{\beta}\right]. \quad (136)$$

In the absence of interactions between monopoles the effective theory for φ_1, φ_2 reads

$$S_\varphi = \int_0^\beta d\tau \int d^3x \left(\frac{1}{2} \overline{\partial_\tau \varphi_1} \partial_\tau \varphi_1 + \frac{1}{2} \overline{\partial_\tau \varphi_2} \partial_\tau \varphi_2 + \frac{1}{2} \frac{\Lambda_M^6}{\bar{\varphi}_1 \varphi_1} + \frac{1}{2} \frac{\Lambda_M^6}{\bar{\varphi}_2 \varphi_2} \right). \quad (137)$$

3.2. A macroscopic ground state

In close analogy to the electric phase we now derive the full macroscopic ground-state dynamics. First, we establish the quantum mechanical and statistical inertness of the fields φ (SU(2)) and φ_1, φ_2 (SU(3)). Subsequently, we solve the equations of motion for the topologically trivial dual gauge field in these backgrounds to obtain pure-gauge configurations describing, on a macroscopic level, the interaction between monopoles in the ground state. It will turn out that the Polyakov loops when evaluated on these pure-gauge configurations are trivial: The electric Z_2 (SU(2)) and Z_3 (SU(3)) degeneracies observed in the electric phase no longer exist. Thus the magnetic phase confines fundamental test charges.

The ratios of the mass-squared of potential φ -field fluctuations with $|\varphi|^2$ and T^2 are

$$\frac{\partial_{|\varphi|^2}^2 V_M(\varphi)}{|\varphi|^2} = 6 \lambda_M^3, \quad \frac{\partial_{|T|^2}^2 V_M(\varphi)}{T^2} = 24\pi^2, \quad (138)$$

where $\lambda_M \equiv \frac{2\pi T}{\Lambda_M}$. We will show below that $\lambda_M \geq 7.075$ (SU(2)) and $\lambda_M \geq 6.467$ (SU(3)). Thus φ -field (SU(2)) and φ_1, φ_2 -field (SU(3)) fluctuations neither exist on-shell nor off-shell.

3.2.1. Pure-gauge configurations

SU(2) case:

The topologically trivial sector is coupled to φ in a minimal fashion, and the following effective action arises

$$S = \int_0^\beta d\tau \int d^3x \left[\frac{1}{4} G_{\mu\nu}^D G_{\mu\nu}^D + \frac{1}{2} \overline{\mathcal{D}_\mu \varphi} \mathcal{D}_\mu \varphi + \frac{1}{2} \frac{\Lambda_M^6}{\bar{\varphi} \varphi} \right], \quad (139)$$

where $G_{\mu\nu}^D = \partial_\mu a_\nu^D - \partial_\nu a_\mu^D$ denotes the Abelian field strength of the dual gauge field a_μ^D and $\mathcal{D}_\mu \equiv \partial_\mu + ig a_\mu^D$ denotes the covariant derivative involving the magnetic gauge coupling g .

Since the field φ does not fluctuate it is a background to the macroscopic gauge-field equations of motion which follows from Eq. (139):

$$\partial_\mu G_{\mu\nu}^D = ig [\overline{\mathcal{D}_\nu \varphi} \varphi - \bar{\varphi} \mathcal{D}_\nu \varphi]. \quad (140)$$

A pure-gauge solution to Eq. (140) with $D_\mu \varphi \equiv 0$ is given as

$$a_\mu^{D,bg} = \pm \delta_{\mu 4} \frac{2\pi}{g\beta}. \quad (141)$$

On φ and on $a_\mu^{D,bg}$ only the potential does not vanish in Eq. (139): Interactions between magnetic monopoles create a nonvanishing energy density ρ^{gs} and pressure P^{gs} where

$$\rho^{gs} = \pi \Lambda_M^3 T = -P^{gs}. \quad (142)$$

54 *Ralf Hofmann*

We shall see in Sec. 4.1.1, compare with Eq. (165), that the negative ground-state pressure in Eq. (142) originates from center-vortex loops which collapse as soon as they are created.

SU(3) case:

The situation is the same as for SU(2) except that we have gauge dynamics subject to $U(1)_D^2$ and not only $U(1)_D$. The effective action reads

$$S = \int_0^\beta d\tau \int d^3x \left[\frac{1}{4} G_{\mu\nu,1}^D G_{\mu\nu,1}^D + \frac{1}{4} G_{\mu\nu,2}^D G_{\mu\nu,2}^D + \frac{1}{2} \overline{\mathcal{D}_{\mu,1}\varphi_1} \mathcal{D}_{\mu,1}\varphi_1 + \frac{1}{2} \overline{\mathcal{D}_{\mu,2}\varphi_2} \mathcal{D}_{\mu,2}\varphi_2 + \frac{1}{2} \frac{\Lambda_M^6}{\bar{\varphi}_1\varphi_1} + \frac{1}{2} \frac{\Lambda_M^6}{\bar{\varphi}_2\varphi_2} \right]. \quad (143)$$

The Abelian field strengths $G_{\mu\nu,1}^D, G_{\mu\nu,2}^D$ and the covariant derivatives $\mathcal{D}_{\mu,1}, \mathcal{D}_{\mu,2}$ are defined as for the SU(2) case with the replacements $a_\mu^D \rightarrow a_{\mu,1}^D, a_\mu^D \rightarrow a_{\mu,2}^D$, respectively. (The magnetic gauge coupling g is universal since both species of monopoles couple with the same strength to their respective gauge field.)

The equations of motion for the fields $a_{\mu,1}^D, a_{\mu,2}^D$ in the background of the fields φ_1, φ_2 are

$$\partial_\mu G_{\mu\nu,1}^D = ig [\overline{\mathcal{D}_{\nu,1}\varphi_1} \varphi_1 - \bar{\varphi}_1 \mathcal{D}_{\nu,1}\varphi_1], \quad \partial_\mu G_{\mu\nu,2}^D = ig [\overline{\mathcal{D}_{\nu,2}\varphi_2} \varphi_2 - \bar{\varphi}_2 \mathcal{D}_{\nu,2}\varphi_2]. \quad (144)$$

Pure-gauge solutions to these equations with $\mathcal{D}_{\nu,1}\varphi_1 = \mathcal{D}_{\nu,2}\varphi_2 = 0$ are given as

$$a_{\mu,1}^{D,bg} = \pm \delta_{\mu 4} \frac{2\pi}{g\beta}, \quad a_{\mu,2}^{D,bg} = \pm \delta_{\mu 4} \frac{2\pi}{g\beta}. \quad (145)$$

On φ_1, φ_2 and on $a_{\mu,1}^{D,bg}, a_{\mu,2}^{D,bg}$ only the potentials do not vanish in Eq. (143): Interactions between magnetic monopoles create a nonvanishing energy density ρ^{gs} and pressure P^{gs} where

$$\rho^{gs} = 2\pi \Lambda_M^3 T = -P^{gs}. \quad (146)$$

Again, the negative ground-state pressure in Eq. (146) originates from center-vortex loops which collapse as soon as they are created.

3.2.2. Polyakov loop and rotation to unitary gauge

SU(2) case:

The Polyakov loop $\mathbf{P} \equiv \exp \left[ig \int_0^\beta d\tau a_4^D \right]$, when evaluated on the pure-gauge configuration in Eq. (141), reads

$$\mathbf{P} = \exp \left[\pm ig \int_0^\beta d\tau \frac{2\pi}{g\beta} \right] = 1. \quad (147)$$

A gauge rotation $a_\mu^{D,bg} \rightarrow a_\mu^{D,bg} + \frac{i}{g} (\partial_\mu \Omega^\dagger) \Omega$ to unitary gauge $\varphi = |\varphi|, a_\mu^{D,bg} = 0$ is mediated by the U(1) group element $\Omega = \exp \left[\pm 2\pi i \frac{\tau}{\beta} \right]$: The Polyakov loop \mathbf{P} is invariant under this gauge transformation. We conclude that the electric Z_2

ground-state degeneracy, which was observed in the electric phase, no longer exists in the magnetic phase: The ground state confines fundamentally charged, heavy and fermionic test charges.

SU(3) case:

Here the Polyakov loop \mathbf{P} is a product of the Polyakov loops \mathbf{P}_1 and \mathbf{P}_2 computed on the respective pure-gauge configurations $a_{\mu,1}^{D,bg}$ and $a_{\mu,1}^{D,bg}$ in Eq. (145). We have

$$\mathbf{P} = \mathbf{P}_1 \mathbf{P}_2 = \exp[\pm 2ig \int_0^\beta d\tau \frac{2\pi}{g\beta}] = 1 \quad \text{or} \quad \mathbf{P} = \mathbf{P}_1 \mathbf{P}_2 = \exp[0] = 1. \quad (148)$$

Gauge rotations to unitary gauge $\varphi_1 = |\varphi_1| = \varphi_2$, $a_{\mu,1}^{D,bg} = a_{\mu,2}^{D,bg} = 0$ are mediated by the U(1) group elements $\Omega_1 = \exp[\pm 2\pi i \frac{\tau}{\beta}] = \Omega_2$. Again, \mathbf{P} is invariant under these gauge rotations. We conclude that the electric Z_3 ground-state degeneracy does not exist in the magnetic phase: Fundamentally charged, heavy and fermionic test charges are confined by the monopole condensates.

3.3. Excitations

3.3.1. Mass spectrum of thermal quasiparticles

The dual Abelian Higgs mechanism generates tree-level quasiparticle masses m and m_1, m_2 for the fluctuations δa_μ^D (SU(2)) and $\delta a_{\mu,1}^D, \delta a_{\mu,2}^D$ (SU(3)), respectively. We have

$$m = g|\varphi| = m_1 = m_2 = aT, \quad (a \equiv 2\pi g \lambda_M^{-3/2}) \quad (149)$$

where $\lambda_M \equiv \frac{2\pi T}{\Lambda_M}$.

3.3.2. Thermodynamical selfconsistency and evolution equation

Due to the absence of interactions between the dual gauge fields the thermodynamics of the magnetic phase is exact on the one-loop level. Again, a magnetic modification of the compositeness condition Eq. (95) applies.

Let us first compare the contribution ΔV_M of quantum fluctuations to the pressure arising from dual gauge modes with the tree-level result $-1/2 V_M = -\pi \Lambda_M^3 T$ (SU(2)) and $-1/2 V_M = -2\pi \Lambda_M^3 T$ (SU(3)). In both cases we have

$$\frac{\Delta V_M}{V_M} = \frac{\lambda_M^{-3}}{24\pi^2}. \quad (150)$$

Considering that $\lambda_M \geq 7.075$ (SU(2)) and $\lambda_M \geq 6.467$ (SU(3)) this is smaller than 1.2×10^{-5} and 1.6×10^{-5} , respectively. Thus the quantum contribution to the one-loop pressure can safely be neglected.

For SU(2) the thermal contribution to the pressure reads

$$P(\lambda_M) = -\Lambda_M^4 \left[\frac{6\lambda_M^4}{(2\pi)^6} \bar{P}(a) + \frac{\lambda_M}{2} \right] \quad (151)$$

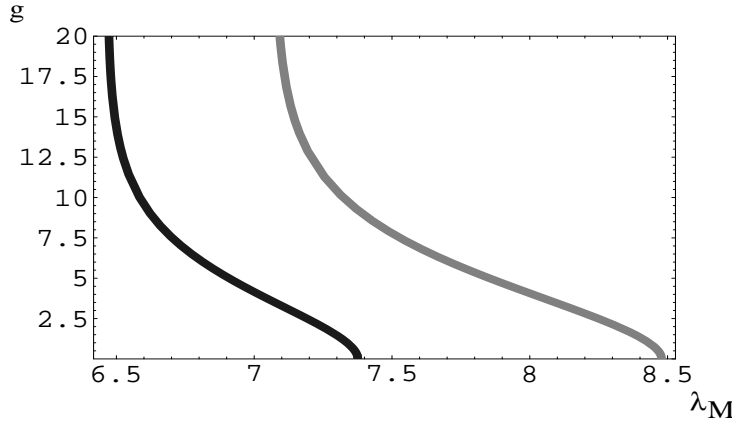


Fig. 17. The evolution of the effective gauge coupling g in the magnetic phase for SU(2) (thick grey line) and SU(3) (thick black line). At $\lambda_{c,M} = 7.075$ (SU(2)) and $\lambda_{c,M} = 6.467$ (SU(3)) g diverges logarithmically, $g \sim -\log(\lambda_M - \lambda_{c,M})$.

where the (negative) function $\bar{P}(a)$ is defined in Eq. (100). The SU(3) pressure is just twice the SU(2) pressure. From the condition $\partial_a P = 0$ of thermodynamical selfconsistency the following evolution equation arises for both SU(2) and SU(3):

$$\partial_a \lambda_M = -\frac{12\lambda_M^4 a}{(2\pi)^6} \frac{D(a)}{1 + \frac{12\lambda_M^3 a^2}{(2\pi)^6} D(a)} \quad (152)$$

where the (positive) function $D(a)$ is defined in Eq. (104). In analogy to the electric phase the λ_M dependence of the gauge coupling constants g is obtained by inverting the solutions to Eq. (152) and by subsequently using the relation between g , λ_M and a in Eq. (149). The temperature evolution of g is shown in Fig. 17.

3.3.3. Interpretation of results

The magnetic gauge coupling g increases continuously from $g = 0$ at the electric-magnetic phase boundary ($T = T_{c,E}$) until it diverges logarithmically at $T_{c,M}$. A variation of the magnetic coupling with temperature is not in contradiction with magnetic charge conservation since no *isolated* magnetic charges appear in the magnetic phase: Magnetic monopoles either are condensed or they conspire to form unstable magnetic flux loops (center-vortex loops), see Fig. 1. From Fig. 17 one can see that the magnetic phase is more narrow for SU(3) than it is for SU(2). Despite the fact that the ground-state degeneracies with respect to the electric Z_2 symmetry (SU(2)) and the electric Z_3 symmetry (SU(3)) are absent in the magnetic phase the fully averaged Polyakov loop (including the massive dual gauge-mode excitations) does not vanish at $T_{c,E}$, see Sec. 3.4. The expectation of the Polyakov loops only vanishes at $T_{c,M}$ where *all* dual gauge modes are decoupled because of a diverging mass. If we take the mass of the dual gauge modes to be the order parameter for the dynamical breaking of $U(1)_D$ (SU(2)) and $U(1)_D^2$ (SU(3)) then the electric-magnetic

transition is second order with mean-field exponents in both cases. The best one can do to relate this order-parameter to electric Z_2 or Z_3 restoration is to look for the point where its exponent is least sensitive to the length $\Delta\lambda_M$ of the fitting interval. The expectation of the 't Hooft loop, which is a dual order parameter for complete confinement and which is nonzero if center-vortices are condensed, vanishes inside the magnetic phase where center-vortex loops are isolated and instable defects. At $T_{c,M}$ the expectation of the 't Hooft loop jumps to a finite value. The associated transition is, however, neither second nor first order but of the Hagedorn type see Sec.4.4. Because of the infinite correlation length (massless condensed magnetic monopoles) a finite-size lattice simulation of the order parameter as well as infrared sensitive thermodynamical quantities such as the pressure is problematic.

3.4. Polyakov loop in the electric and the magnetic phase

In this section we show, on a qualitative level, that the expectation of the Polyakov loop $\langle \mathbf{P} \rangle$, which is an order parameter for the confinement-deconfinement transition, is finite both in the electric phase and the magnetic phase. Deep in the magnetic phase $\langle \mathbf{P} \rangle$ is, however, strongly suppressed as compared to its value at $T_{c,E}$.

In each phase the Polyakov-loop expectation $\langle \mathbf{P} \rangle$ can be computed in unitary(-Coulomb) gauge. Let us first discuss the electric phase. The sector $S_{f,E}$ in the effective action (73), which involves fluctuating fields, is given as

$$S_{f,E} = \int_0^\beta d\tau d^3x \left[\frac{1}{4} G_{\mu\nu}^a G_{\mu\nu}^a + \frac{1}{2} \sum_a m_a^2 (\delta a_\mu^a)^2 \right]. \quad (153)$$

Here $a = 1, 2, 3$ and $m_1 = m_2 > 0, m_3 = 0$ for SU(2) and $a = 1, \dots, 8$ and $m_1 = m_2 = \frac{1}{2}m_3 = \frac{1}{2}m_4 = \frac{1}{2}m_5 = \frac{1}{2}m_6 > 0, m_7 = m_8 = 0$ for SU(3). Since in unitary gauge the Polyakov loop is unity in the ground state no direct ground-state contribution arises in the expectation $\langle \mathbf{P} \rangle$: The associated factor in the numerator cancels that in the denominator. We have

$$\langle \mathbf{P} \rangle = Z_{f,E}^{-1} \times \int [d\delta a_\mu] \exp \left[ie \int_0^\beta d\tau \delta a_4 \right] \exp[-S_{f,E}], \quad (154)$$

where $[d\delta a_\mu]$ denotes the path-integral measure and $Z_{f,E} \equiv \int [d\delta a_\mu] \exp[-S_{f,E}]$.

Since the fluctuations δa_μ are periodic in τ they can be decomposed into a Matsubara sum:

$$\delta a_\mu(\tau, \vec{x}) = \sum_{n=-\infty}^{n=\infty} \exp \left[2\pi i n \frac{\tau}{\beta} \right] \delta \bar{a}_{\mu,n}(\vec{x}). \quad (155)$$

Modes with $n \neq 0$ in Eq. (155) render the Polyakov-loop phase in Eq. (154) to be unity and are action-suppressed. Zero modes ($n = 0$) contribute to $\langle \mathbf{P} \rangle$ sizably if they are not action-suppressed. This is the case if and only if both of the following conditions are met: (i) as compared to T some or all masses m_a in Eq. (153) are small and (ii) $\partial_i \delta \bar{a}_{\mu,0}(\vec{x})$ is small compared with T^2 and the field configuration is

still localized in space. Here ∂_i denotes a spatial derivative. In the electric phase there are massless modes, the conditions (i) and (ii) can be satisfied, and thus a finite Polyakov-loop expectation emerges.

A similar consideration can be performed for the magnetic phase. Deep inside this phase condition (i) is badly violated since the mass of *all* dual gauge modes is much larger than T by virtue of Fig. 17 and the mass formula in Eq. (149). Thus $\langle \mathbf{P} \rangle$, though nonvanishing, is strongly suppressed deep inside the magnetic phase as compared to its value at $T_{c,E}$. For quantitative results the average $\langle \mathbf{P} \rangle$ can be performed on a lattice or analytically by using the respective effective theory for the electric and the magnetic phase.

3.5. *Critical behavior at the electric-magnetic transition*

The electric-magnetic transition, which goes with the dynamical breakdown of $U(1)_D$ ($SU(2)$) and $U(1)_D^2$ ($SU(3)$), is second order in both cases. The difference is that in the $SU(3)$ case the magnetic phase is more narrow than for $SU(2)$, see Fig. 17, and that the peak-value of the specific heat per volume is much larger for $SU(3)$ than it is for $SU(2)$, see Fig. 29. In addition, the entropy density, which measures the mobility of dual gauge modes and which is used to extract an apparent latent heat on the lattice⁷⁸, drops much more rapidly in the magnetic phase for $SU(3)$ as compared to the $SU(2)$ case. This is a plausible explanation for the apparent first-order nature of the confinement-deconfinement transition observed in lattice simulations^{82,83}.

The order parameter for the electric-magnetic transition is the mass $\propto a\lambda_M$ of the dual gauge bosons. (The monopole mass vanishes like an inverse *logarithm* on the electric side of the transition, and thus it is not an order parameter.) The following model applies to the behavior of $a\lambda_M$ close to the critical temperature $\lambda_c = 9.24$ ($SU(2)$) and $\lambda_c = 6.81$ ($SU(3)$):

$$a\lambda_M(\lambda_M) = K |\lambda_M - \lambda_c|^\nu, \quad (156)$$

where K and ν are constants, and λ_c is the critical temperature $T_{c,E}$ in units of $\frac{\Lambda_M}{2\pi}$. By demanding continuity of the pressure across the electric-magnetic transition, see Sec. 5, we derive $\lambda_c = 8.478$ ($SU(2)$) and $\lambda_c = 7.376$ ($SU(3)$).

The magnetic phase is not entirely confining (dual gauge bosons propagate although fundamental, heavy, and fermionic test charges are confined), and thus the expectation of the Polyakov loop $\langle \mathbf{P} \rangle$ is not exactly zero. The best one can do in order to compare the behavior of $a\lambda_M$ to the behavior of $\langle \mathbf{P} \rangle$ inferred from universality arguments^{69,70} is to look for the point where the fitted value of ν in Eq. (156) is least sensitive to a variation of the length $\Delta\lambda_M$ of the fitting interval.

To perform the fit to the model in Eq. (156) we have used Mathematica's `NonlinearFit` function which is contained in the statistics package. The function $a(\lambda_M)$, subject to the initial conditions $a(\lambda_c = 8.478) = 0$ ($SU(2)$) and $a(\lambda_c = 7.376) = 0$ ($SU(3)$), was generated by an inversion of the corresponding numerical solutions to

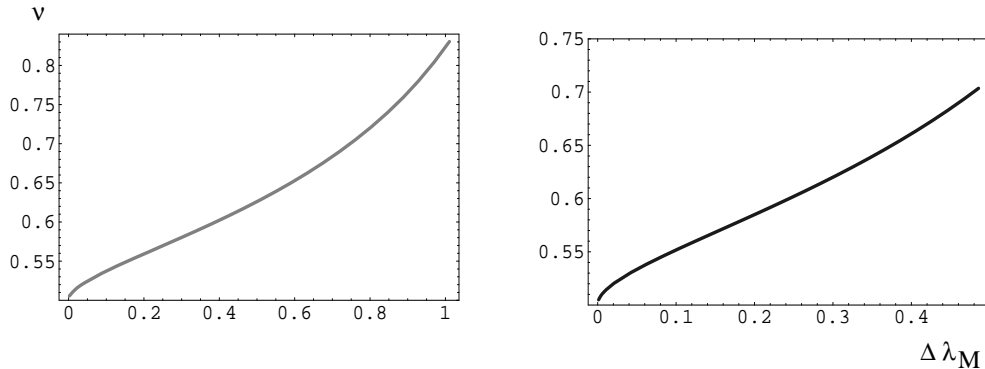


Fig. 18. The critical exponent ν for the mass of the dual gauge modes and for the magnetic-electric transition as a function of the length $\Delta\lambda_M$ of the fitting interval. The left panel is the SU(2) and the right panel the SU(3) result.

Eq. (152). (A step-size $\delta a = 5 \times 10^{-9}$ was used in the Runge-Kutta algorithm^f.) In Fig. 18 the fitted exponent ν is shown as a function of $\Delta\lambda_M$. Two things are important to observe. First, the magnetic-electric transition is second order with the mean-field exponent $\nu = 0.5$ for both SU(2) and SU(3). Second, for each case there is a point $\Delta\lambda_M^*$ of least sensitivity for ν under variations in $\Delta\lambda_M$. For SU(2) we have $\Delta\lambda_M^* = 0.28 \pm 0.03$ and $\nu(\Delta\lambda_M^*) = 0.576 \pm 0.008$, and for SU(3) $\Delta\lambda_M^* = 0.16 \pm 0.02$ and $\nu(\Delta\lambda_M^*) = 0.572 \pm 0.006$. By universality we expect $\nu(\Delta\lambda_M^*)$ for SU(2) to be close to the exponent ν_{IM} for the corresponding order parameter of a 3D Ising model^{69,70}. One has $\nu_{\text{IM}} \sim 0.63$. The SU(2) exponent $\nu(\Delta\lambda_M^*)$ only deviates by about 8.5% from ν_{IM} .

4. The center phase

4.1. Prerequisites

4.1.1. ANO vortex in the BPS limit

Just like the isolated defects in the electric phase are screened BPS monopoles, the isolated defects in the magnetic phase are screened and closed magnetic flux lines (vortex-loops). In Fig. 1, see also⁶⁶, we have given a figurative interpretation of these flux lines: They are composed of magnetic monopoles and antimonopoles which move into opposite directions. Thus there is a net magnetic current in the vortex core. A vortex core can be viewed as locations in space where $U(1)_D$ (SU(2)) or one of the factors in $U(1)_D^2$ (SU(3)) are restored. Hence the picture of isolated monopoles, contributing to the magnetic current, applies to the vortex core.

We have explained in Sec. 1 why the magnetic flux carried by a vortex-loop is independent of the state of motion of a particular monopole contributing to the vortex: The amount of flux carried by a vortex solely is a function of the charge of each

^fThe author would like to thank Jochen Rohrer for performing the numerical calculation.

60 *Ralf Hofmann*

BPS monopole contributing to it. Because large-holonomy calorons of topological charge one and thus monopoles with one unit of magnetic charge only are thermodynamically excited Abrikosov-Nielsen-Olesen (ANO) vortices are center vortices in the magnetic phase of an SU(2) or an SU(3) Yang-Mills theory.

A mesoscopic description of a static ANO vortex in the BPS limit is given by the action Eq. (139) when omitting the potential for φ . (This potential measures the energy density of the *macroscopic* ground state and thus must be subtracted when discussing the typical energy of a solitonic configuration on a mesoscopic level.) The following cylindrically symmetric (with axis along the x_3 direction) and static ansatz for the gauge field a_μ^D is made to describe the vortex⁶⁷:

$$a_4^D = 0, \quad a_i^D = \epsilon_{ijk} \hat{r}_j e_k A(r), \quad (157)$$

where \hat{r} is a radial unit vector in the $x_1 x_2$ plane, and \vec{e} is a unit vector along the x_3 direction. Writing $\varphi = |\varphi|(r) \exp[i\theta]$, the equations of motion for $|\varphi|(r)$ and $A(r)$ read

$$-\frac{1}{r} \frac{d}{dr} \left(r \frac{d}{dr} |\varphi| \right) + \left(\frac{1}{r} - g A \right)^2 |\varphi| = 0, \quad (158)$$

$$-\frac{d}{dr} \left(\frac{1}{r} \frac{d}{dr} (rA) \right) + g |\varphi|^2 \left(g A - \frac{1}{r} \right) = 0. \quad (159)$$

We keep in mind that $|\varphi|(r \rightarrow \infty) = \sqrt{\frac{\Lambda_M^3 \beta}{2\pi}}$, see Eq. (134). Let us first search for BPS saturated solutions to the system (158,159). The question is under what condition a solution to the first-order equation

$$\frac{d}{dr} |\varphi| = \left(\frac{1}{r} - g A \right) |\varphi| \quad (160)$$

also solves Eq. (158). Substituting Eq. (160) into Eq. (158), we observe that

$$A = -r \frac{d}{dr} A. \quad (161)$$

The solution to Eq. (161) is

$$A(r) = \frac{\text{const}}{r}. \quad (162)$$

Substituting Eq. (162) into Eq. (159), the constant in Eq. (162) is determined to be $\frac{1}{g}$. Eq. (160) is solved for $r > 0$ by

$$|\varphi|(r) \equiv \sqrt{\frac{\Lambda_M^3 \beta}{2\pi}}. \quad (163)$$

We have found an analytical solution to the system (158,159) for $r > 0$ which has one unit of magnetic flux $F_v(r) \equiv \frac{2\pi}{g} = \oint_C dz_\mu a_\mu^D$, where C is a circular curve of radius r in the $x_1 x_2$ plane centered at $x_1 = x_2 = 0$, and which has a vanishing vortex core. The energy density $\rho_v(r)$, when evaluated on the configuration $A(r) = \frac{1}{gr}$, $|\varphi|(r) \equiv \sqrt{\frac{\Lambda_M^3 \beta}{2\pi}}$, reduces to that of the magnetic field $H(r) = \frac{1}{2\pi r} \frac{d}{dr} F_v(r)$: (By Stoke's

theorem the magnetic field H must be proportional to a two-dimensional δ -function at $r = 0$. Thus the energy per unit vortex length diverges on the configuration (162) and (163).

$$\rho_v(r) = \frac{1}{2} H^2(r) \equiv 0, \quad (r > 0). \quad (164)$$

The (isotropic in the x_1x_2 plane) pressure $P_v(r)$ outside the vortex core is given as

$$P_v(r) = -\frac{1}{2} \frac{\Lambda_M^3 \beta}{2\pi} \frac{1}{g^2 r^2}, \quad (r > 0). \quad (165)$$

Eq.(165) is the mesoscopic reason for the macroscopic results in Eqs.(142) and (146). Because of the *negative* pressure in Eq. (165) vortex-loops start to collapse as soon as they are created at finite coupling g . (The pressure is more negative inside than outside of the vortex-loop.) Notice that in the limit $g \rightarrow \infty$ we have $P_v(r) \rightarrow 0$: For temperatures below $T_{c,M}$ vortex-loops do exist as particle-like excitations.

4.1.2. Leaving the BPS limit

Let us now discuss how the solutions in Eqs.(163) and (162) are deformed when the BPS limit is left at finite coupling g . In this case only approximate analytical solutions to the second-order system (158) and (159) are known⁶⁷. Assuming $|\varphi|$ to be constant, which is viable sufficiently far away from the core around $r = 0$, the solution to Eq. (159) reads

$$A(r) = \frac{1}{gr} - |\varphi| K_1(g|\varphi|r) \rightarrow \frac{1}{gr} - |\varphi| \sqrt{\frac{\pi}{2g|\varphi|r}} \exp[-g|\varphi|r], \quad (r \rightarrow \infty), \quad (166)$$

where K_1 is a modified Bessel function. (Notice that the $1/r$ divergence at $r = 0$ of the solution in Eq. (162) is absent in the configuration in Eq. (166).) Now $|\varphi|$ is not constant inside the vortex core but smoothly approaches zero for $r \rightarrow 0$. So there is a gradient contribution from $|\varphi|$ to the energy per unit length $\frac{E_v}{2\pi R}$ along the vortex where R denote the typical radius of a vortex loop. Let us first calculate the magnetic energy per unit length $\frac{E_{m,v}}{2\pi R}$. One has⁶⁷

$$\frac{E_{m,v}}{2\pi R} = \frac{1}{2} \int_0^\infty dr 2\pi r H^2(r) = \pi |\varphi|^2 \int_0^\infty dy K_0^2(y) y = \frac{\pi}{2} |\varphi|^2, \quad (167)$$

where $|\varphi|$ is given in Eq. (163). The gradient contribution $\frac{E_{\varphi,v}}{2\pi R}$ is comparable to $\frac{E_{m,v}}{2\pi R}$. Thus the typical energy E_v of the vortex loop is obtained by multiplying $\frac{E_{m,v}}{2\pi R} + \frac{E_{\varphi,v}}{2\pi R}$ with the typical circumference $2\pi R \sim \frac{1}{g|\varphi|}$ of the loop. We have

$$E_v \sim 2 \frac{\pi}{2} |\varphi|^2 \times \frac{1}{g|\varphi|} = \pi \frac{|\varphi|}{g}. \quad (168)$$

From Eq. (168) we conclude that vortex loops become massless in the limit $g \rightarrow \infty$. For $r \gg \frac{1}{g|\varphi|}$ the (isotropic in the x_1x_2 plane) pressure $P_v(r)$ of the vortex configuration is still given by Eq. (165): For finite coupling g vortex loops collapse as soon as they are created.

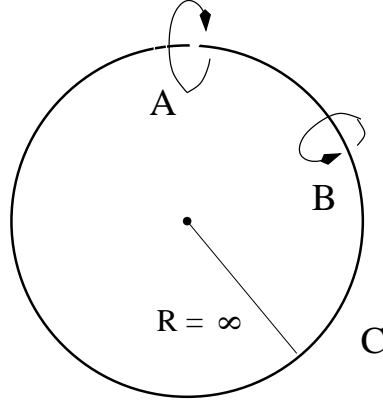


Fig. 19. Two center-vortex loops of opposite flux being pierced by an S_1 of infinite radius.

4.2. Derivation of the phase of a macroscopic complex scalar field

We consider a pair of center-vortex loops that are pierced by a circular contour C of infinite radius, see Fig. 19. The total center flux $F_{\pm,0}$ through the minimal surface spanned by C is

$$F_{\pm,0} = \begin{cases} \pm \frac{2\pi}{g} \\ 0 \end{cases} \quad (169)$$

depending on whether at finite coupling g the loop A (B) collapses to nothing well before the loop B (A) or whether this roughly happens at the same time. (In any case, vortex loops which start out *without* getting pierced by C do not contribute a center flux through C .)

Unlike in the case of a pair of a monopole and an antimonopole discussed in Sec. 3.1.2 the flux $F_{\pm,0}$ takes *discrete* values. In analogy to the derivation of a macroscopic monopole condensate we may investigate the thermally averaged flux of the vortex-antivortex (spin-0) system in the limit where there is no spatial momentum of this system and where $g \rightarrow \infty$:

$$\begin{aligned} \lim_{g \rightarrow \infty} F_{\pm,0;\text{th}}(\delta) &= 4\pi \int d^3p \delta^{(3)}(\vec{p}) n_B(\beta |2 E_v(\vec{p})|) F_{\pm,0} \\ &= 0, \pm \frac{2}{\beta |\varphi|} = 0, \pm \frac{\lambda_{c,M}^{3/2}}{\pi}. \end{aligned} \quad (170)$$

The phase of a macroscopic complex field Φ is defined as

$$\Gamma \frac{\Phi}{|\Phi|}(x) \equiv \lim_{g \rightarrow \infty} \left\langle \exp \left[ig \oint_{C(x)} dz_\mu (a^D)^\mu \right] \right\rangle \quad (171)$$

where Γ is a complex constant, and $(a^D)^\mu$ denotes the gauge field of a center vortex. The expectation on the right-hand side of Eq. (171) is proportional to the expectation of 't Hooft's loop operator⁶⁸. (Green functions of this operator change their

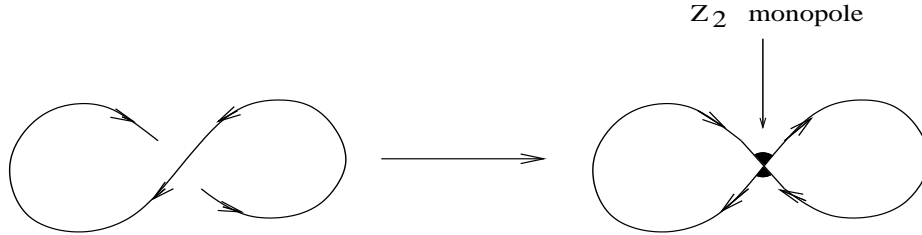


Fig. 20. The creation of an isolated Z_2 monopole by self-intersection of a center-vortex loop.

phase by -1 (SU(2)) and $\exp[\pm \frac{2\pi i}{3}]$ (SU(3)) under an exchange of the order of any two of their arguments: A feature which is familiar from Green functions of fermionic fields.) The possible values of Φ 's phase are parametrized by the average center flux $\lim_{g \rightarrow \infty} F_{\pm,0;\text{th}}(\delta)$ in Eq. (170).

According to Eq. (170) the condensate Φ of center-vortex loops is determined by discrete parameter values which can be normalized as $\hat{\tau} = \pm 1, 0$. Recall that at $\lambda_{c,M}$ vortex loops start to be stable excitations since their pressure $P_v(r)$ is zero outside the (infinitely thin) vortex core. Once the field Φ acquires a nonzero modulus its phase is observed to jump locally in space. (Each jump corresponds to a stable vortex loop travelling in from infinity and getting pierced by \mathcal{C} .) Thus we are led to interpret jumps in Φ 's phase as creation processes for (fermionic) particles. (There are two degenerate polarizations of these particles: The two possible directions of center flux in a given vortex-loop. By travelling in from infinity the vortex loop makes Φ 's phase jump twice: A created unit of flux is associated with a forward jump (piercing by \mathcal{C}) while a backward jump corresponds to minus this flux (no piercing by \mathcal{C} , center-vortex loop lies inside \mathcal{C} .) If a single center-vortex loop is created with sufficiently large momentum then a part of its kinetic energy can be converted into the mass of self-intersection points by subsequent twisting. Self-intersection points are Z_2 magnetic monopoles, each contributing $\sim \Lambda_C$ to the mass of the state where Λ_C is a mass scale. Twisting does not alter the fact that only two possible polarizations (spin-1/2 fermions) occur. (The magnetic flux is reversed by a Z_2 monopole⁷¹, see Fig. 20.) We conclude that the mass spectrum m_n of fermionic excitations is equidistant:

$$m_n \sim n \Lambda_C, \quad (n = 0, 1, 2, \dots). \quad (172)$$

The process of fermion creation violates the spatial homogeneity of the system and thus thermal equilibrium. Fermion creation, that is, the process of sucking in stable center-vortex loops from infinity, can only go on so long as the energy density provided by the field Φ is finite. Thus the field Φ must eventually relax to one of the

possible zero-energy minima of its potential. This phenomenon is generally known as tachyonic pre- and re-heating⁷⁴.

SU(2) case:

The symmetry, which is dynamically broken by center-vortex condensation, is a local magnetic Z_2 . After a relaxation of Φ to zero energy density the ground state must exhibit the associated Z_2 degeneracy. We conclude that for SU(2) the parameters $\hat{\tau} = \pm 1$ must be identified: They describe the same minimum of Φ 's potential. The parameter value $\hat{\tau} = 0$ corresponds to the other degenerate minimum. The center flux carried by a given flux line is associated with the differences in Φ 's phase in each minimum of Φ 's potential.

SU(3) case:

For SU(3) the dynamically broken symmetry is a local magnetic Z_3 . As a consequence, each of the three possible values $\hat{\tau} = \pm 1, 0$ describes one of the three possible, distinct minima of Φ 's potential. Before relaxation to zero energy density local jumps of Φ 's phase generate two distinct species of flux loops: Each associated with the three differences in Φ 's phase modulo three. (A short jump between two neighbouring unit roots is equivalent to a long jump into the opposite direction involving the third unit root as a brief stop-over.)

4.3. *The potential of the macroscopic complex scalar field*

At $T_{c,M}$ dual gauge modes decouple. Moreover, a condensate of (Cooper-like) pairs of single center-vortex–center-antivortex loops confines fundamental electric and fermionic test charges. This happens because each condensed center-vortex loop represents an electric dipole. A condensate of such dipoles squeezes an externally applied electric field into a flux tube: Oppositely charged test particles are subject to a linear potential at large distances. Thus the center phase is confining both test charges and *all* gauge modes: There is complete confinement. (The Polyakov loop expectation is zero below $T_{c,M}$, the 't Hooft loop expectation $\bar{\Phi}$, which is the dual order parameter for confinement, jumps to a finite value.)

The effective action for the center phase thus is only a functional of Φ and $\bar{\Phi}$. Moreover, thermal equilibrium (that is, periodicity in Euclidean time) is no longer applicable to constrain Φ 's potential. According to our discussion in the last section Φ 's potential V_C must be (i) invariant under center jumps only (invariance under a larger (continuous or discontinuous) symmetry is forbidden), (ii) it must allow for fermion creation by center jumps, and (iii) center-degenerate minima of zero energy density have to occur. Moreover, (iv) we insist on the occurrence of a single mass scale Λ_C only. From (i) we conclude that V_C can not be a function of $\bar{\Phi}\Phi$ alone.

SU(2) case:

The only potential V_C satisfying (i),(ii), (iii), and (iv) is given by

$$V_C = \overline{v_C} v_C \equiv \overline{\left(\frac{\Lambda_C^3}{\Phi} - \Lambda_C \Phi \right)} \left(\frac{\Lambda_C^3}{\Phi} - \Lambda_C \Phi \right). \quad (173)$$

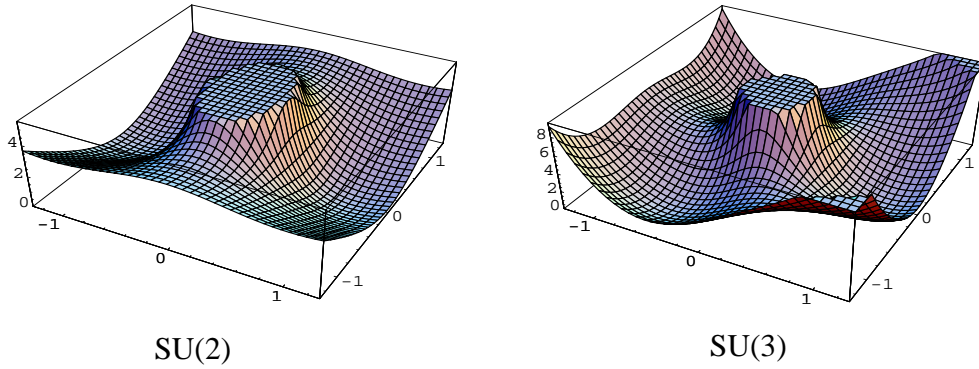


Fig. 21. The potential $V_C = \overline{v_C(\Phi)}v_C(\Phi)$ for the center-vortex condensate Φ . Notice the regions of negative tangential curvature inbetween the minima.

The zero-energy minima of V_M are at $\Phi = \pm\Lambda_C$. It is easy to show that adding or subtracting powers $(\Phi^{-1})^{2l+1}$ or Φ^{2k+1} in v_C , where $k, l = 0, 1, 2, 3, \dots$, generates additional minima and thus destroys the center degeneracy of the ground state after relaxation and/or violates the demand for zero energy-density at a finite value of Φ in these minima (requirement (iii)).

SU(3) case:

The only potential V_C satisfying (i),(ii), (iii), and (iv) is given by

$$V_C = \overline{v_C} v_C \equiv \overline{\left(\frac{\Lambda_C^3}{\Phi} - \Phi^2\right)} \left(\frac{\Lambda_C^3}{\Phi} - \Phi^2\right). \quad (174)$$

The zero-energy minima of V_C are at $\Phi = \Lambda_C \exp\left[\pm\frac{2\pi i}{3}\right]$ and $\Phi = \Lambda_C$. Again, adding or subtracting powers $(\Phi^{-1})^{3l+1}$ or $(\Phi)^{3k-1}$ in v_C , where $l = 0, 1, 2, 3, \dots$ and $k = 1, 2, 3, 4, \dots$, violates requirement (iii).

In Fig. 21 plots of the potentials in Eq. (173) and Eq. (174) are shown. The ridges of negative tangential curvature are classically forbidden: The field Φ tunnels through these ridges, and a phase change, which is determined by an element of the center Z_2 (SU(2)) or Z_3 (SU(3)), occurs locally in space. This is the afore-mentioned generation of one unit of center flux.

4.4. Thermodynamics close to the Hagedorn transition

The action describing the process of relaxation of Φ to one of V_M 's minima is

$$S = \int d^4x \left(\frac{1}{2} \overline{\partial_\mu \Phi} \partial^\mu \Phi - \frac{1}{2} V_C \right). \quad (175)$$

In contrast to the electric and magnetic phases the action S in Eq. (175) does not determine a classical, macroscopic ground state if Φ is not in one of V_C 's minima.

Though tunneling processes occur in real time they can be described by a Euclidean simulation, WKB-like approximations are thinkable. Alternatively, the computation of fermion creation rates can be performed on a finite-temperature lattice based on the theory (175). An interesting object to be measured is Φ 's two-point correlator $\Pi(x) \equiv \langle \bar{\Phi}(x)\Phi(0) \rangle$. Projecting onto a given spatial momentum \vec{p} at a given temperature, the strength of intermediate tachyonic modes can be extracted by a Fourier analysis of the τ dependence in $\int d^3x \exp[i\vec{p} \cdot \vec{x}] \Pi(\tau, \vec{x})$. This gives a measure for the density of states ρ_n for fermions of mass $\sim n \Lambda_C$ and spatial momentum \vec{p} ⁷².

Let us estimate ρ_n for SU(2). The multiplicity of fermion states with n self-intersections is given by twice the number L_n of bubble diagrams with n vertices in a scalar $\lambda\phi^4$ theory. In ⁷³ the minimal number of such diagrams $L_{n,min}$ was estimated to be $L_{n,min} = n!3^{-n}$. Using Stirling's formula this can be approximated as

$$\begin{aligned} L_{n,min} &\sim \frac{1}{3} \sqrt{2\pi n} (3e)^{-n} n^n \\ &= \frac{\sqrt{2\pi}}{3} \exp \left[n \left(\log n - (\log 3 + 1) \right) + \frac{1}{2} \log n \right] \\ &\sim \frac{\sqrt{2\pi}}{3} \exp [n \log n] \end{aligned} \quad (176)$$

for $n \gg 1$. So the number F_n of fermion states with mass $m_n \sim n \Lambda_C$ is bounded from below roughly by

$$F_n \sim 2 \times \frac{\sqrt{2\pi}}{3} \exp [n \log n] = \frac{\sqrt{8\pi}}{3} \exp [n \log n]. \quad (177)$$

We now estimate the density $\rho_{n,0}$ of fermion states at rest $\vec{p} = 0$ (or $\tilde{\rho}(E = n\Lambda_C)$) by differentiating F_n with respect to n and dividing the result by the level-spacing $\delta m_n = \Lambda_C$. We have

$$\begin{aligned} \rho_{n,0} &> \frac{\sqrt{8\pi}}{3\Lambda_C} \exp [n \log n] (\log n + 1) \quad \text{or} \\ \tilde{\rho}(E) &> \frac{\sqrt{8\pi}}{3\Lambda_C} \exp \left[\frac{E}{\Lambda_C} \log \frac{E}{\Lambda_C} \right] \left(\log \frac{E}{\Lambda_C} + 1 \right). \end{aligned} \quad (178)$$

Eq. (178) tells us that the density of static fermion states is more than exponentially increasing with energy E . The partition function Z_Φ thus is estimated as

$$\begin{aligned} Z_\Phi &> \int_{E^*}^{\infty} dE \tilde{\rho}(E) n_F(\beta E) \\ &> \frac{\sqrt{8\pi}}{3\Lambda_C} \int_{E^*}^{\infty} dE \exp \left[\frac{E}{\Lambda_C} \right] \exp[-\beta E], \end{aligned} \quad (179)$$

where $E^* \gg \Lambda_C$ is the energy where we start to trust our approximations. Thus Z_Φ diverges at some temperature $T_H < \Lambda_C$. (Strictly speaking, $T_H = 0$ according to Eq. (178). This is an artefact of our assumption that all states are infinitely narrow. There are, however, finite widths for higher-charge states ($n > 1$) since

contact interactions exist between vortex lines and intersection points. Moreover, in the real world higher-charge states are even broader due to their decay and their mutual annihilation into charge-one and charge-zero states. This happens because an SU(2) theory, which is not confining at the present temperature of the Universe, mixes with the theory under consideration at large temperatures and thus couples its massless gauge mode – the photon – to the Z_2 charges of the latter. The larger n the broader the associated state and the less reliable our assumption of infinitely narrow states.) This is the celebrated Hagedorn transition. (At T_H the entropy diverges and the system condenses self-intersecting center-vortex loops into a new ground state: The monopole condensate of the magnetic phase. The process of monopole condensation from below violates the spatial homogeneity of the system: Z_2 charges loose their mass by dense packing only. Thus the Hagedorn transition is genuinely nonthermal.)

Once Φ has settled into V_C 's minima Φ_{\min} there are no quantum fluctuations $\delta\Phi$. Writing $\Phi = |\Phi| \exp\left[i\frac{\theta}{\Lambda_c}\right]$, this is a consequence of the following fact:

$$\left.\frac{\partial_\theta^2 V_C(\Phi)}{|\Phi|^2}\right|_{\Phi_{\min}} = \left.\frac{\partial_{|\Phi|}^2 V_C(\Phi)}{|\Phi|^2}\right|_{\Phi_{\min}} = \begin{cases} 8 & (\text{SU}(2)) \\ 18 & (\text{SU}(3)) \end{cases}. \quad (180)$$

Thus radial *and* tangential fluctuations around Φ_{\min} would have a mass $m_{\delta\Phi}$ which is sizably larger than the compositeness scale $|\Phi_{\min}|$ for both SU(2) and SU(3). Since $|p_{\delta\Phi}^2 + m_{\delta\Phi}^2| \leq |\Phi_{\min}|^2$ for any allowed Euclidean momentum $p_{\delta\Phi}^2 > 0$ this means that the fluctuations $\delta\Phi$ are absent: After relaxation the ground state of the center phase has a vanishing pressure and a vanishing energy density.

5. Matching the pressure

The mass scales Λ_E and Λ_M , which determine the modulus of the adjoint Higgs field ϕ and the moduli of the monopole condensates φ (SU(2)) and φ_1, φ_2 (SU(3)), respectively, are related. This derives from the fact that across a second-order transition the pressure is continuous. We have

$$\begin{aligned} \Lambda_M &= \left(4 + \frac{\lambda_{c,E}^3}{720\pi^2}\right)^{1/3} \Lambda_E, & (\text{SU}(2)), \\ \Lambda_M &= \left(2 + \frac{\lambda_{c,E}^3}{720\pi^2}\right)^{1/3} \Lambda_E, & (\text{SU}(3)). \end{aligned} \quad (181)$$

Across the magnetic-center transition the pressure is not continuous. We may, however, estimate the scale Λ_C by assuming thermal equilibrium at the *onset* of this transition. (This assumption underlies Eq. (170).) This gives

$$\Lambda_M \sim 2^{1/3} \Lambda_C, \quad (\text{SU}(2)) \quad \text{and} \quad \Lambda_M \sim \Lambda_C, \quad (\text{SU}(3)). \quad (182)$$

68 *Ralf Hofmann*

6. Thermodynamical quantities

6.1. Results

In this section we present our numerical results for one-loop temperature evolutions of thermodynamical quantities throughout the electric and magnetic phase.

SU(2) case:

In the electric phase the ratio of pressure P and T^4 is given as

$$\frac{P}{T^4} = -\frac{(2\pi)^4}{\lambda_E^4} \left[\frac{2\lambda_E^4}{(2\pi)^6} (2\bar{P}(0) + 6\bar{P}(2a)) + 2\lambda_E \right] \quad (183)$$

where the function $\bar{P}(a)$ and the dimensionless mass parameter a are defined in Eq. (100) and Eq. (99), respectively. In the magnetic phase we have

$$\frac{P}{T^4} = -\frac{(2\pi)^4}{\lambda_M^4} \left[\frac{6\lambda_M^4}{(2\pi)^6} \bar{P}(a) + \frac{\lambda_M}{2} \right] \quad (184)$$

where a is defined in Eq. (149).

In the electric phase the ratio of energy density ρ and T^4 is given as

$$\frac{\rho}{T^4} = \frac{(2\pi)^4}{\lambda_E^4} \left[\frac{2\lambda_E^4}{(2\pi)^6} (2\bar{\rho}(0) + 6\bar{\rho}(2a)) + 2\lambda_E \right] \quad (185)$$

where the function $\bar{\rho}(a)$ is defined as

$$\bar{\rho}(a) \equiv \int_0^\infty dx x^2 \frac{\sqrt{x^2 + a^2}}{\exp(\sqrt{x^2 + a^2}) - 1}. \quad (186)$$

In the magnetic phase we have

$$\frac{\rho}{T^4} = \frac{(2\pi)^4}{\lambda_M^4} \left[\frac{6\lambda_M^4}{(2\pi)^6} \bar{\rho}(a) + \frac{\lambda_M}{2} \right]. \quad (187)$$

The ratio of entropy density and T^3 is given as

$$\frac{s}{T^3} = \frac{1}{T^4} (\rho + P). \quad (188)$$

Because the ground-state contributions cancel in $\frac{s}{T^3}$ this quantity is not as infrared sensitive as, e. g., $\frac{\rho}{T^4}$ or $\frac{P}{T^4}$: Lattice simulations are in a position to correctly measure the entropy density at low temperatures.

SU(3) case:

In the electric phase we have

$$\frac{P}{T^4} = -\frac{(2\pi)^4}{\lambda_E^4} \left[\frac{2\lambda_E^4}{(2\pi)^6} (4\bar{P}(0) + 3(4\bar{P}(a) + 2\bar{P}(2a))) + 2\lambda_E \right] \quad (189)$$

and

$$\frac{\rho}{T^4} = \frac{(2\pi)^4}{\lambda_E^4} \left[\frac{2\lambda_E^4}{(2\pi)^6} (4\bar{\rho}(0) + 3(4\bar{\rho}(a) + 2\bar{\rho}(2a))) + 2\lambda_E \right]. \quad (190)$$

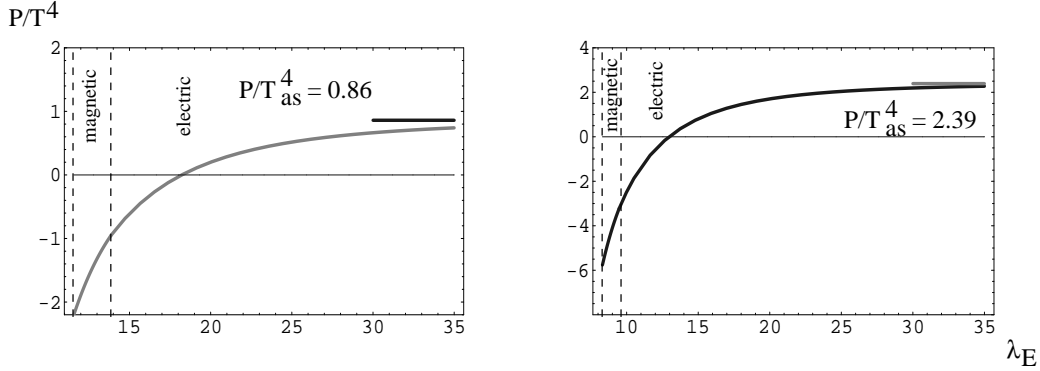


Fig. 22. $\frac{P}{T^4}$ as a function of temperature for SU(2) (left panel) and SU(3) (right panel). The horizontal lines indicate the respective asymptotic values, the dashed vertical lines are the phase boundaries.

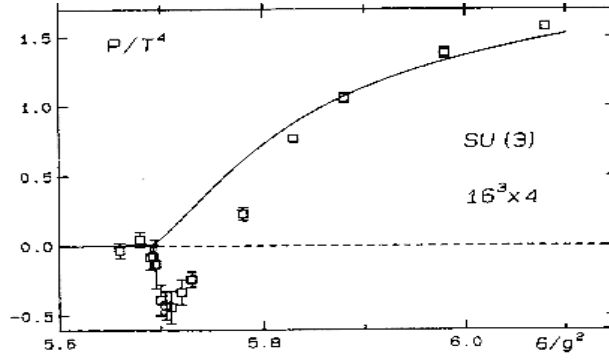


Fig. 23. $\frac{P}{T^4}$ as a function of temperature for SU(3) as obtained on a $(16^3 \times 4)$ -lattice using the differential method with a universal two-loop perturbative β function^{78,79} and using the integral method (solid line)⁸⁰. The figure is taken from⁸⁰.

In the magnetic phase we have

$$\frac{P}{T^4} = -\frac{(2\pi)^4}{\lambda_M^4} \left[\frac{12\lambda_M^4}{(2\pi)^6} \bar{P}(a) + \lambda_M \right] \quad (191)$$

and

$$\frac{\rho}{T^4} = \frac{(2\pi)^4}{\lambda_M^4} \left[\frac{12\lambda_M^4}{(2\pi)^6} \bar{\rho}(a) + \lambda_M \right]. \quad (192)$$

The ratio of entropy density and T^3 is given in Eq.(188) where now the SU(3)-expressions for P and ρ have to be used.

The result for $\frac{P}{T^4}$ is plotted in Fig. 22 as a function of temperature throughout the electric and magnetic phase, Fig. 23 depicts SU(3)-lattice results. Notice that the pressure is negative in the electric phase close to $\lambda_{E,c}$ and even more so in the magnetic phase where the ground state strongly dominates the thermodynamics of

infrared sensitive quantities. Notice also the negative pressure in Fig. 23 obtained close to the phase transition when the differential method is used in the lattice simulation. (For a discussion of differential versus integral method see Sec. 6.2.2.) We conclude that the finite-size constraints of realistic lattices have a severe effect on the obtained values of the pressure shortly above the first confining transition and even more so below this transition.

Let us now discuss the behavior close to $T_{c,M}$ where the thermodynamical relation

$$dP = S dT \quad (193)$$

starts to be violated. Eq. (193) implies that in a homogeneous, thermalized system the pressure needs to be a strictly monotonic increasing function of temperature since S is never negative. Crossing the point $T_{c,M}$ from above, the pressure jumps from a negative to a positive value. (On the magnetic side of the phase boundary the ground state strongly dominates the excitations, on the center side the vortex-condensate has zero pressure while fermionic excitations give a positive contribution.) There are two ways of seeing that thermal equilibrium must break down close to $T_{c,M}$. First, spatial homogeneity starts to be badly violated by discontinuous and local phase changes of the field Φ as soon as the system starts to condense center-vortex loops. The derivation of Eq. (193), however, relies on thermal equilibrium and thus on spatial homogeneity. Second, one may assume thermal equilibrium and then lead this assumption to a contradiction. In thermal equilibrium the spectral density $\rho(E)$ in the center phase is more than exponentially increasing with energy E , see Eq. (178). Thus the partition function diverges at $T = T_H < \Lambda_C$: A homogeneous system would need an infinite amount of energy per volume to increase its temperature beyond T_H . But this is a contradiction to the fact that a magnetic phase exists for $T > T_H$. (In an extended thermalized system the transition from the center phase to the magnetic phase is accomplished by an increase of the overall energy density: The excitation of very massive dual gauge modes, though very unlikely, is furnished energetically by the large energy residing in the system. If the considered system is of a small spatial extent, such as the interaction vertex in a scattering process, then the total energy of the system, e.g., the center-of-mass energy being deposited into a vertex, needs to be larger than the very large mass of the dual gauge modes on the magnetic side of the phase boundary.) Thus thermal equilibrium breaks down for $T \sim T_H$.

The result for $\frac{\rho}{T^4}$ as a function of temperature throughout the electric and magnetic phase is shown in Fig. 24. Fig. 25 depicts an SU(2)-lattice result⁷⁵. Notice the (small) discontinuities at $\lambda_{c,E}$. Their occurrence is explained by the fact that by crossing the electric-magnetic phase boundary the system needs to generate an extra polarization for each dual gauge mode compared to the two polarizations of a TLM mode. Extra polarizations are extra fluctuating degrees of freedom which increase the energy density on the magnetic side of the phase boundary. The situation is somewhat peculiar: On the one hand, the order parameter for the dynamical

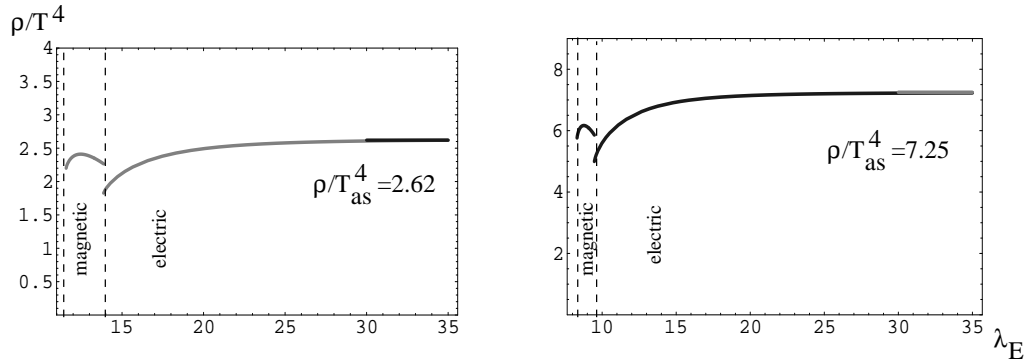


Fig. 24. $\frac{\rho}{T^4}$ as a function of temperature for SU(2) (left panel) and SU(3) (right panel). The horizontal lines indicate the respective asymptotic values, the dashed vertical lines are the phase boundaries.

breaking of the dual gauge groups $U(1)_D$ (SU(2)) and $U(1)_D^2$ (SU(3)) is continuous. On the other hand, there is a small amount of latent heat being released across the *magnetic-electric* transition. (That is, by heating up the system starting in the magnetic phase.) As we shall see in Sec. 7, this is the reason for a dynamical stabilization of the temperature of the cosmic microwave background against gravitational expansion. (Thus we may look forward to enjoy the privilege of the photon's masslessness for another sizable fraction of today's age of the Universe⁸¹.) Again, the energy density is dominated by the ground-state contribution in the electric phase close to the electric-magnetic transition and even more so in the magnetic phase. Notice also that $\rho = -P$ at the point, where the system starts to condense center-vortex loops, that the magnetic phase is narrower for SU(3) than it is for SU(2), and that $\frac{\rho}{T^4}$ dips in a much steeper way at the electric-magnetic transition for SU(3) than for SU(2).

The result for the interaction measure $\frac{\Delta}{T^4} \equiv \frac{(\rho - 3P)}{T^4}$ is shown in Fig. 26. Figs. 27 and 28 are lattice results. Notice the rapid approach to the free-gas limit in Fig. 26 and the large values of $\frac{\Delta}{T^4}$ in the magnetic phase. Interestingly, there is a small bump to the left of the phase boundary in Fig. 27.

The result for the ratio of the specific heat per unit volume $c_V \equiv \frac{d\rho}{dT}$ and T^3 is shown in Fig. 29, Fig. 30 is an SU(2)-lattice result⁷⁵. The quantity $\frac{c_V}{T^3}$ peaks both at the electric-magnetic and the magnetic-center transition. The finite peak at the former phase boundary is in agreement with the electric-magnetic transition being second-order. Moreover, we have $\frac{c_V}{T^3}|_{T_{c,E};SU(3)} \sim 3 \frac{c_V}{T^3}|_{T_{c,E};SU(2)}$. This explains why lattice simulations prefer to identify the confining transition as weakly first order for SU(3), see^{82,83} and references therein. Now, $3 \neq \infty$ but in the vicinity of $T_{c,E}$ lattice results for infrared sensitive quantities, such as $\frac{c_V}{T^3}$, are not reliable anyway.

72 *Ralf Hofmann*

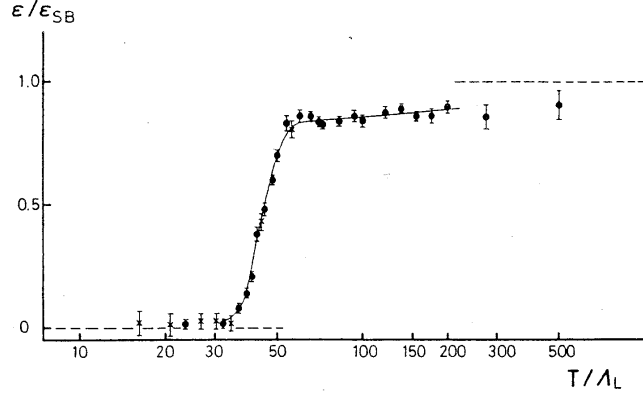


Fig. 11. The ratio ϵ/ϵ_{SB} for a $10^3 \times 3$ lattice versus temperature. The full points are icosahedral, the crosses full SU(2) group Monte Carlo results; the line is a spline fit to the data.

Fig. 25. $\frac{\rho}{T^4}$ as obtained from the SU(2)-lattice simulation in ⁷⁵.

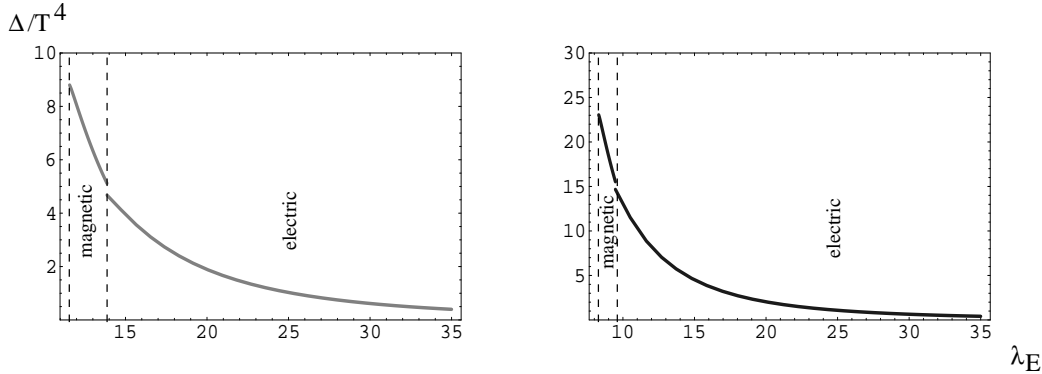


Fig. 26. The interaction measure $\frac{\Delta}{T^4}$ as a function of temperature for SU(2) (left panel) and SU(3) (right panel). The asymptotic value in both cases is $\frac{\Delta}{T^4} = 0$, the dashed vertical lines are the phase boundaries.

The result for $\frac{S}{T^3}$ is shown in Fig. 31. Fig. 32 depicts a lattice result for SU(3) obtained with the differential method ⁷⁸. The entropy density S is a measure for the ‘mobility’ of gauge modes. Notice the jump of S/T^3 which, again, is explained by the additional polarization of the dual gauge mode in the magnetic phase. Notice also that $\frac{S}{T^3}$ vanishes at the point $T_{c,M}$ where the system condenses center vortices. At this point dual gauge modes are infinitely heavy: The thermodynamics is completely determined by the ground state. The numerical agreement between the lattice result (d) (largest lattice) in Fig. 32 and the SU(3)-result in Fig. 31 is striking. The two data points to the left of the jump in (d) indicate that an ambiguity exists for the

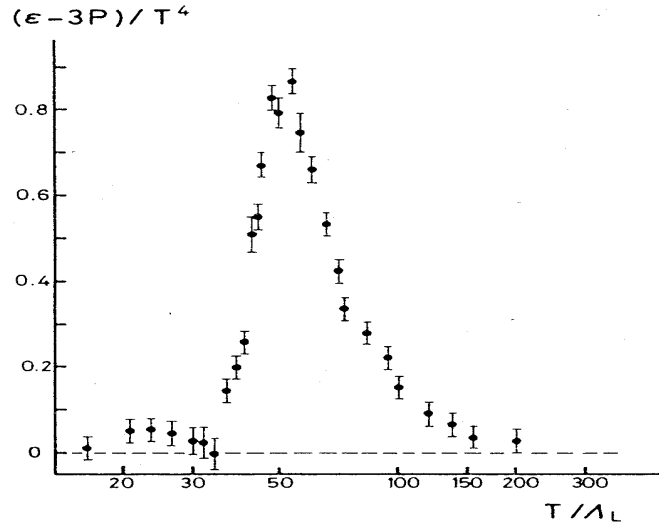


Fig. 15. The difference $(\epsilon - 3P)/T^4$ versus temperature for a $10^3 \times 3$ lattice.

Fig. 27. $\frac{\Delta}{T^4}$ as obtained from the SU(2)-lattice simulation in ⁷⁵.

value of $\frac{S}{T^3}$ very close to the transition. The jump itself corresponds to the large slope of $\frac{S}{T^3}$ on the electric side of the phase boundary in Fig. 31. The observed agreement is explained by the small sensitivity of the quantity $\frac{S}{T^3}$ on the ground-state physics making the finite-volume lattice simulation reliable close to the electric magnetic transition.

The data files needed to generate the plots in Figs. 22, 24, 26, 29, and 31 are provided by the author upon request.

6.2. Comparison with the lattice

6.2.1. Specific observations

SU(2) case:

The results of an early lattice measurements of the energy density ρ and the interaction measure $\Delta \equiv \rho - 3P$ in a pure SU(2) gauge theory were reported in ⁷⁵. In that work the critical temperature T_c for the deconfinement transition was determined from the critical behavior of the Polyakov-loop expectation and the peak position of the specific heat using a Wilson action. The function $\Delta(T)$ was extracted by multiplying the lattice β function with the difference of plaquette expectations at finite and zero temperature (symmetric lattice). This assures that Δ vanishes for $T \rightarrow 0$. What is subtracted in ⁷⁵ at finite T is, however, *not* the value $\Delta(T = 0)$ since the plaquette expectation on the symmetric lattice is multiplied with the *finite-T* value of the β function. Apart from this approximation, the use of a perturbative

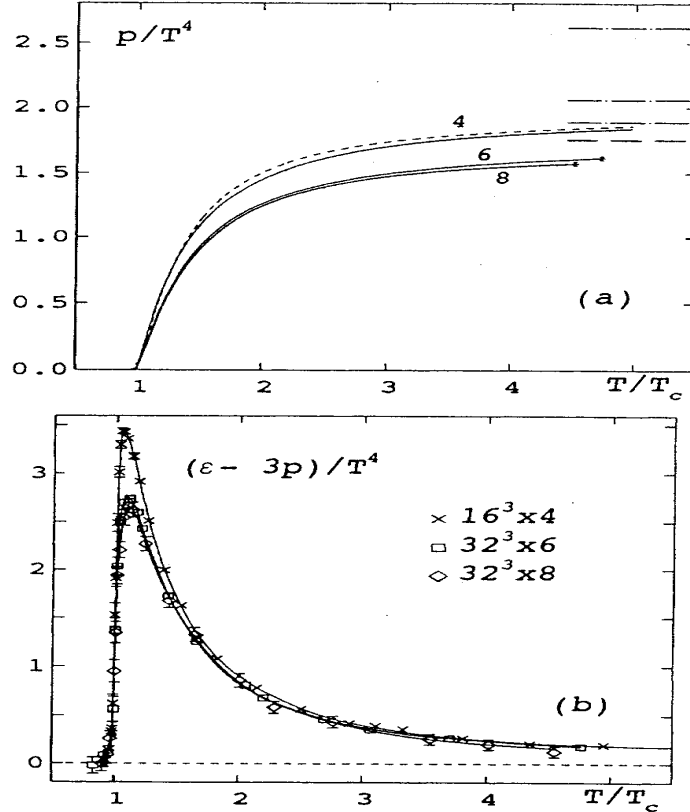


FIG. 2. (a) The pressure versus T/T_c for $N_\tau = 4, 6,$ and $8,$ integrating the interpolations for the action density. Solid curves show our parametrization. The dashed curve for $N_\tau = 4$ is the result of using the temperature scale from the effective coupling scheme. The horizontal dash-dotted lines show the ideal gas values for $N_\tau = 4, 6,$ and $8;$ the horizontal dashed line is the continuum value. In (b) we show the difference $(\epsilon - 3p)/T^4.$

Fig. 28. $\frac{P}{T^4}$ and $\frac{\Delta}{T^4}$ as obtained from the SU(3)-lattice simulation in ⁷⁶.

β function was assumed for all temperatures. The simulation was carried out on a (rather small) $(10^3 \times 3)$ -lattice.

Let us compare our results with those of ⁷⁵. The lattice results for ρ in ⁷⁵ differ drastically from our results for temperatures close the first confinement, that is, the electric-magnetic transition. (The lattice is doomed to produce incorrect results for infrared sensitive quantities close to the electric-magnetic transition and in the magnetic phase: A finite spatial lattice size L cuts off *physical* correlations on length scales $> L$ since the correlation length $l_M = M_m^{-1} > L$ close to the electric-magnetic transition and $l_M = \infty$ in the magnetic phase. Here M_m denotes the mass of a magnetic monopole.)

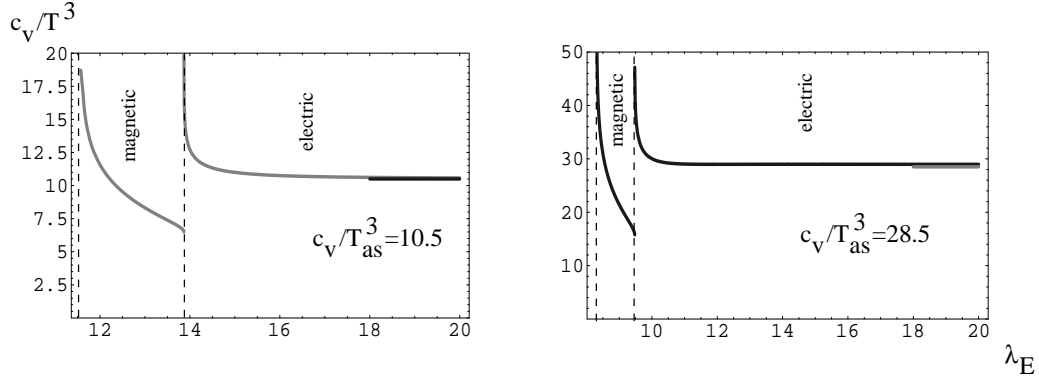


Fig. 29. $\frac{c_V}{T^3}$ as a function of temperature for SU(2) (left panel) and SU(3) (right panel). The horizontal lines signal the respective asymptotic values, the dashed vertical lines are the phase boundaries.

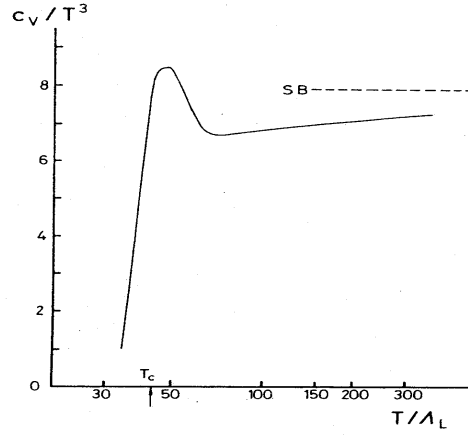


Fig. 12. The specific heat per unit volume divided by T^3 versus temperature, obtained from the fit in fig. 11 to ϵ/ϵ_{SB} .

Fig. 30. $\frac{c_V}{T^3}$ as obtained from the SU(2)-lattice simulation in 75.

We obtain

$$\frac{\rho}{\rho_{SB}} \Big|_{T \sim 1.5 T_{c,E}} \sim 1.27, \quad (194)$$

where $\rho_{SB} \equiv \frac{\pi^2}{5} T^4$ denotes the Stefan-Boltzmann limit (ideal gas of three species of massless gluons with two polarizations each). On the lattice this ratio is measured to be smaller than unity: $\frac{\rho}{\rho_{SB}} \Big|_{T \sim 1.5 T_{c,E}} = 0.84$. At $T \sim 5 T_{c,E}$ we obtain

$$\frac{\rho}{\rho_{SB}} \Big|_{T \sim 5 T_{c,E}} \sim 1.33 \quad (195)$$

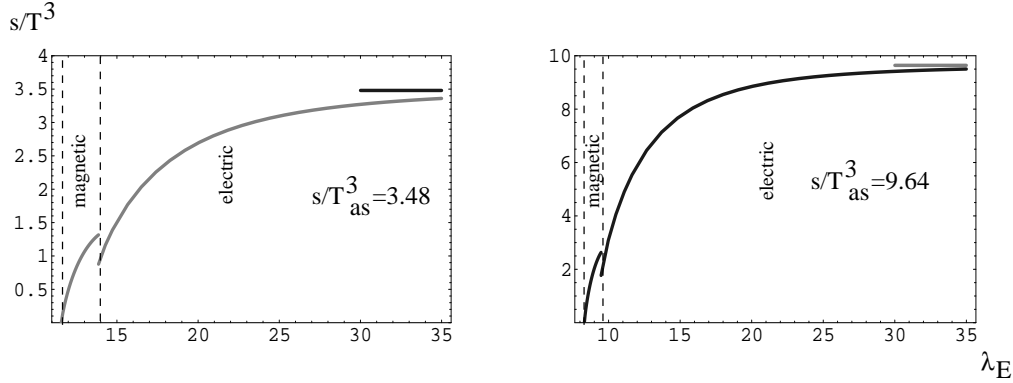
76 *Ralf Hofmann*


Fig. 31. $\frac{s}{T^3}$ as a function of temperature for SU(2) (left panel) and SU(3) (right panel). The horizontal lines signal the respective asymptotic values.

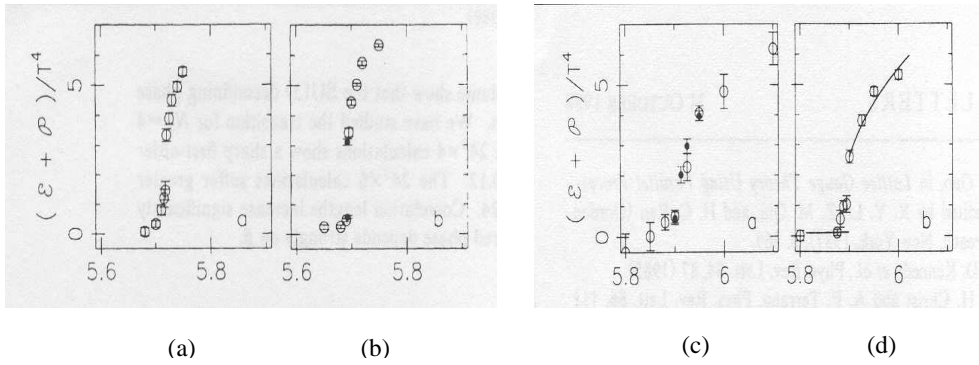


Fig. 32. $\frac{s}{T^3}$ as a function of β obtained in SU(3) lattice gauge theory using the differential method and a perturbative beta function⁷⁸. The simulations were performed on (a) $16^3 \times 4$ -, (b) $(24^3 \times 4)$ -, (c) $(16^3 \times 6)$ - (open circles) and $(20^3 \times 6)$ - (closed circles), and (d) $(24^3 \times 6)$ -lattices. Using the $(24^3 \times 6)$ -lattice, the critical value of β is between 5.8875 and 5.90.

while the lattice measures $\left. \frac{\rho}{\rho_{SB}} \right|_{T \sim 5 T_{c,E}} = 0.85$.

Our results for the pressure P are *negative* for T close to $T_{c,E}$ (see Fig. 22) – much in contrast to the positive values obtained in⁷⁵. At $T \sim 5 T_{c,E}$ we obtain

$$\left. \frac{P}{P_{SB}} \right|_{T \sim 5 T_{c,E}} \sim 1.31 \quad (196)$$

while the lattice measures $\left. \frac{P}{P_{SB}} \right|_{T \sim 5 T_{c,E}} \sim 0.88$. (On the lattice P is extracted from the measured values of Δ and ρ , and $P_{SB} \equiv \frac{\pi^2}{15} T^4$ denotes the Stefan-Boltzmann limit.)

Notice that the results in Eq.(195) and Eq.(196) are very close to the ratio

$\frac{2 \times 3 + 2}{6} \frac{4}{3}$ of the number of degrees of freedom in a gas of two species of (nearly) massless gluons (three polarizations per species) and one massless species and a gas of massless gluons. (At $\lambda_E \sim 75$ the value of the mass parameter is $a \sim 2\pi \frac{5.5}{650} \sim 0.086$. Thus the Boltzmann suppression is small for TLH modes, compare also with Fig. 26.) At extremely high temperatures a TLH mode ‘remembers’ its massiveness at low temperatures in terms of an extra polarization. The latter originates from a tiny mass which solves the infrared problem of loop expansions, for formal arguments see ⁵⁰.

The peak-value of the specific heat is about $\frac{c_V}{T^3} \Big|_{T_{c,E}} \sim 20$ while it is measured to be ~ 8 on the lattice. Moreover, we have $\frac{\Delta}{T^4} \Big|_{T_{c,E}} \sim 4.8$ while the lattice obtains a value ~ 0.85 . The much lower values obtained on the lattice are not surprising: Finite lattice sizes cut off existing long-range correlations at $T_{c,E}$.

No result for the entropy density was directly reported in ⁷⁵.

SU(3) case:

Here we discuss the results obtained in ⁷⁶ with a Wilson action on the lattice of the largest time extension, $N_\beta = 8$, and the results obtained in ^{79,78}.

In the vicinity of the transition point $T_{c,E}$ the situation for both ρ and P is similar to the SU(2) case: Drastic differences between the lattice measurements and our results occur. Again, P is negative close to $T_{c,E}$ contradicting the positive values obtained with the integral method in ⁷⁶. A lattice simulation ⁷⁹ of P , which used the differential method, has reported negative pressure for T shortly above the transition already in 1988. The most negative value of $P/T^4 \sim -0.5$ obtained in ⁷⁹ very close to the phase transition is down by a factor of about 0.19 as compared to our result at the electric-magnetic transition, see Figs. 22 and 23. Again, this is explained by the finite lattice-size cutoff on physical long-range correlations. The lattice-result obtained with the integral method ⁷⁶ is by construction positive definite, see Sec. 6.2.2, and thus it is *unphysical*. For that reason we renounce a (useless) comparison of our results for pressure, energy density, and interaction measure with those obtained in ⁷⁶. In ⁷⁹ only the dependence of $\frac{P}{T^4}$ on the lattice coupling was presented. One can use Fig. 23 and the temperature dependence of $\frac{P}{T^4}$ in Fig. 28 to gauge particular values of this quantity against temperature. (In both simulations ⁷⁹ and ⁷⁶ the universal part of the two-loop perturbative β function was used to relate lattice coupling to lattice spacing.) For example, a value of $\frac{P}{T^4} \sim 1.6$ in ⁷⁹ corresponds to a value $\frac{P}{T^4} \sim 1.5$ in ⁷⁶. The latter is associated with a temperature $T = 3.2 T_{c,E}$ by virtue of Fig. 28. We have

$$\frac{P}{T^4} \Big|_{T \sim 3.2 T_{c,E}} \sim 2.2. \quad (197)$$

This is larger than the result obtained in ⁷⁹ and explained by the insufficient account of infrared correlations in the lattice simulation. These correlations generate masses for six out of eight gluon species, thus extra polarizations, and therefore a larger value for $\frac{P}{T^4}$.

78 *Ralf Hofmann*

Our asymptotic ($\lambda_E = 35$) values for P and ρ are

$$\left. \frac{P}{P_{SB}} \right|_{as} \sim 1.30, \quad \left. \frac{\rho}{\rho_{SB}} \right|_{as} \sim 1.37, \quad (198)$$

where $\rho_{SB} = \frac{8}{15}\pi^2 T^4 = 3P_{SB}$. Both values in Eq. (198) are close to the ratio $R = \frac{11}{8} = 1.375$ of the numbers of polarization in a free gluon gas, where six gluon species have a tiny mass, and in a free gluon gas where all gluon species are massless.

The entropy density approaches zero for $T \searrow T_{c,M}$, see Fig. (31). This expresses the fact that dual gauge modes are decoupled (infinite masses): The ground state strongly dominates the thermodynamics.

6.2.2. *Differential versus integral method*

What are the reasons for the qualitative difference between the pressure-results obtained in ^{76,77} using the integral method and in ^{78,79} using the differential method? While the differential method is based on the definition

$$P = T \frac{\partial \ln Z}{\partial V}, \quad (199)$$

which is proper for a lattice of *finite* volume V , the integral method assumes the thermodynamical limit $V \rightarrow \infty$ from the start. In this limit one has

$$P = T \frac{\ln Z}{V}, \quad (200)$$

and thus the pressure equals minus the free energy density. In Eqs. (199) and (200) Z denotes the partition function.

The official reason for the introduction of the integral method, see for example ⁸⁰, was that one wanted to avoid the use of the imprecisely known β function in the strong-coupling regime of the theory. (Based on the definition in Eq. (199), the β function multiplies the sum of spatial and time plaquette averages in the expression for the pressure.) When using the definition in Eq. (200), the derivative of the pressure with respect to the bare coupling $\bar{\beta}$ ($\bar{\beta} = \frac{6}{g^2}$ for SU(3)) can be expressed as an expectation over minus the sum of spatial and time-like plaquettes without the beta-function prefactor. Thus the pressure is, up to an unknown integration constant, obtained in terms of an integral of a sum of plaquette averages over β . The integration constant is chosen in such a way that the pressure vanishes at a temperature well below T_c . Instead of only integrating over minus the sum of spatial and time-like plaquette expectations an extra term was added to the *integrand* ^{76,77} to assure that the pressure vanishes at $T = 0$. The added term equals twice the plaquette expectation taken on a symmetric lattice (the expectation at $T = 0$). We stress that this prescription does not follow from the definition in Eq. (200). Moreover, the assumption that $P = 0$ for $T \sim 0.8 T_c$ or so is a strong bias. (There are massless fermionic particles in the center phase which keep the total pressure positive for temperatures comparable to this value.)

The results for $P(T)$ obtained when using the integral method show a rather large dependence on the spatial size and the time extent N_τ of the lattice⁷⁶. We believe that this reflects the considerable deviation from the assumed thermodynamical limit for realistic lattice sizes. The problem was addressed in⁷⁷ where a correction factor r was introduced to relate P , obtained with the integral method, to P , obtained with the differential method. For a given value of N_τ the factor r was determined from the pressure-ratio at $\bar{g} = 0$. Subsequently, this value of r was used at *finite* coupling \bar{g} to extract the spatial anisotropy coefficient c_σ (essentially the β function) by demanding the equality of the pressure obtained with the integral and the differential method. In doing so, twice the plaquette expectation at $T = 0$ was, again, added to minus the sum of spatial and time-like plaquette expectations in the differential-method expression for the pressure. It may be questioned whether a simple correction factor r does correctly account for finite-size effects and, if yes, whether it is justified to determine r in the limit of noninteracting gluons. (The c_σ -values obtained in this way do not coincide with those obtained in⁸⁵.) In addition, it seems that the imprecise knowledge of the β function, which contains information about fluctuations in the ultraviolet, is much less of a problem for a lattice simulation of the pressure than the missing infrared physics is (finite lattice size)⁸⁴.

Using the universal part of the two-loop perturbative beta function in the differential method, negative values for the pressure were obtained for T close to T_c in⁷⁹. Moreover, a rapid approach of ρ and P to their respective free-gas limits was observed. This is in qualitative (but not quantitative) agreement with our results, see Figs. 26, 22, and 24.

7. Implications for particle physics and cosmology

In this section we provide outlooks on the implications of the nonperturbative approach to SU(2) and SU(3) Yang-Mills thermodynamics in view of so-far unexplained phenomena in particle physics and cosmology. The way of how selected problems are addressed in this section is preliminary, mostly qualitative and thus should not be understood as the final say on the matter. Rather, we try to provide a certain amount of stimulus for future developments.

7.1. A Planck-scale axion: Cosmic coincidence today and CP violation

Among the gauge groups SU(N) (N finite) we regard SU(2) and SU(3) as particular due to their unique phase diagrams. We have come to appreciate that nature seems to prefer situations with a unique outcome. Thus we tend to believe that dynamics subject to a finite gauge symmetry, that is, dynamics below the Planck scale $M_P \sim 1.2 \times 10^{19}$ GeV, obeys the SU(2) or SU(3) gauge principle. A possible scenario would be that at M_P an SU(N) gauge symmetry ($N = \infty$) is dynamically broken into a four-dimensional low-energy manifestation involving several SU(2) and SU(3) factor

groups, which can behave in an electric-magnetically dual way to one another, and into nonfluctuating gravity.

This set-up may, in fact, be described by the low-energy sector of a bosonic string theory whose vacuum instability is resolved in terms of tachyon condensation in the presence of a D-brane⁸⁶. A low-energy Kaluza-Klein^{64,65} compactification of the Weyl-invariant and thus d -dimensional bosonic string theory (in a flat background $d = 26$) to four dimensions yields gauge symmetries which are associated with the isometries of the $d-4$ dimensional compactification manifold: We assume that these isometries are products of SU(2) and SU(3) corresponding to a compactification manifold which, locally, is $S_3 \times (S_3 \times S_5) \times \dots$ ^{60,59}. In addition, there are a low-mass scalar dilaton field φ and a massless antisymmetric tensor $B_{\mu\nu}$. While the former may drive the monopole condensation process within, say, an SU(2) theory of Yang-Mills scale $\Lambda_1 \sim M_P$ and thus may trigger the inflation of the Universe (making it spatially flat) the latter may be responsible for adiabatically generated density perturbations⁸⁷.

The scales of the SU(2) and SU(3) factors would dynamically be set into a certain hierarchy: $\Lambda_1 \sim M_P > \Lambda_2 > \dots > \Lambda_{\text{CMB}}$. The scale Λ_{CMB} is associated with an SU(2) theory that is not confining at the present temperature of the Universe: Being *at* the electric-magnetic transition this theory generates the photon as its only massless excitation, see Sec. 7.2. Being in its center phase at a temperature $T \sim \Lambda_1 \sim M_P$, $SU(2)_1$ generates fermions by re-heating (single and self-intersecting center-vortex loops). Because $SU(2)_1$ used to be part of $SU(N = \infty)$ and thus was mixing with the other factors these fermions couple to the gauge fields of these factors. Since higher-charge states (self-intersecting center-vortex loops) with opposite charges are generated in equal amounts we would expect that they quickly annihilate into charge-zero states (no self-intersections). (Re-creation of higher-charge states after annihilation is less likely due to the redshift of the spectrum by the rapid power-law expansion of the Universe furnished by a free-gas equation of state. The latter originates from the gauge-mode excitations of the other factors). Although the massless fermions (single center-vortex loops) do not couple to the propagating gauge fields of the other factors by naked gauge charges they do so by their dipole moments. Considering these massless fermions to be fundamental, there is a global, axial U(1) symmetry which, however, is dynamically broken⁸⁸ and anomalous due to the calorons of the other factors^{89,90}.

Integrating out $SU(2)_1$'s massless fermions, the relevant composite field is a (canonically normalized) axion field a whose coupling to the gauge fields of the other factors is

$$\mathcal{L}_{a.a.} = \frac{a}{F} \sum_{i=2}^{\text{CMB}} \text{tr} \tilde{F}_{\mu\nu,i} F_{\mu\nu,i} \quad (201)$$

where $F \sim M_P$ denotes the Peccei-Quinn scale⁹¹: The scale at which $SU(2)_1$'s fermions come into existence and which measure the magnitude of the Cooper-pair condensate involving the massless species. The sum is over the other factors, and

$\tilde{F}_{\mu\nu,i} = \frac{1}{2} \epsilon_{\mu\nu\alpha\beta} F_{\alpha\beta,i}$ is the dual field strength. Eq. (201) represents a term in the action for the other factors (deconfining at $T \sim M_P$) which violates parity (P) and charge conjugation (C) symmetries.

While a would be a massless phase if the axial anomaly was absent and the axial U(1) only was broken dynamically the anomaly-induced coupling in Eq. (201) gives rise to an axion potential $V_a = \sum_{i=2}^{\text{CMB}} V_{a,i}$. The operator $\text{tr} \tilde{F}_{\mu\nu,i} F_{\mu\nu,i}$ measures the average topological charge density carried by *propagating* gauge fields. This is a conserved quantity for $T \gg \Lambda_i$, and thus it is independent of temperature. Integrating over topologies and accounting for dimensional transmutation we have

$$V_{a,i} \sim \begin{cases} (1 - \cos \frac{a}{F}) \Lambda_i^4, & (\text{theory } i \text{ in electric or magnetic phase}), \\ 0 & (\text{theory } i \text{ in center phase}). \end{cases} \quad (202)$$

For a smaller (but not much smaller) than F the cosine in Eq. (202) can be expanded, and the axion mass-squared at $T \sim M_P$ reads

$$m_a^2 \sim \frac{1}{F^2} \sum_{i=2}^{\text{CMB}} \Lambda_i^4 \sim \sum_{i=2}^{\text{CMB}} \frac{\Lambda_i^4}{M_P^2}. \quad (203)$$

As the temperature of the Universe falls below Λ_2 the associated theory fails to contribute to the axion mass-squared and so forth.

Now in an expanding Friedmann-Robertson-Walker Universe the (spatially homogeneous) axion field a satisfies the following equation of motion

$$\ddot{a} + 3H\dot{a} + m_a^2 a = 0. \quad (204)$$

The Hubble parameter $H \equiv \frac{\dot{R}}{R} = \sqrt{\frac{8\pi\rho(T)}{3M_P^2}}$ is determined by the energy density $\rho(T) = \sum_{i=2}^{\text{CMB}} \rho_i(T)$ of the Universe. At $T \sim M_P$ this energy density is given by the Stefan-Boltzmann limit of the theories $i = 2, \dots, \text{CMB}$ if the hierarchy between M_P and Λ_2 is sufficiently large. (The SU(2) theory with $i = 1$ went center, subsequently experienced a strong dilution of its massive excitations, and does not produce a ground-state contribution to ρ at $T \sim M_P$.) We have $\rho_i(T) = \frac{4\pi^2}{15} T^4$ (SU(2)) and $\rho_i(T) = \frac{11\pi^2}{15} T^4$ (SU(3)). Thus H is radiation-dominated at $T \sim M_P$ and $H^2 \gg m_a^2$. But this means that a is frozen to the slope of its potential with an amplitude $a \sim M_P$. For $T \sim \Lambda_2$ the Universe's energy density remains radiation-dominated. The axion mass-squared, however, is reduced by the value $\frac{\Lambda_2^4}{M_P^2}$ since the theory with $i = 2$ went center. If $\Lambda_2 \ll M_P$ then the mass-squared $\sim \sum_{i=3}^{\text{CMB}} \frac{\Lambda_i^4}{\Lambda_2^2}$ of the axion generated by the theory with $i = 2$ is much larger than H^2 . By Eq. (204) this means that this axion rapidly relaxes to the minimum of its potential and thus is irrelevant for subsequent cosmology. Moreover, the fermions generated by the center transition of the theory with $i = 2$ exhibit a large asymmetry in fermion number. This is qualitatively true since all three Sakharov conditions⁹² are satisfied: (i) the center transition is nonthermal (Hagedorn), (ii) there is a local violation of fermion number since fermions are nonlocal objects, and (iii) the generation of fermions takes place in the presence of CP violation (the frozen-in Planck-scale axion a).

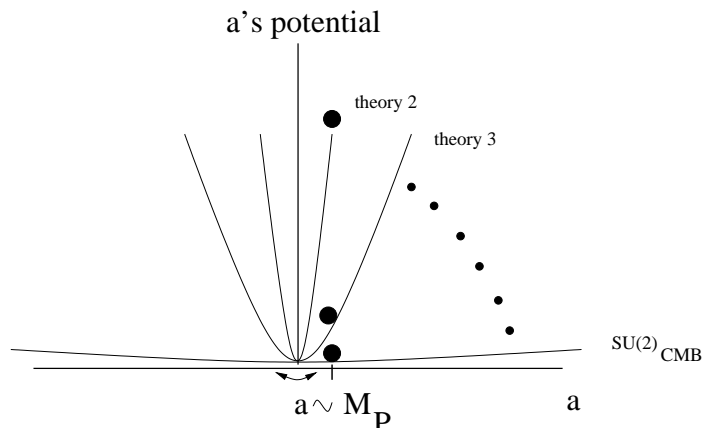


Fig. 33. The fate of a Planck-scale axion along the Universe's evolution. At temperatures sizably larger than T_{CMB} the axion is frozen to the slope of its potential by cosmological friction ($H \gg m_a$), for $T \sim T_{\text{CMB}}$ axion mass and Hubble parameter become comparable: The axion starts to roll down its potential.

This goes on until $T = T_{\text{CMB}}$ where the last theory in the chain, $\text{SU}(2)_{\text{CMB}}$, is close to its center transition (more specifically, at the electric-magnetic phase boundary today), see Fig. 33. Here H^2 is dominated by the ground-state energy. We have

$$H^2 \sim \frac{8\pi}{3} \frac{4\pi T_{\text{CMB}} \Lambda_{\text{CMB}}^3 + \rho_V + \rho_K}{M_{\text{P}}^2} \gtrsim m_a^2 \sim \frac{\Lambda_{\text{CMB}}^4}{M_{\text{P}}^2}. \quad (205)$$

In Eq. (205) ρ_V denotes the energy density associated with the value of the axion potential at T_{CMB} , and ρ_K is an energy density due to axion rolling. Both contributions are comparable since H is not much larger than m_a , compare with Eq. (204). The formerly frozen-in axion field a slowly starts to roll down its potential. While ρ_V has an equation of state $\rho_V = -P_V$ the kinetic contribution ρ_K is associated with an equation of state $P_K = 0$ which is the same as that of nonrelativistic matter.

Cosmic coincidence may have an explanation in terms of a Planck-scale axion and an $\text{SU}(2)$ Yang-Mills theory of scale Λ_{CMB} comparable to the present temperature of the CMB. For related ideas see ⁹³. The alert reader may object that the θ angle in Quantum Chromodynamics (QCD) is constrained to be an extremely small number by a measurement of the neutron's electric dipole moment. On the other hand, the mass of the η' is much larger than the pion mass. Thus one would conclude that the Planck-scale axion is irrelevant in the former while it is relevant in the latter case. What is the resolution of this puzzle? The electric dipole moment of the neutron is measured with a photon of momentum much smaller than the QCD confinement scale. Thus this photon does not probe a phase of QCD with propagating gauge bosons: The operator $\tilde{F}_{\mu\nu} F_{\mu\nu}$ has a vanishing expectation. The η' , on the other hand, is generated in a scattering process involving propagating gluons: Inside the vertex the operator $\tilde{F}_{\mu\nu} F_{\mu\nu}$ has a finite expectation.

We will see in Sec. 7.2 that the ground-state contribution of $\text{SU}(2)_{\text{CMB}}$ in the

absence of the Planck-scale axion is small in comparison with the measured value of today's cosmological constant. The scenario outlined above does not yet explain the origin of *clustering* dark matter as it is observed in the anomalous rotation curves of galaxies but we will see below that the decoupled TLH modes of $SU(2)_{\text{CMB}}$ are candidates for this form of matter.

7.2. Electroweak sector of the Standard Model: Nature of leptons, electroweak symmetry breaking, masses of intermediary vector bosons, intergalactic magnetic fields, and solar wind

Here we would like to propose a formulation of the electroweak sector of the Standard Model in terms of pure $SU(2)$ Yang-Mills theories.

$SU(2)_{\text{CMB}}$:

Let us first discuss the $U(1)_Y$ factor of the electroweak gauge group $SU(2)_W \times U(1)_Y$. We claim that this factor is the unbroken subgroup of an $SU(2)$ Yang-Mills theory of scale comparable to that of the CMB temperature: $T_{\text{CMB}} = 2.728 \text{ K} = 2.351 \times 10^{-4} \text{ eV}$. Only one point in the phase diagram of this theory exists, the boundary between the electric and magnetic phases, where this claim is in accord with observations: The photon is unscreened and practically massless ($m_\gamma < 10^{-14} \text{ eV}$ from a precision measurement of the Coulomb potential⁹⁴, see⁹⁵ for a discussion on why stronger bounds are unreliable), see Fig. 14. Thus we identify $T_{\text{CMB}} = T_{c,E}$. Notice that isolated charges in the electric phase of $SU(2)_{\text{CMB}}$ have a dual interpretation: What is a magnetic monopole in $SU(2)$ is an electrically charged particle w.r.t. $U(1)_Y$.

The energy density ρ^{gs} of the ground-state at T_{CMB} is $\rho^{gs} = 4\pi T_{\text{CMB}} \Lambda_E^3 = 4\pi \times (2.351 \times 10^{-4} \text{ eV}) \Lambda_E^3 = 2\lambda_{c,E} \Lambda_E^4 = 27.7 \Lambda_E^4$. Moreover, we have $\Lambda_E = 1.065 \times 10^{-4} \text{ eV}$. Substituting this into ρ^{gs} , we have $\rho^{gs} = (2.444 \times 10^{-4} \text{ eV})^4$. This is about 0.36% of the commonly accepted value of today's dark energy density $(10^{-3} \text{ eV})^4$. The dominating, missing part would be generated by a slowly rolling Planck-scale axion, see Sec. 7.1.

An immediate question to answer is why the masslessness and the unscreened propagation of the photon is a singled-out situation. The answer to this question is encoded in Fig. 24: The energy density of an $SU(2)$ Yang-Mills theory dips at the electric-magnetic phase boundary. On the electric side this is explained by the thermodynamical decoupling of TLH modes, on the magnetic side an extra polarization, which costs energy, needs to be generated for the photon. To facilitate the jump in energy density for $SU(2)_{\text{CMB}}$ to reach the magnetic phase thermal equilibrium needs to be violated by the eventually fast rolling Planck-scale axion. The photon acquires mass and the ground state becomes superconducting (electrically charged monopoles condense). It is suggestive that the occurrence of intergalactic magnetic fields is related to the Universe being slightly out of thermal equilibrium due to (slow) axion rolling today.

At T_{CMB} TLH modes decouple thermodynamically. Recall that their mass is

given by $m_{\text{TLH}} = 2e|\phi|$ and $e_{dec} = \infty$ at $T_{c,E} = T_{\text{CMB}}$. In the real world e_{dec} is large but not infinite because $\text{SU}(2)_{\text{CMB}}$ is not the only Yang-Mills theory in the Universe. Taking $e_{dec} \sim 10^6$, say, the mass of a decoupled TLH mode is $m_{\text{TLH}} \sim 57 \text{ eV}$. (The reason why we chose this value for e_{dec} is mildly justified by our discussion of the gauge group $\text{SU}(2)_e$ below.) Since the two TLH modes do not interact and thus are stable (no decay into light fermions is possible because $\text{SU}(2)_{\text{CMB}}$ is not in its center phase yet) they yield a tiny contribution to clustering dark matter.

Finally, we would like to make a remark concerning the observed large-angle anomaly in the temperature-(electric)polarization cross correlation seen by WMAP 96. The standard explanation is that this effect is generated by CMB photons scattering off electric charges which are released by an early re-ionization of the interstellar medium at redshift $z \sim 10 - 20$. We would like to propose that CMB photons scatter off electrically charged and dilute monopoles at temperatures $> T_{\text{CMB}}$ which are condensed at T_{CMB} . Since static magnetic (electric with respect to $\text{SU}(2)$) fields are completely screened in the photon propagator deep inside the electric phase of $\text{SU}(2)_{\text{CMB}}$, see Eq. (112), the effect should be weaker in the temperature-(magnetic)polarization cross correlation.

$\text{SU}(2)_e \times \text{SU}(2)_\mu \times \text{SU}(2)_\tau$:

To relate the existence and the interactions of leptons, as they are described by the electroweak sector of the Standard Model (SM), of which Quantum Electrodynamics (QED) is an integral part, with pure $\text{SU}(2)$ Yang-Mills dynamics is motivated by the following observations. (i) The masses of charged leptons are unexplained parameters in the SM. In particular, their small values on the scale of their apparent pointlikeness is unexplained. (ii) No deeper explanation for the value of the magnetic dipole moment of a charged lepton other than that following from the Dirac equation and small radiative corrections is given. (iii) There are experimental indications that scattering processes involving the electron or the positron do not obey the QED predictions if the momentum transfer is close to the mass of a charged lepton. (iv) No Higgs particle has been observed experimentally up to a hypothetical Higgs mass of $\sim 115 \text{ GeV}$ suggesting that electroweak symmetry breaking takes place by a different mechanism than assumed in the SM. (v) The naive ground state of the SM generates a cosmological constant which is many orders of magnitude larger than the observed value.

Points (i), (ii), (iv), and (v) are undisputed facts. To see that there is some truth to point (iii) we present experimental results. In Fig. 34 a plot of the ratio of experiment to theory of the wide-angle e^+e^- pair-creation cross section through γ scattering off of the field of a carbon nucleus is shown as a function of the invariant mass M of the created lepton pair. Notice the substantial deviation from unity for $M \sim 2m_\mu \dots 4m_\mu \sim (210 \dots 420) \text{ MeV}$. Notice also that for $M > 500 \text{ MeV}$ theory and experiment do agree. A much more drastic deviation within the same kinematic regime was seen earlier in 98. This, however, was not confirmed in 97.

In Fig. 35 a plot of the differential cross section for e^-e^- scattering (electron in-

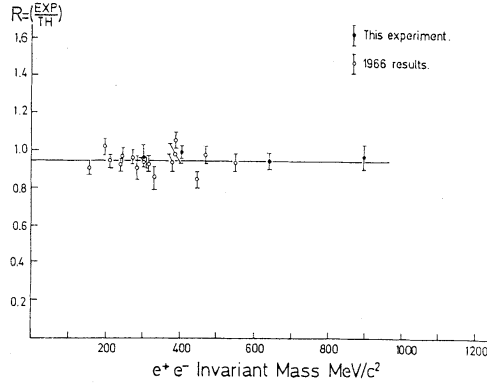


FIG 2. The ratio R of experiment to theory is shown for this measurement together with our earlier results. The normalization uncertainty of $\approx 5\%$ is not included.

Fig. 34. Ratio of experiment to theory of the wide-angle e^+e^- pair-creation cross section by γ scattering off the field of a carbon nucleus as a function of the invariant mass M of the lepton pair. Plot taken from ⁹⁷.

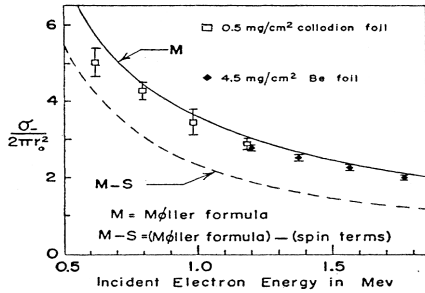


FIG. 5. Comparison with theory of the measured absolute differential electron-electron scattering cross section at $\nu=0.5$ as a function of the kinetic energy of the incident electron taken with the 270° apparatus.

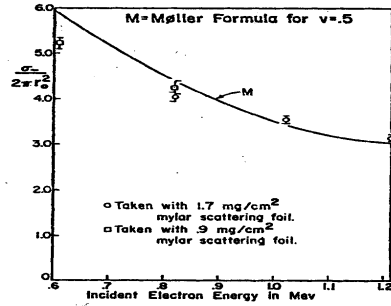


FIG. 6. Comparison with theory of the measured absolute differential electron-electron scattering cross section at $\nu=0.5$ as a function of the kinetic energy of the incident electron taken with the 180° apparatus.

Fig. 35. Møller scattering of electrons, for an explanation see text. Taken from ⁹⁹.

cident on an atomic electron of a target) at a fixed fraction $\nu = 0.5$ of the incident kinetic energy E_{kin} transferred in the collision is shown for $0.6 \text{ MeV} \leq E_{\text{kin}} \leq 1.7 \text{ MeV}$ taken with a 270° apparatus (left panel) and for $0.6 \text{ MeV} \leq E_{\text{kin}} \leq 1.2 \text{ MeV}$ taken with a 180° apparatus (right panel) ⁹⁹. The solid line indicates the theoretical result obtained by using the Møller formula. Notice the agreement with QED for large values of E_{kin} (in particular in the left panel of Fig. 35). In ¹⁰⁰ the differential cross section for Møller scattering was measured for $E_{\text{kin}} = 15.7 \text{ MeV}$ as a function of the scattering angle and found to be in agreement with QED on the 0.4% error level.

The disagreement at the lowest value $E_{\text{kin}} = 0.6 \text{ MeV}$ in Fig. 35, which corresponds to a center-of-mass energy of about $2.5 m_e$, is conspicuous.

If the Yang-Mills scales of the factors $SU(2)_e$, $SU(2)_\mu$, and $SU(2)_\tau$ are about m_e , m_μ , and m_τ , respectively, then the masses of the charge-one states in the center phase of each theory, see Fig. 20, are determined to be these values. Since $T_{\text{CMB}} \ll m_e, m_\mu, m_\tau$ these theories are in their center phases. By looking at Fig. 20 a g -factor of two is imperative by the assignment of angular momentum one half in the presence of one unit of (electric) center flux in the vortex loop. The latter generates the lowest nonvanishing quantum of magnetic moment (Bohr magneton). Notice that Fig. 20 provides for an intuitive manifestation of the concept of spin-1/2: Inside the intersection core the center flux is diverted to the right above and to the left below such that an eddy is generated. The latter carries the electric charge of the soliton.

Let us now give some qualitative arguments why the gauge group $SU(2)_{\text{CMB}} \times SU(2)_e \times SU(2)_\mu \times SU(2)_\tau$ together with a Planck-scale axion may be a viable candidate to describe the phenomenology of electroweak interactions. Why do the photon ($SU(2)_{\text{CMB}}$) and the massive intermediate vector bosons (magnetic and electric phase of $SU(2)_e$) couple to the charge and/or the magnetic moment of charge-one and charge-zero states? The answer to this question is rooted in the symmetry breakdown at $T \sim M_P$ where the factors $SU(2)_{\text{CMB}}$, $SU(2)_e$, $SU(2)_\mu$, and $SU(2)_\tau$ were generated out of one large gauge group whose gauge bosons were mixing. (In the SM the mixing of the 'photon' of $U(1)_Y$ with that of $SU(2)_W$ is parametrized by the Weinberg angle θ with $\sin^2 \theta = 0.23$.) The interaction of the photon of $SU(2)_{\text{CMB}}$ with the electrically charged soliton of, say, $SU(2)_e$ thus is furnished by an adiabatic rotation into the (massive) photon of $SU(2)_e$ when approaching the charge of the latter and an adiabatic back-rotation into the photon of $SU(2)_{\text{CMB}}$ after the interaction has taken place. Where are the higher charge states? These states are unstable by repulsion mediated by the photon of $SU(2)_{\text{CMB}}$, and thus they are very broad. The density of these states, however, is over-exponentially rising. Why do we only see the structure of a charged lepton in scattering experiments with a center-of-mass energy \sqrt{s} comparable to the mass of the lepton, see Figs. 34,35? Radial excitations of a 't Hooft monopole have been investigated in ⁶³. The first excited level is comparable to twice the mass of the monopole ground state. This must semi-quantitatively also hold for a Z_2 monopole (self-intersection of a center-vortex loop). For $\sqrt{s} \ll m_e, m_\mu, m_\tau$ the Z_2 monopole is not excitable, a QED point-particle description holds. For $m_Z \gg \sqrt{s} \gg m_e, m_\mu, m_\tau$, where $m_Z \sim 90 \text{ GeV}$ is the mass of the Z boson, the energy deposited into the vertex is converted into a large entropy carried by the Hagedorn spectrum of unstable states. The latter protect the Z_2 monopole against radial excitations, a QED point-particle description again holds. For $\sqrt{s} \sim 2 m_e, 2 m_\mu, 2 m_\tau$ the Z_2 monopole is excited radially: A QED point-particle description fails. For $\sqrt{s} \gg m_Z$ the Hagedorn phase boundary of $SU(2)_e$ is locally overcome (the Z boson is interpreted as the decoupled dual gauge mode on the magnetic side of the magnetic-center phase boundary, the W^\pm bosons as the

decoupled gauge modes on the electric side of the electric-magnetic phase boundary): The multiplicity of final states should be in stark contradiction to the SM prediction (we expect charge nonconservation in such processes). Where does the parity violation come from? This is an intermediate consequence of the existence of a Planck-scale axion. What is the nature of the charge-zero state (single center-vortex loop)? The mass of this state for $SU(2)_e$ is roughly given by $m_\nu \sim \frac{m_e}{g_{dec}}$, compare with Eq. (168). Moreover, the mass of the Z boson is given as $m_Z \sim g_{dec} m_e$. From the experimentally known values $m_e \sim 5 \times 10^5$ eV and $m_Z \sim 9 \times 10^{10}$ eV we thus have $g_{dec} \sim \frac{9}{5} \times 10^5$ and therefore $m_\nu \sim \frac{25}{9}$ eV. This is close to the upper bound for the mass of the electron neutrino obtained from a tritium β decay experiment: $m_\nu < 2.3$ eV¹⁰¹. Thus a single center-vortex loop of $SU(2)_e$ viably is a candidate for the electron neutrino. Notice that this soliton has no antiparticle: Neutrinos need to be of the Majorana type in accord with the successful search for neutrinoless double beta decay¹⁰². A similar situation holds for $SU(2)_\mu$ and $SU(2)_\tau$. We expect the masses of their intermediary vector bosons $m_{Z'}, m_{W',\pm}$ and $m_{Z'', m_{W'',\pm}}$ to scale with their Yang-Mills scales m_μ and m_τ and large values of the gauge couplings at the respective phase boundaries. Thus there are very weak and very, very weak interactions in addition to the weak interactions which, however, will be very hard to detect experimentally. (To detect, say, $m_{Z'}$ directly would need a center-of-mass energy in e^+e^- annihilation which should at least be two-hundred times $m_{Z'}$.) A remark concerning point (v) is in order: Since $SU(2)_e \times SU(2)_\mu \times SU(2)_\tau$ are in their center phases at present their contribution to the ground-state energy density and pressure of the Universe is nil. Above, we have computed the contribution arising from $SU(2)_{CMB}$ when assuming the Planck-scale axion to be absent.

Let us make a short remark on the solar wind. This particle flux is mainly composed of protons (about 3×10^{43} protons depart annually from the solar surface¹⁰³). If the conservation of electric charge, which is a built-in feature of the SM, would hold then the sun would continuously acquire negative charge: A disastrous implication for earth's orbit would arise. The problem is resolved by the observation that in the solar core temperatures are greater than m_e . Electronic charge, however, is absent in the magnetic or electric phase of $SU(2)_e$. According to the phase diagram of $SU(2)_e$ the solar core contains a superconducting mantle (magnetic phase, Bose condensate of electric monopole-antimonopole pairs) whose negative pressure together with gravity balances the positive thermal pressure of the innermost core (electric phase) where fusion takes place. Within the core region there is a clear dominance of positive charge which the sun deposes off by means of the solar wind. A superconducting core of the sun is also demanded in¹⁰³ for other reasons.

We conclude this section by stressing that no fundamental Higgs field is needed to break the weak symmetry $SU(2)_W$ or $SU(2)_e$. In contrast to the SM, where this symmetry breaking is complete by a nonvanishing expectation of a fundamental Higgs field, the dynamical breakdown of $SU(2)_e$ proceeds in a two-stage, Higgs-particle free way: $SU(2)_e \rightarrow U(1)$ (electric phase; adjoint nonfluctuating Higgs field) and $U(1)_D \rightarrow 1$ (magnetic phase; complex nonfluctuating Higgs field). Moreover,

the electron and its neutrino are stable solitons in the center phase of $SU(2)_e$.

7.3. *Quantum chromodynamics: Quark confinement and fractional quantum Hall effect*

In this section we pursue an admittedly speculative and not very matured idea about the nature of quarks and their interactions.

Quantum chromodynamics (QCD) is an integral part of the SM. QCD is the gauge theory of strong interactions: Pointlike current quarks, which are spin-1/2 fermions of to-be-measured masses, are fundamentally charged under the gauge group $SU(3)_C$ and interact by the exchanges of massless gluons, the gauge bosons of $SU(3)_C$. The latter interact with one another according to a pure Yang-Mills action. The electric charges of quarks are $2/3$ or $-1/3$. Let us only discuss the three quark flavors of lowest mass $m_u = (3 \cdots 5) \text{ MeV}$ (charge $2/3$), $m_d = (5 \cdots 7) \text{ MeV}$ (charge $-1/3$), and $m_s = (100 \cdots 140) \sim \text{ MeV}$ (charge $-1/3$) (all $\overline{\text{MS}}$ scheme, results depend on the renormalization point).

Since leptons are likely to be the stable solitons in the center phases of pure $SU(2)$ Yang-Mills theories it is tempting to speculate that quarks are related to the charge-one solitons (center-vortex loops with one self-intersection, spin-1/2 fermions) in the center phases of pure $SU(3)$ Yang-Mills theories. If we assign an $SU(3)_u$ and $SU(3)_d$ theory of Yang-Mills scale $\sim m_u$ and m_d to the quark flavors u and d , respectively, then we need to understand why these quarks are confined and why the electric charge appears to be $2/3$ or $-1/3$. A plausible way of generating quark confinement would be to add an additional $SU(3)$ Yang-Mills theory of scale, say $\Lambda = 140 \text{ MeV}$ which, however, is a magnetic dual to the other $SU(3)$ theories. A center-vortex condensate of this theory constrains the (color)electric flux between a u or d quark and a u or d antiquark into a tube and thus confines. The additional $SU(3)$ theory also has charge-one solitons in its center phase which are confined by the center-vortex condensates of the theories $SU(3)_u$ and $SU(3)_d$. It is tempting to interpret these solitons as strange quarks s and thus to invoke the label $SU(3)_s$.

What about the electric quark charges? Due to confinement the trajectories of each quark flavor are forced onto a more or less two-dimensional spherical surface if the ground state of a given hadron is considered. A flux dual to the flux in the confining tube is readily available in the center-vortex condensate being responsible for confinement. This is the set-up for the occurrence of the fractional quantum Hall effect: Quarks that would be integer charged spin-1/2 fermions in the absence of the dual fluxes form bound states with these fluxes. Bound states with three dual flux quanta are bosons, and thus they condense. Excitations above this condensate have fractional electric charge. For a thorough discussion of this phenomenon, see 104.

Again, all of what was said in this section is preliminary. We would like to stress though that the above scenario has the potential to explain why the equation of state in hydrodynamical simulations of the elliptic flow measured in ultra-relativistic

heavy-ion collisions at RHIC seems to be so close to the free-gas limit despite the fact that strong correlations thermalize the system very rapidly¹⁰⁵. (At $T_c \sim 170$ MeV the two theories $SU(3)_u$ and $SU(3)_d$ are deep inside their electric phases while $SU(3)_s$ is just above the electric-magnetic transition.)

8. Conclusions

We have developed a nonperturbative approach to $SU(2)$ and $SU(3)$ Yang-Mills thermodynamics. The formation of a macroscopic, adjoint, and nonfluctuating Higgs field in the deconfining (electric) phase of each theory, which involves the (admissible part of the) moduli space of a caloron-anticaloron system, the Bose condensation of thermalized magnetic monopole-antimonopole systems into a macroscopic, nonfluctuating complex field in a preconfining (magnetic) phase, and the nonthermal condensation of systems composed of a center-vortex and an anti-center-vortex in a confining (center) phase were shown. A change of the statistics of the excitations from bosonic to fermionic was observed across the last phase transition. The degeneracy of the ground state with respect to a (global) electric Z_2 ($SU(2)$) and Z_3 ($SU(3)$) symmetry was observed in the electric phase, and the uniqueness of the ground state with respect to these symmetries was derived in the magnetic phase. Moreover, the nature of the phase transitions, electric-magnetic and magnetic-center, was clarified. The evolution of thermodynamical quantities with temperature was computed within the electric phase and the magnetic phase, and the density of fermionic states was estimated in the center phase.

It did not escape the author's attention that the results obtained may resolve a number of long-standing problems in particle physics and cosmology.

Acknowledgments

The author would like to thank B. Garbrecht, H. Gies, Th. Konstandin, T. Prokopec, H. Rothe, K. Rothe, M. Schmidt, I.-O. Stamatescu, and W. Wetzel for very helpful, continuing discussions. Important support for numerical calculations was provided by J. Rohrer and is thankfully acknowledged. The author acknowledges vivid discussion with Francesco Giacosa and Markus Schwarz. In particular, I am grateful to Francesco Giacosa for pointing out the need for a modification of the evolution equations for the effective gauge couplings which was overlooked in the previous version. Very useful discussions with P. van Baal, E. Gubankova, J. Moffat, J. Polonyi, D. Rischke, and F. Wilczek and illuminating conversations with D. Bödeker, R. Brandenberger, G. Dunne, Ph. de Forcrand, A. Guth, F. Karsch, A. Kovner, M. Laine, H. Liu, C. Nunez, J. Pawłowski, R. D. Pisarski, K. Rajagopal, K. Redlich, E. Shuryak, D. T. Son, A. Vainshtein, J. Verbaarschot, and F. Wilczek are gratefully acknowledged. A very useful correspondence with O. Manuel on solar models is thankfully acknowledged. The warm hospitality of the Center for Theoretical Physics at M.I.T, where part of this research was carried out (sponsored by Deutsche Forschungsgemeinschaft), is thankfully acknowledged.

90 *Ralf Hofmann*

This paper is dedicated to my family and in particular to my wife Karin Thier. Thank you for your continuing encouragement, your persistent moral support, and your unconditional love.

References

1. G. Gomez-Ceballos *et al.*, *Int. J. Mod. Phys. A* **16S1B**, 839 (2001).
2. U. W. Heinz and P. F. Kolb, *Nucl. Phys. A* **702**, 269 (2002).
3. D. Teaney, J. Lauret, and E. V. Shuryak, *nucl-th/0110037*.
4. C. L. Bennett *et al.*, *Astrophys. J.* **464**, L1 (1996).
K. M. Gorski *et al.*, *Astrophys. J.* **464**, L11 (1996).
G. Hinshaw *et al.*, *Astrophys. J.* **464**, L17 (1996).
5. S. Perlmutter *et al.*, *Astrophys. J.* **517**, 565 (1999).
S. Perlmutter *et al.*, *Bull. Am. Astron. Soc.* **29**, 1351 (1997).
6. A. G. Riess *et al.*, *Astron. J.* **116**, 1009 (1998).
7. D. N. Spergel *et al.*, *Astrophys. J. Suppl.* **148**, 175 (2003).
8. A. D. Linde, *Phys. Lett. B* **108**, 389 (1982).
9. A. H. Guth and S. Y. Pi, *Phys. Rev. Lett.* **49**, 1110 (1982).
10. E. B. Gliner and I.G. Dymnikova, *Sov. Astron. Lett.* **1** (1975) 93.
I. G. Dymnikova, *Sov. Phys. JETP* **63** (1986) 1111.
11. A. A. Starobinsky, *Phys. Lett. B* **117**, 175 (1982).
12. A. Kogut *et al.*, *Astrophys. J. Suppl.* **148**, 161 (2003).
13. Z. G. Dai *et al.*, *Astrophys. J.* **580**, L7 (2002).
14. J. Bagchi *et al.*, *New Astron.* **7**, 249 (2002).
15. R. Hagedorn, *Nuovo Cim. Suppl.* **3**, 147 (1965).
16. D. J. Gross and F. Wilczek, *Phys. Rev. Lett.* **30**, 1343 (1973).
D. J. Gross and F. Wilczek, *Phys. Rev. D* **8**, 3633 (1973).
17. H. D. Politzer, *Phys. Rev. Lett.* **30**, 1346 (1973).
18. A. D. Linde, *Phys. Lett. B* **96**, 289 (1980).
19. J. C. Taylor and S. M. H. Wong, *Nucl. Phys. B* **346**, 115 (1990).
E. Braaten and R. D. Pisarski, *Nucl. Phys. B* **337**, 569.
20. D. Bödeker, *Phys. Lett. B* **426**, 351 (1998).
21. P. Arnold, D. T. Son, and L. G. Yaffe, *Phys. Rev. D* **59**, 105020 (1999).
J.-P. Blaizot and E. Iancu, *Nucl. Phys. B* **557**, 183 (1999).
D. F. Litim and C. Manuel, *Phys. Rev. Lett.* **82**, 4981 (1999).
22. K. Kajantie, M. Laine, K. Rummukainen, and Y. Schroder, *Phys. Rev. D* **67**, 105008 (2003).
K. Kajantie, M. Laine, K. Rummukainen, and Y. Schroder, *Phys. Rev. Lett.* **86**, 10 (2001).
23. J.-P. Blaizot, E. Iancu, and A. Rebhan, *hep-ph/0303185*.
24. R. Hofmann, *Phys. Rev. D* **62**, 065012 (2000).
R. Hofmann, *Phys. Rev. D* **62**, 105021 (2000).
R. Hofmann, *Phys. Rev. D* **65**, 125025 (2002).
R. Hofmann, *Phys. Rev. D* **68**, 065015 (2003).
R. Hofmann, *hep-ph/0312046*.
25. V. L. Ginzburg and L. D. Landau, *JETP* **20**, 1064 (1950).
26. A. A. Abrikosov, *Sov. Phys. JETP* **5**, 1174 (1957).
27. D. F. Litim and J. M. Pawłowski, *publ. in Faro 1998, The exact renormalization group*, 168, *hep-th/9901063*.
28. A. Belavin, A. Polyakov, A. Schwartz, and Yu. Tyupkin, *Phys. Lett.* **59**, 85 (1975).

29. B. J. Harrington and H. K. Shepard, Phys. Rev. D **17**, 105007 (1978).
30. M. K. Prasad and C. M. Sommerfield, Phys. Rev. Lett. **35**, 760 (1975).
E. B. Bogomolnyi, Sov. J. Nucl. Phys. **24**, 449 (1976).
31. W. Nahm, Phys. Lett. B **90**, 413 (1980).
W. Nahm, Lect. Notes in Physics. 201, eds. G. Denaro, e.a. (1984) p. 189.
32. T. C. Kraan and P. van Baal, Nucl. Phys. B **533**, 627 (1998).
33. T. C. Kraan and P. van Baal, Phys. Lett. B **428**, 268 (1998).
T. C. Kraan and P. van Baal, Phys. Lett. B **435**, 389 (1998).
34. K.-M. Lee and C.-H. Lu, Phys. Rev. D **58**, 025011 (1998).
35. R. C. Brower, D. Chen, J. Negele, K. Orginos, and C-I Tan, Nucl. Phys. Proc. Suppl. **73**, 557 (1999).
36. D. J. Gross, R. D. Pisarski, and L. G. Yaffe, Rev. Mod. Phys. **53**, 43 (1981).
37. L. Brown, R. Carlitz, and C. Lee, Phys. Rev. D **16**, 417 (1977).
38. L. Brown, R. Carlitz, D. Creamer, and C. Lee, Phys. Rev. D **17**, 1583 (1978).
39. L. Brown and D. Creamer, Phys. Rev. D **18**, 3695 (1978).
40. G. 't Hooft, Phys. Rev. D **14**, 3432 (1976), Erratum-ibid. D **18**, 2199 (1978).
41. D. Diakonov, N. Gromov, V. Petrov, and S. Slizovskiy, Phys. Rev. D **70**, 036003 (2004).
42. Th. Schafer and E. V. Shuryak, Rev. Mod. Phys. **70**, 323 (1998).
43. A. Actor, Ann. Phys. (N. Y.) **148**, 32 (1983).
44. A. Chakrabarti, Phys. Rev. D **35**, 696 (1987).
45. G. 't Hooft, Phys. Rev. D **14**, 3432 (1976), D **18**, 2199 (E) (1976).
G. 't Hooft, unpublished.
M. Atiyah, W. Drinfeld, N. Hitchin, and Yu. Manin, Phys. Lett. **A**, 65 (1978).
46. U. Herbst and R. Hofmann, hep-th/0411214.
47. Y. Hosotani, Phys. Lett. B **126**, 309 (1983).
48. U. Herbst, R. Hofmann, and J. Rohrer, Acta Phys. Pol. B **36**, 881 (2005).
49. M. Schwarz, R. Hofmann, and F. Giacosa, hep-th/0603078.
50. R. Hofmann, hep-th/0609033.
51. M. I. Gorenstein and S. N. Yang, Phys. Rev. D **52**, 5206 (1995).
52. J. Rohrer and R. Hofmann, work in progress.
53. C. P. Korthals Altes, hep-ph/0406138, hep-ph/0408301.
C. P. Korthals Altes, Acta Phys. Polon. B **34**, 5825 (2003).
P. Giovannangeli and C. P. Korthals Altes, Nucl. Phys. B **608**, 203 (2001).
C. Korthals-Altes, A. Kovner, and M. A. Stephanov, Phys. Lett. B **469**, 205 (1999).
54. Ch. Hoelbing, C. Rebbi, and V. A. Rubakov, Phys. Rev. D **63**, 034506 (2001).
55. G. 't Hooft, Nucl. Phys. B **79**, 276 (1974).
56. A. M. Polyakov, JETP Lett. **20**, 194 (1974).
57. M. K. Prasad and C. M. Sommerfield, Phys. Rev. Lett. **35**, 760 (1975).
58. B. Julia and A. Zee, Phys. Rev. D **11**, 2227 (1975).
59. M. A. Aguilar and M. Socolovsky, Int. J. Theor. Phys. **38**, 2485 (1999).
60. N. Steenrod, *The topology of Fibre Bundles*, Princeton University Press, Princeton, New Jersey.
61. G. 't Hooft, Phys. Rev. D **14**, 3432 (1976).
62. N. P. Landsman and C. G. van Weert, Phys. Rep. **145**, 141 (1987)
63. P. Forgacs and M. Volkov, Phys. Rev. Lett. **92**, 151802.
64. T. Kaluza, Sitzungsber. Preuss. Akad. Wiss. Berlin (Math.Phys.) **1921**, 966 (1921).
65. O. Klein, Z. Phys. **37**, 895 (1926).
O. Klein, Surveys High Energ.Phys. **5**, 241 (1986).
66. L. Del Debbio *et al.*, proc. NATO Adv. Res. Workshop on Theor. Phys., Zakopane

92 *Ralf Hofmann*

- (1997) [hep-lat/9708023].
67. H. B. Nielsen and P. Olesen, Nucl. Phys. B **61**, 45 (1973).
 68. G. 't Hooft, Nucl. Phys. B **138**, 1 (1978).
 69. B. Svetitsky and L. G. Yaffe, Nucl. Phys. B **210**, 423 (1982).
 70. B. Svetitsky and L. G. Yaffe, Phys. Rev. D **26**, 963 (1982).
 71. H. Reinhardt, Nucl. Phys. B **628**, 133 (2002).
 72. R. Hofmann, S. Scheffler, and I.-O. Stamatescu, work in progress.
 73. C. M. Bender and T. T. Wu, Phys. Rev. **184**, 1231 (1969).
 74. J. H. Traschen and R. H. Brandenberger, Phys. Rev. D **42**, 2491 (1990).
L. Kofman, A. D. Linde and A. A. Starobinsky, Phys. Rev. Lett. **73**, 3195 (1994).
J. Berges and J. Serreau, Phys. Rev. Lett. **91**, 111601 (2003).
 75. J. Engels *et al.*, Nucl. Phys. B **205**[FS5], 545 (1982).
 76. G. Boyd *et al.*, Phys. Rev. Lett. **75**, 4169 (1995).
G. Boyd *et al.*, Nucl. Phys. **B469**, 419 (1996).
 77. J. Engels, F. Karsch, T. Scheideler, Nucl. Phys. B **564**, 302 (1999).
 78. F. R. Brown *et al.*, Phys. Rev. Lett. **61**, 2058 (1988).
 79. Y. Deng, in BATAVIA 1988, proc. LATTICE 88, 334.
 80. J. Engels *et al.*, Phys. Lett. B **252**, 625 (1990).
 81. F. Giacosa and R. Hofmann, hep-th/0512184.
 82. B. Lucini, M. Teper, and U. Wenger, JHEP **0401**, 061 (2004).
 83. B. Lucini, M. Teper, and U. Wenger, JHEP **0502**, 033 (2005).
 84. Th. Blum, private conversation.
 85. T. R. Klassen, Nucl. Phys. B **533**, 557 (1998).
 86. A. Sen and B. Zwiebach, JHEP03 **002** (2000).
 87. T. Prokopec, astro-ph/0503289.
 88. M. F. Atiyah and I. M. Singer, Proc. Nat. Acad. Sci. **81**, 2597 (1984).
 89. J. S. Bell and R. Jackiw, Nuovo Cim. A **60**, 47 (1969).
 90. K. Fujikawa, Phys. Rev. Lett. **42**, 1195 (1979).
 91. R. D. Peccei and H. R. Quinn, Phys. Rev. D **16**, 1791 (1977).
R. D. Peccei and H. R. Quinn, Phys. Rev. Lett. **38**, 1440 (1977).
 92. A. D. Sakharov, Pisma Zh. Eksp. Teor. Fiz. **5**, 32 (1967); JETP Lett. **5**, 24 (1967);
Sov. Phys. Usp. **34**, 392 (1991); Usp. Fiz. Nauk **161**, 61 (1991).
 93. F. Wilczek, hep-ph/0408167.
 94. E. R. Williams, J. E. Faller, and H. A. Hill, Phys. Rev. Lett. **26**, 721 (1971).
 95. E. Adelberger, G. Dvali, and A. Gruzinov, hep-ph/0306245.
 96. D. N. Spergel *et al.*, Astrophys. J. Suppl. **148**, 175 (2003).
 97. H. Alvensleben *et al.*, Phys. Rev. Lett. **21**, 1501 (1968).
 98. R. B. Blumenthal *et al.*, Phys. Rev. **144**, 1199 (1966).
 99. A. Ashkin, L. A. Page, and W. M. Woodard, Phys. Rev. **94**, 357 (1953).
 100. M. B. Scott, A. O. Hanson, and E. M. Lyman, Phys. Rev. **84**, 638 (1951).
 101. Ch. Kraus *et al.*, hep-ex/0412056.
 102. H. V. Klapdor-Kleingrothaus, I. V. Krivosheina, A. Dietz, and O. Chkvorets, Phys. Lett. B **586**, 198 (2004).
 103. O. Manuel, in proc. Fourth Intern. Conf. on Beyond Standard Model Physics 2003, astro-ph/0411658.
 104. R. B. Laughlin, Nobel lecture publ. in NOBEL LECTURES IN PHYSICS (1996-2000), World Scientific Publishing Co.
 105. E. Shuryak, J. Phys. G **30**, S1221 (2004).